2005

Geologic variability and Holocene sedimentary record on the Northern Gulf of Mexico inner to mid-continental shelf

Triniti A. Dufrene
Louisiana State University and Agricultural and Mechanical College

GEOLOGICAL VARIABILITY AND HOLOCENE SEDIMENTARY RECORD ON THE NORTHERN GULF OF MEXICO INNER TO MID-CONTINENTAL SHELF

A Thesis

Submitted to the Graduate Faculty of the
Louisiana State University and
Agricultural and Mechanical College
in partial fulfillment of the
requirements for the degree of
Master of Science

in

The Department of Oceanography and Coastal Sciences

by
Triniti Ann Dufrene
B.S. Coastal Carolina University, 2001
May 2005

ACKNOWLEDGEMENTS

First and foremost, I would like to thank Dr. Sam Bentley for taking a chance on me and I am ever grateful for his patience, guidance, and understanding. I would also like to thank my committee members Dr. Harry H. Roberts and Dr. Chuck Wilson for their help and insight along the way.

I would like to extend a big thanks to those who have helped me with field work and analysis: Kristina Rotondo, Brian Velardo, Luke Patterson, Brian Vosburg, Zahid Muhammad, Chris Dautreve, Jonathon Mitchell, Will Vienne, and Mark Miller. I would like to send a special thanks to Yvonne Allen and Walker Winans, who both helped guide me through the wonderful world of sonar and chirp. I could not have done it without them.

I would like to extend thanks to the captains and crew of the R/V Acadiana and Caretta. Also thanks to the Pascagoula NMFS office. I would also like to thank Dr. Will Patterson and Dave Wells for their help and insight on the fisheries aspect of this project. And I would like to thank the Coastal Studies Field Support Unit for all of their help in cruise preparation and to CSI and CFI for instrumentation and software used in this study.

I would also like to thank my family and friends, who have been very understanding through this journey and who I am sure are very happy to have me finished and back to normal.

Support for this project was provided by National Sea Grant.

TABLE OF CONTENTS

Acknowledgements……..…..ii

Abstract……..……iv

Introduction…….1
Overall Objectives & Rationale……..1
General Geologic History of the Northern Gulf of Mexico……...1
Study Area…….….5
Essential Fish Habitats: The Need for Geological Characterization……..7

Methods…….……..8
Geoacoustics……....8
Sampling & Analysis……..10

Results……....16
Geologic and Geoacoustic Results……..…16
Juvenile Red Snapper EFH……..…59

Discussion…….…..63
Geologic Interpretations…….….63
Implications to Juvenile Red Snapper Essential Fish Habitat……..…81

Conclusions…….83

References……...85

Appendix A: Chirp Subbottom Profiles……...90

Appendix B: Sediment Data from Site D……96

Vita…….…….100

ABSTRACT

Side-scan Sonar, Chirp sub-bottom profiles, and grab samples were collected on the north-central Gulf of Mexico continental shelf as part of an interdisciplinary study of juvenile red snapper habitat. Demarcation of essential fish habitat for juvenile red snapper (*Lutjanus campechansis*) in the Gulf of Mexico is considered to be critical for maintaining viable stocks of this valuable species. The first goal of the study is to map and describe the geology of this region. The second goal is to attempt to relate variations in geology to juvenile red snapper distribution and habitat preferences.

Sidescan mosaics were created for ten polygons, ranging in size from 2-20km² on the inner to middle shelf south of Mississippi-Alabama, in water depths of 17-40 m. Geological observations have delineated three contrasting seabed types: (1) linear to patchy shell regions on the inner and middle shelf, (2) muddy sand sheets on the middle shelf, and (3) prodeltaic muds in the southwest of the study area, marking the eastern extent of recent shelf deposits from the modern Mississippi delta. The shell ridges stand 1-3 m above the surrounding seabed, and extend up to 200 m across. They are composed of $> 50\%$ $CaCO_3$, including shell fragments from both estuarine and marine taxa, and contrast sharply with adjacent muddy sands containing minor shell. AMS ^{14}C dating of shell material, along with the geological characteristics of the ridges suggests that they are remnants of Holocene coastal environments.

This region has been previously described as either an extension of the MAFLA sand sheet or a transitional zone between the MAFLA sands and prodelta muds (Ludwick, 1964). In the present study, we have identified a range of geological features of estuarine, shoreface, and wholly marine origin. The diversity of deposits described

here thus records a wide range of geological processes active from early-middle Holocene to recent time. The integration of geological observations with coordinated biological observations reveals that geologic structures and sediment composition on the northern Gulf of Mexico continental shelf are major controls on the distribution of juvenile red snapper (Patterson et al, in press), and record both coastal depositional histories and open-shelf processes active during the Holocene transgression.

INTRODUCTION

Overall Objectives & Rationale

The overall goal of this study is to evaluate the Holocene geological variability and depositional history of the seabed along the Northern Gulf of Mexico inner to mid-continental shelf as part of a larger study evaluating juvenile red snapper Essential Fish Habitat (EFH). In this context, EFH refers to the bottom habitat (substrate) that is necessary for the growth and survival of the juvenile red snapper. The geological seabed characterization gained from this study will be used to characterize the habitat of the commercially threatened species in order to better evaluate stock and aid in future decisions regarding red snapper management (Patterson et al., in press).

To meet these goals, we have mapped ten sites, ranging in size from 2 to 20 km² and extending 20-85 km offshore, on the Mississippi-Alabama continental shelf. We have employed both large-scale acoustic mapping techniques (sidescan sonar and chirp sonar subbottom profiling) along with groundtruthing (sediment sampling at study areas to 'calibrate' acoustic reflectance) to develop a more complete geological understanding of the seabed (e.g. Valentine et al., 2003).

General Geologic History of the Northern Gulf of Mexico

The northern Gulf of Mexico (GOM) continental shelf, along the Mississippi-Alabama coast (Figure 1), is gently sloping (<0.1º) and broad with the shelf edge occurring between approximately 60 and 100 m water depth (Kindinger, 1989; Parker, 1992; and Schroeder et al., 1995). Longitudinally, it extends from the Mississippi River to the DeSoto Canyon. South of Mississippi, the shelf is approximately 122 km wide and

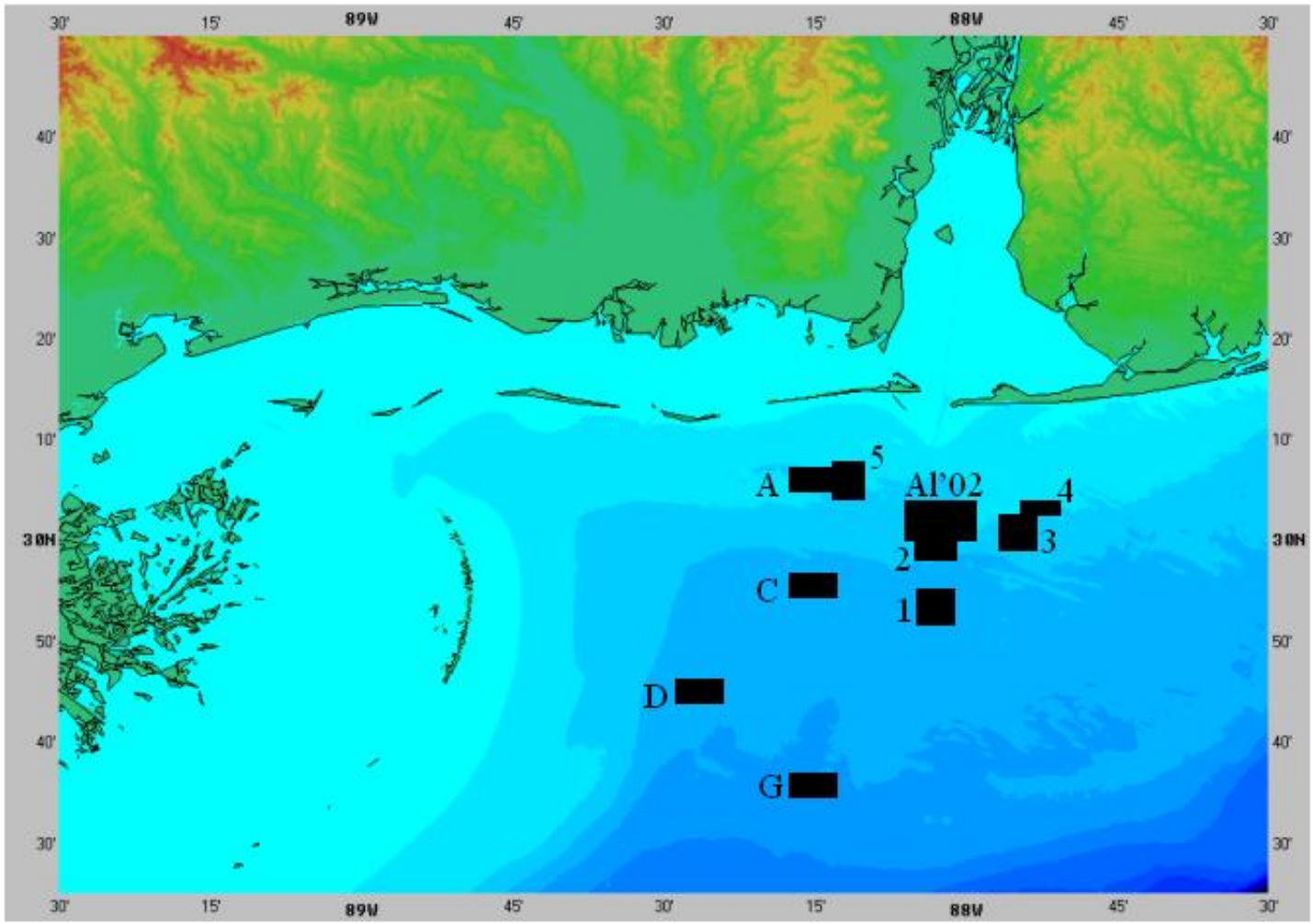

Figure 1. Study location along the Mississippi-Alabama continental shelf. Text refers to site name. Bathymetry 10m intervals.

narrows to 44 km near the head of the DeSoto Canyon (Parker et al., 1992). It is bordered to the west by the Chandeleur Islands and to the north by the Mississippi-Alabama barrier island system. The Northern GOM shelf is characterized as a slowly subsiding passive continental margin (Sydow and Roberts, 1994) with little evidence of structural deformation apparent at present. Salt diapirs (from underlying Louann Salts of the Jurassic), with associated faulting, on the shelf edge (water depth of 75-80 m) are the only evidence for structural complexity (Kindinger, 1989; Bryant et al., 1991).

Owing to glacio-eustatic sea level fluctuations during the Pleistocene and Quaternary, a thick sedimentary wedge of sediment has been deposited at the shelf-slope transition of the GOM (Winker, 1982). Extension of the coastal plain onto the continental shelf during lowstands resulted in the deposition of shelf edge deltas (Suter & Berryhill, 1985). High-resolution seismic profiling indicated that shelf margin bathymetry and progradation seem to be a result of deposition associated with major lowstands during Quaternary time (Winker, 1982). The shallow subsurface of the Mississippi-Alabama shelf edge was characterized seismically by a series of offlapping depositional sequences overlying onlapping sequences with intermittent periods of erosion (Kindinger, 1989). Present topographic relief seems to represent geologic structure of the basin remnant of the most recent Late Wisconsinian glaciation approximately 18,000-20,000 ybp (Bryant et al., 1991; Kindinger, 1989).

According to Donoghue (1983), the geologic history of the Gulf of Mexico continental shelf has been dominated by the activity of the Mississippi River since the Early Tertiary. As a result of deltaic progradation, sediments underlying a thin Holocene veneer consist of fluvial sands and gravels within fluvial and deltaic depositional

fairways. These were believed to be deposited around 18,000 ybp during the last sea-level lowstand. At this time, sea level is believed to have been around 120 m lower than present level. Marine processes have reworked some of this sediment during sea-level rise (Parker et al., 1992).

The modern northern GOM is a low energy, microtidal environment that has been strongly influenced in the past by the Mississippi River, its associated deltas, and by rising sea level (Ludwick, 1964; Mazzullo and Bates, 1985; Kindinger, 1988, 1989; McBride et al., 1991, 1999; McBride, 1997). Doyle and Sparks (1980) indicated that under present conditions only small amounts of terrigenous sediments reach the Mississippi-Alabama continental shelf because most fluvial material trapped in coastal bays and estuaries. Since less than 30% of fluvial material is believed to reach the continental shelf (Parker, 1992), relict or palimpsest topographic features and sediments characterize the Mississippi-Alabama continental shelf. Low sediment accumulation on the shelf and exposure of relict features is considered unique to the present highstand situation, especially since deltaic processes and associated sedimentation have deposited most of the underlying continental shelf sediments (Sager et al., 1999).

Surficial sediments in the area are believed to depict different depositional episodes and divide the shelf into two regions: delta complexes to the west, and a sand sheet to the east (Kindinger, 1989 & Parker et al., 1992). The delta complexes, including the St. Bernard and the Modern Balize lobe have been extensively studied (Coleman and Gagliano, 1964; Ludwick, 1964; Frazier, 1967; Mazzullo and Bates, 1985, Brooks et al., 1995) and include a range of fluvial deltaic, estuarine, and marine depositional environments of muddy and sandy character. To the east, a homogeneous clean sand

sheet (MAFLA) has been produced by rivers of relatively low sediment yield and sediment winnowing during the Holocene transgression (Ludwick, 1964; Doyle and Sparks, 1980; Mazzullo and Bates, 1985; Kindinger, 1988, 1989; McBride et al, 1991; Kennicutt et al., 1995; Anderson and McBride, 1996; McBride, 1997; McBride et al, 1999).

Study Area

Our area of interest lies between these two geologic provinces and on the western margin of the eastern sand sheet (Figure 1). Ludwick (1964) found spatially variable bottom types in a grab sample study, and described this region as a transitional zone between the MAFLA sand sheet and the prodelta muds associated with the Balize and St. Bernard delta complexes (Figure 2). Despite the development of new tools and approaches, few studies in the recent decades have concentrated on the surficial deposits in this transitional zone. Prior to the late 1980's, the Mississippi-Alabama continental shelf was thought of as a featureless extension of the eastern sand sheet consisting primarily of quartz sand with smaller amounts of carbonate sands, gravel, and mud (Parker et al., 1992). Only in the past 15 years have topographic features been observed with the use of geoacoustics and more detailed sampling. Although the presence of some of these low relief structures has been documented previously, their geologic origin has not been clearly established.

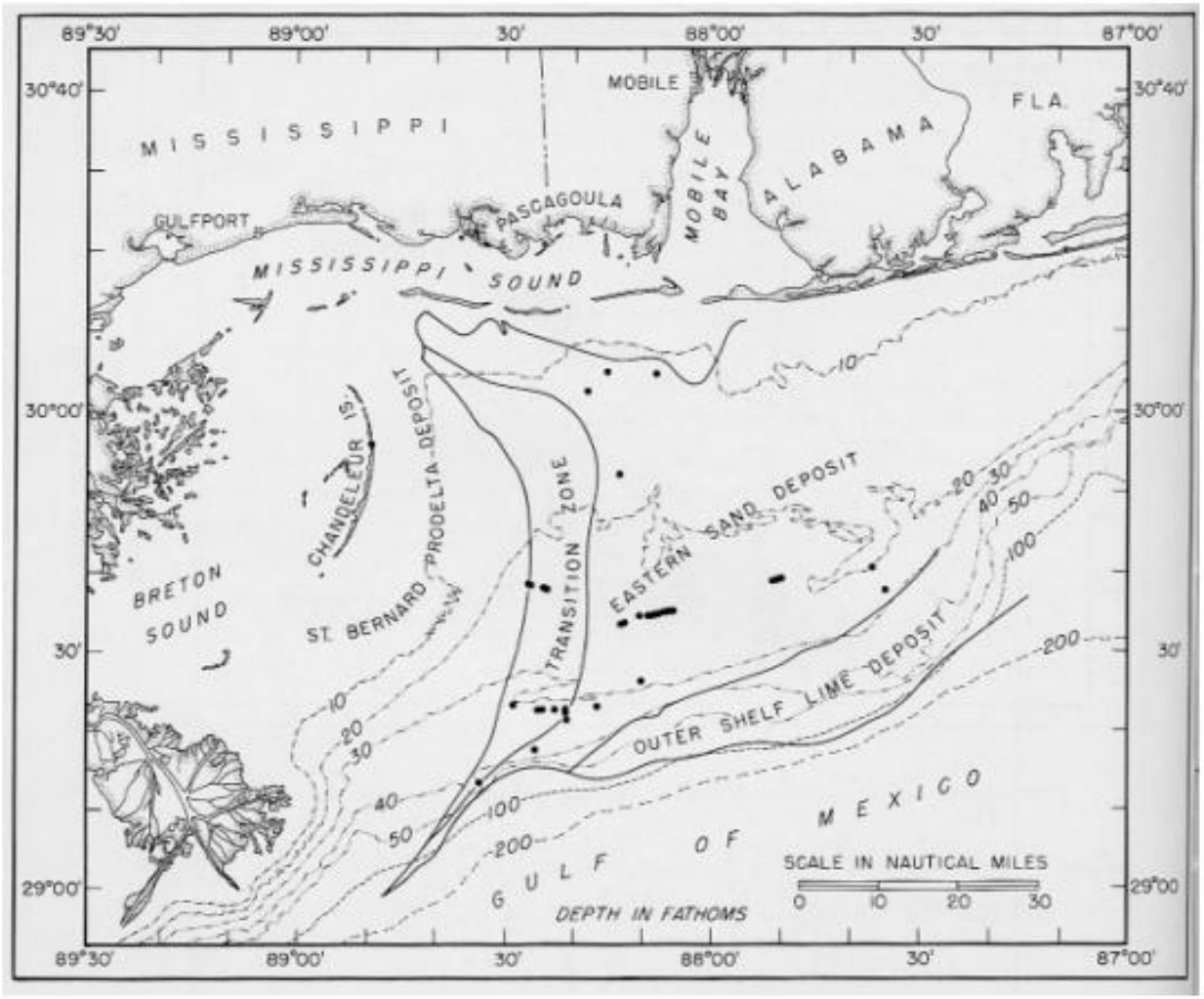

Figure 2. Locations of major Northern Gulf of Mexico surficial sediment provinces. (From Ludwick, 1964)

Essential Fish Habitats: The Need for Geological Characterization

One of the main fishery concerns in the Gulf of Mexico is the overfished status of the red snapper, *Lutjanus campechanus*. The snapper fishery is either threatened or closed in the Northern Gulf of Mexico and therefore raises serious conservation issues (Patterson et al., in press). Mortality estimates from the National Marine Fisheries Service (NMFS) indicate that there are two main causes of juvenile red snapper population decline: (1) low estimated spawning potential, and (2) bycatch of juveniles by the shrimping industry (Patterson et al., in press). Recent data on red snapper mortality suggest that bycatch of juveniles by trawlers targeting penaeid shrimp species is the most important issue causing of the decline in population. To reduce bycatch mortality, a better understanding of the habitat specific location and distribution of juvenile snapper is needed. Characterization of EFH for juvenile red snapper (*Lutjanus campechanus*) in the Gulf of Mexico is considered to be critical for maintaining viable stocks of this valuable species.

The preference of juvenile snapper to different habitats has been studied in laboratory and small-scale *in-situ* studies (reviewed in Patterson et al., in press). These results indicate that juvenile snapper display some affinity for low-relief shell structures. However, general studies have also reported this species in open-sand, shell rubble, and artificial structures with greater vertical relief (Patterson et al. in press). Surficial sediment characterization, as a result of this study, will be used in classifying EFH of juvenile red snapper within the study area.

METHODS

Geoacoustics

Sound Navigation and Ranging (Sonar) has important geological applications, including the use of acoustic waves to survey large areas of the seafloor. Sonars take advantage of the differing sound-absorbing and sound-reflecting properties of material. This methodology allows scientists to image the seafloor and assess local seabed morphology and sediment texture. In side-scan sonar (SSS), transmission cycles (sound pulses or pings) are transmitted as sonic sweeps from either side of the towfish simultaneously (2 beams). As the high-frequency acoustic beams interact with the seafloor, energy can be reflected back to the towfish, scattered, or absorbed by the seafloor. Signals recorded by the towfish are amplified and then recorded as reflected or backscattered acoustic energy. The backscatter record is affected by the towfish attitude, local geometry (incidence angle), the physical characteristics (microscale and mesoscale morphology), and the properties of the seafloor (composition and density) (Blondel and Murton, 1997).

High (Dual) Frequency digital SSS (100kHz and 500kHz) can give high-resolution images detecting objects on the sea floor ranging from 10's of cm's to 100 m in size. SSS can generate a clear acoustic picture of the seabed once several swaths are combined into a mosaic. The mosaics are overlapping swaths of side-scan data combined into a plan-view gray-scale acoustic image of the seafloor in which brightness is a function of backscatter strength (Schroeder et al., 1989). Since SSS is basically designed to report the strength of the echo or return, the harder the substrate, the harder and

stronger the return. Softer substrate (usually silts and clays) has a weaker return (Blondel & Murton, 1997). Shading intensity within the sonar mosaic thus indicates the difference in acoustic reflectance. In the present study, high reflectance is portrayed as dark (black) and low reflectance as lighter shades. Georeferenced images allow easy detection and location of morphological and sedimentological features (Kenny et al., 2003), and can yield resolutions of less than 1 m if the SSS fish is towed close to the seafloor (Valentine et al., 2003). Therefore, these devices are commonly used to detect and remotely characterize the seafloor and to discriminate different benthic habitats (Freitas et al., 2003). However, relying on acoustic reflectance alone is not sufficient to differentiate between bottom types due to the many variables that affect backscatter (Parker et al., 1992).

Chirp sonar sub-bottom profiling utilizes some of the same general principles as SSS but uses a lower frequency (4-24 kHz) to penetrate the subsurface and provides a vertical 2-D cross section of the sediment into the seabed. Boundaries between different sediment types produce an impedance contrast that reflects some fraction of incident sound back to the instrument (Larsen, 2002). Frequencies used for high-frequency Chirp systems allow for penetration of the top 1- 10m into the seafloor (depending on sediment type), but also allow for vertical resolutions of <1m. By lowering the frequency, penetration can be increased but resolution is decreased. The capacity of sound waves to penetrate into the seafloor is dependent on the type of sediment and pulse amplitude and frequency. Chirp subbottom profile data is useful in descriminating “hard-bottom”, i.e. shells, from other areas of finer material (Roberts et al., 1999). The depositional history

of the area can also be interpreted from a subbottom profile record (Roberts et al., 2000), if groundtruthing for sediment composition is concurrent.

Sampling and Analysis

Ten polygons, or blocks, were selected for seabed characterization with digital side-scan sonar. These blocks were originally chosen based on National Marine Fisheries Service (NMFS) historical snapper catch rates (1-high, 2-median, 1-low) as shown in Figure 3 (Patterson et al., in press). Additional sites were later selected based on their position in an artificial reef area (de-facto no trawl zone). Four research cruises, during 2001-2003, were conducted for survey and sampling. In August 2001, SSS surveys and boxcore sampling occurred aboard the R/V Carretta. This sampling trip was followed by a cruise aboard the R/V Acadiana in August 2002, which completed sampling at the previously surveyed areas (Blocks A, C, D, & G; Al'02). In the June 2003, a second SSS survey cruise (Blocks 1, 2, 3, 4, & 5) was conducted aboard the M/V Spree and then followed by a cruise aboard the R/V Acadiana in August of 2003 for boxcoring, chirp sonar subbottom data acquisition, and benthic photography.

The side-scan data were acquired with a Klein model 2260NV digital dual frequency (100/500 kHz) tow fish, a Klein T2100 transceiver, and a high-fidelity, low loss armored single conductor coaxial tow cable. The data were processed with a Triton-Elics system and exported as geo-referenced tagged image format (TIFF) files in UTM15, NAD27 format. To compress the large files for rapid loading in a GIS, but maintain the highest image quality, Multi-resolution Seamless Image Database (MrSID) files were also created (www.lizardtech.com). Bathymetric data were acquired using an Odum model precision depth recorder on the June 2003 survey.

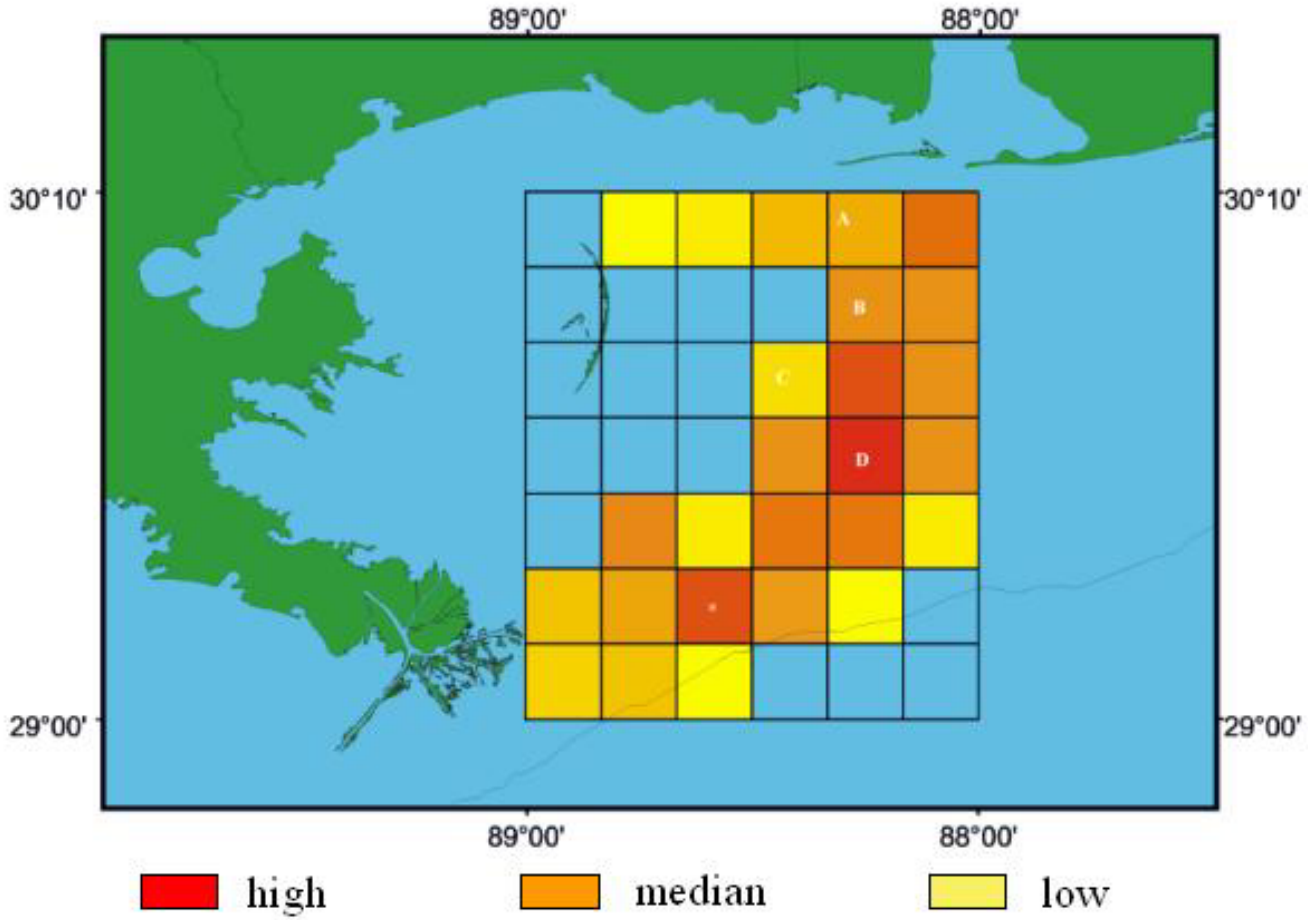

Figure 3. Historical Red Snapper Catch Densities from NMFS archive data (1991-2000). (From Patterson et al., in press)

Side-scan sonar was followed by ground-truthing with boxcore and sediment grab samples. Boxcores were taken with a 45 x 45 cm Ocean Instruments GOMEX cover using differential GPS positioning displayed directly over digitized side-scan mosaics. Sampling locations were chosen to characterize various patterns of reflectance in the side-scan data. At areas of harder substrate, poor boxcore penetration allowed collection of only surface grab samples. For cores that penetrated >15cm into muddy substrate, subcores were obtained by inserting a thin walled PVC pipe into the boxcore; subcores were extruded on deck at 2cm intervals and retained for later analysis. Samples for x-radiography analysis were also taken in the muddy cores. The X-radiograph samples were collected by inserting a thin-walled Plexiglas tray (2 cm thick, 15 cm wide, 40 cm long) into the sediment encased by the boxcore. They were brought back to LSU and X-rayed with a veterinary X-ray unit at 60 KeV and 125 & 150 mAs. The X-radiographs were scanned in using an Epson Expression 1640XL scanner with transparency unit and then converted into tiff files.

Chirp Subottom profiling data was collected in August 2003 aboard the R/V Acadiana. A Geostar Full Spectrum Sub-bottom Profiler was used at 20ms 2-10kHz in order to maximize penetration into hard substrate. Transects were chosen based on previously documented features and sonar reflectance bottom types. Profiles are reported in time (seconds). To calculate the depth scales for the profiles, the speed of sound through sediments was assumed to be comparable to the speed of sound through water, ~1500m/s (H.H. Roberts, personal communication). Therefore, 0.01 seconds (two-way travel time) converts to a vertical distance of 7.5 m.

A benthic camera system was also deployed in the August 2003 cruise and a series of photographic transects were made within the blocks to demonstrate the different bottom types and supplement physical sampling. The photographs are cross-sectional images of the sediment water interface. At all of these locations, GPS capture points were taken for referencing the data.

All cores were subsampled and analyzed for grain size, organic carbon content, and carbonate content. Sand:mud ratio was determined by wet-sieving dispersed sediments through a 63μm sieve. Muddy samples were also analyzed in a Micromeritics Sedigraph particle size analyzer for the fine fraction (Coakley and Syvitski, 1991). Organic content was measured by loss on ignition after 4 hours at 400 ˚C, and carbonate at 950˚C (Carver, 1971).

Processes of deposition and evidence of biological mixing have been evaluated through radioisotopic analysis, in conjunction with the study of sedimentary fabric and structures observed in X-radiographs. Subsamples for porosity and radioisotopic composition were extruded at 2 cm intervals in muddy cores. Radionuclide analysis was completed on a Canberra LeGe Gamma-Spectrometry system for the radioisotopes ^{210}Pb, ^{137}Cs, and ^{7}Be at sites with significant mud content. To estimate sedimentation rates and sediment flux on the time scale of ~100 yrs, ^{210}Pb (45.6 KeV; t ½ = 22 yrs), produced by natural decay of the ^{238}U-series, can be used (Appleby and Oldfield, 1979). Total ^{210}Pb activity within a sample includes the unsupported activity (input from atmospheric decay of ^{222}Rn) and supported (input from decay of ^{226}Ra and ^{222}Rn within sediments and rocks) (Noller, 2000). Total ^{210}Pb activity is directly measured on detectors and then the supported ^{210}Pb (assuming secular equilibrium with ^{222}Radon) is calculated from the

activities of ^{214}Pb ($t_{½}$ = 26.8 min; 295.2 KeV and 352 KeV peaks) and ^{214}Bi ($t_{½}$ = 19.7 min; 609 KeV peak). Total activity minus supported activity equals excess ^{210}Pb activity. By using $^{210}Pb_{ex}$, the presence or absence of new sediments can be measured. Used as an anthropogenic tracer, ^{137}Cs, was (661 KeV; t ½ = 30.7 yrs; MDA = 0.05 dpm/g) produced by atomic bomb testing and nuclear reactors. It was first introduced into the environment in ~1954, and enters the system through atmospheric fallout (Noller, 2000). In 1954, ^{137}Cs appears in the sediment record and can for that reason be an absolute age marker of sediments. A ^{137}Cs maximum can be recorded in sediments as a subsurface peak in activity and can be attributed to 1963, the time of peak atmospheric emissions (Noller, 2000). A natural radioisotope that is a useful tracer for river discharge on coasts where fluvial input is greater than atmospheric input (like the GOM) is ^{7}Be (477 KeV; t ½ = 53.3 d; MDA= ~0.3 dpm/g). Presence of ^{7}Be in sediments may indicate deposition of land-derived material deposited within months of core analysis (Sommerfield et al., 1999).

Four oyster shells from trawls at site G (Figure 1) were radiocarbon dated, in order to constrain ages of reef-like features observed in the areas. Additional samples from the shallow site (block A) were also considered but due to the bored and encrusted nature of the shells, they were judged not suitable for testing. Accelerator mass spectrometry techniques were utilized (Stuvier and Reimer, 1993). To help avoid contamination and provide the most pristine sample possible, the oysters were first sliced open and samples from the unaltered shell interior were selected for dating. These shell samples were sent to the University of Arizona AMS lab for analysis. The dates were

corrected and calibrated using the marine database, methods, and software set forth by Stuiver and Reimer (1993) found online at **www.calib.org**.

RESULTS

Geologic and Geoacoustic Results

Block A & Block 5

Sonar data from block A display highly reflective linear features approaching 700 m long (Figure 4) with widths 50-100 m and oriented NW-SE. Grain size results for Block A indicate that at least 70% of all sediment collected at each location is greater than 63μ (Figure 5). Sites along the shelly linear features exhibit a carbonate content of over 50%, while muddy sand regions immediately adjacent have carbonate content of less than 10% (Figure 6 and Table 1).

Block 5 is located immediately east of block A. Because of their close proximity and constraints on time, this block was not sampled and is assumed to be geologically similar to block A. This block shows similar reflectance patterns with highly reflective linear features trending NW-SE. Bathymetric data obtained from the fathometer indicate that these features have 0.5-1m of vertical relief compared with the rest of the seabed.

When several sidescan sonar survey lines (swaths) are combined to create a mosaic, the ship's path and overlap of the swaths are evident in the image. The long linear horizontal lines that are present in the entire length of the sonar mosaics are merely artifacts of collection and processing rather than seabed features with differing acoustic properties (Blondel and Murton, 1997).

Block C

Block C has what appears to be a homogenous bottom reflectance (Figure 7). Block C has an overall sand fraction greater than 70% (Figure 8 and Table 2). Very few shells are apparent at this site. The carbonate content does not exceed 15% in this

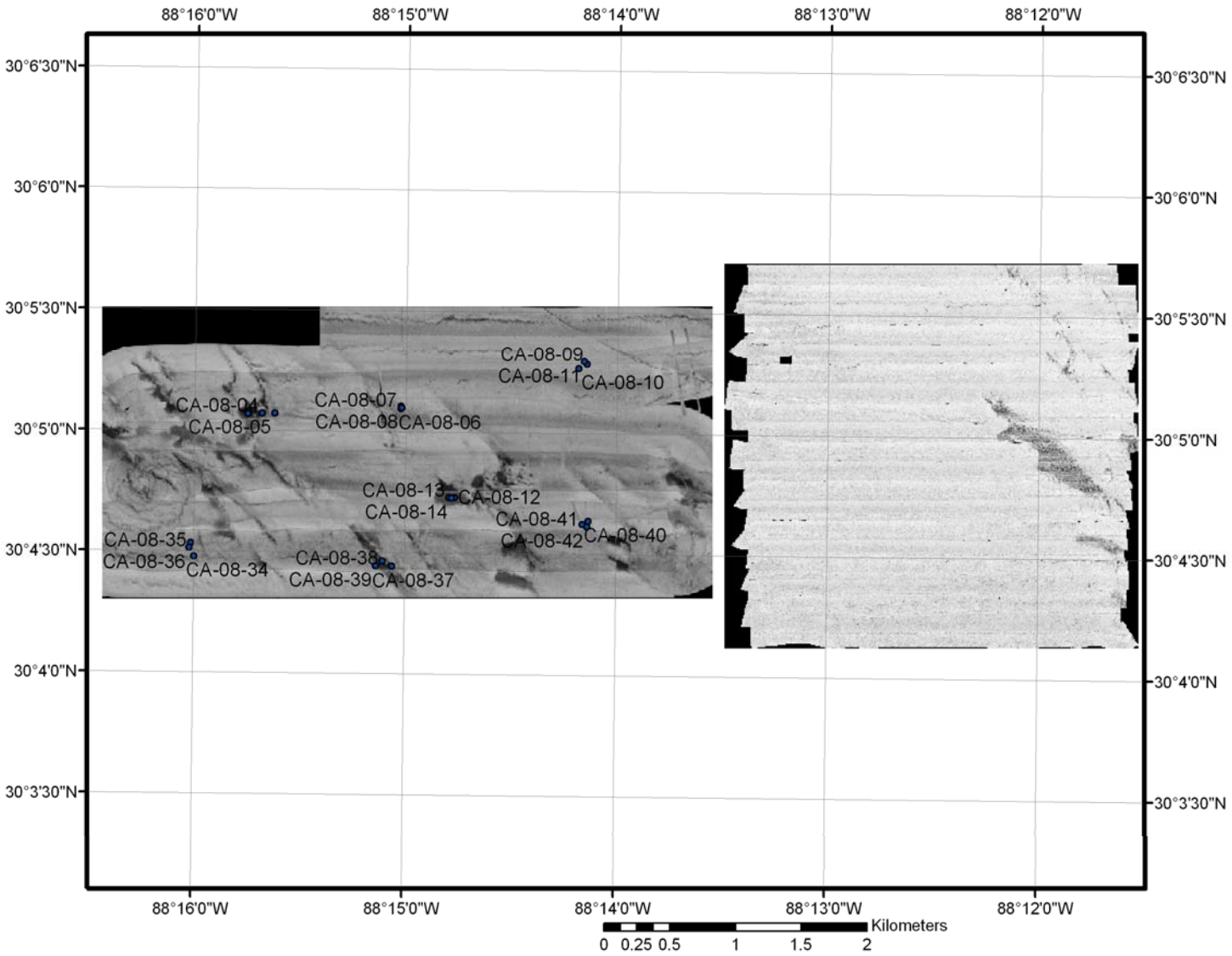

Figure 4. Sidescan sonar mosaic of blocks A & 5. Core locations and names are displayed. Darker linear NW-SE trending features are areas of higher reflectance while lighter gray areas indicate low reflectivity.

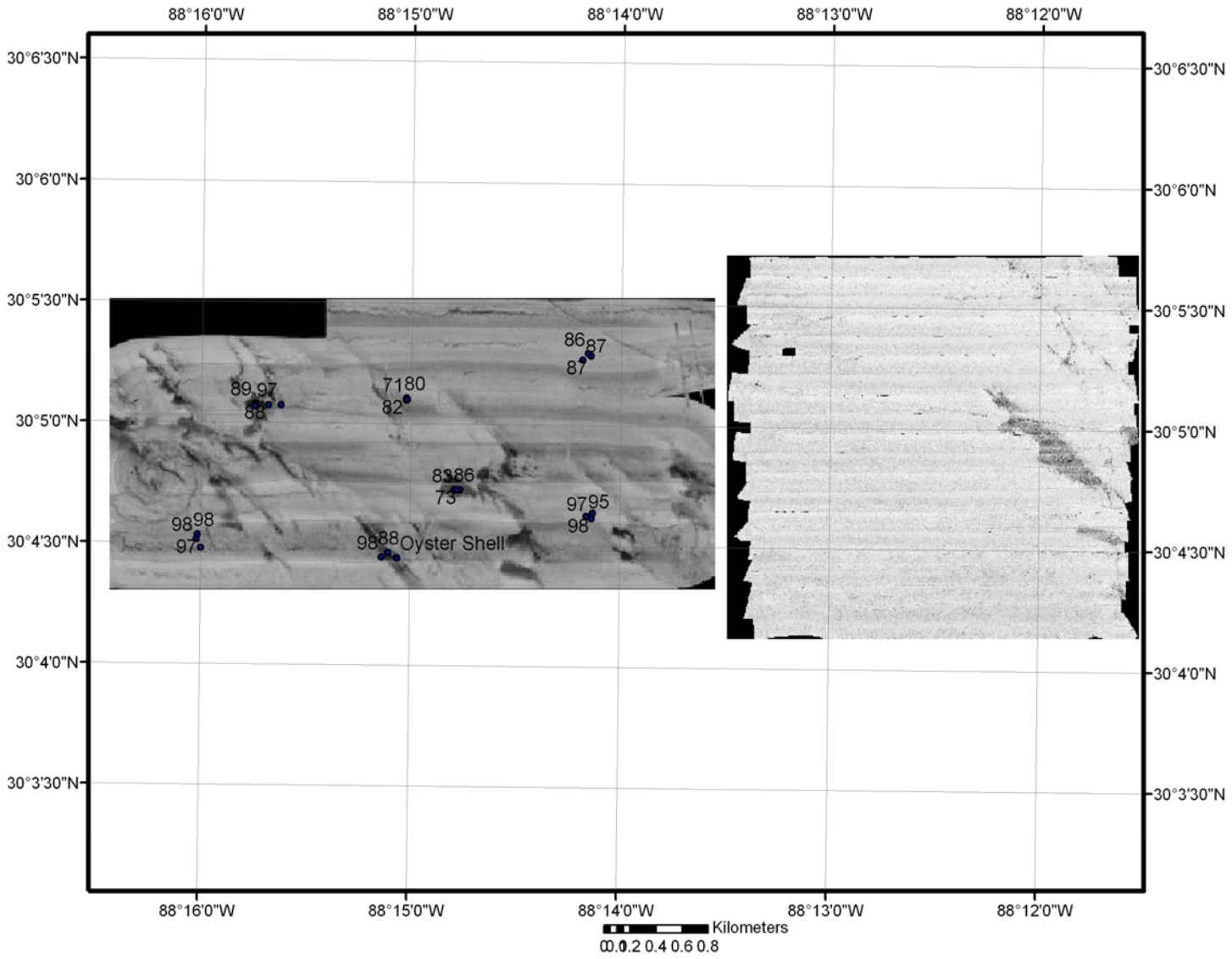

Figure 5. Sidescan sonar image of Blocks A & 5. Values shown represent the fraction of the sample that has a grain size >63µ.

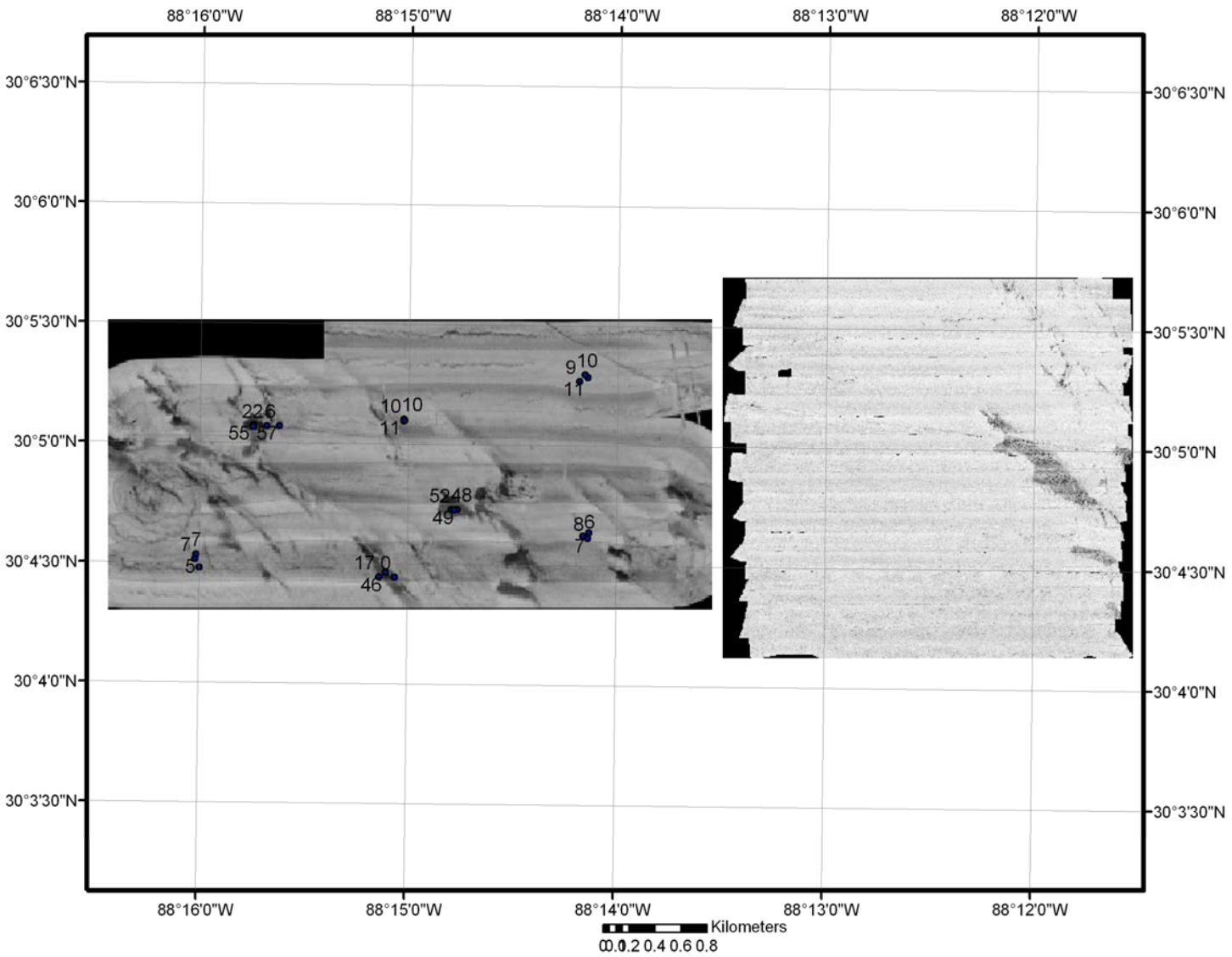

Figure 6. Sidescan sonar image of Blocks A & 5. Sample locations are represented by circles and values refer to the % carbonate content at each location.

Table 1. Physical properties of sediments from blocks A & 5.

Core-ID	% sand	% mud	% CO3	Facies
CA-08-02	89.0	11.0	57.3	shell
CA-08-03	87.8	12.2	55.3	shell
CA-08-04	87.8	12.2	22.0	shell
CA-08-05	96.6	3.5	6.3	sand
CA-08-06	82.5	17.6	10.6	sand
CA-08-07	79.5	20.5	9.9	sand
CA-08-08	70.7	29.3	9.9	sand
CA-08-09	86.7	13.4	10.7	sand
CA-08-10	87.2	12.8	9.0	sand
CA-08-11	85.7	14.3	10.1	shell
CA-08-12	72.7	27.3	48.6	shell
CA-08-13	85.8	14.3	47.9	shell
CA-08-14	83.0	17.0	52.0	sand
CA-08-34	97.0	3.0	5.1	sand
CA-08-35	98.0	2.0	7.2	sand
CA-08-36	98.4	1.6	7.4	shell
CA-08-37	Oyster Shell			shell
CA-08-38	88.4	11.7	46.4	shell
CA-08-39	98.2	1.9	17.1	sand
CA-08-40	97.7	2.4	6.8	sand
CA-08-41	95.3	4.7	6.4	sand
CA-08-42	96.6	3.4	7.9	sand

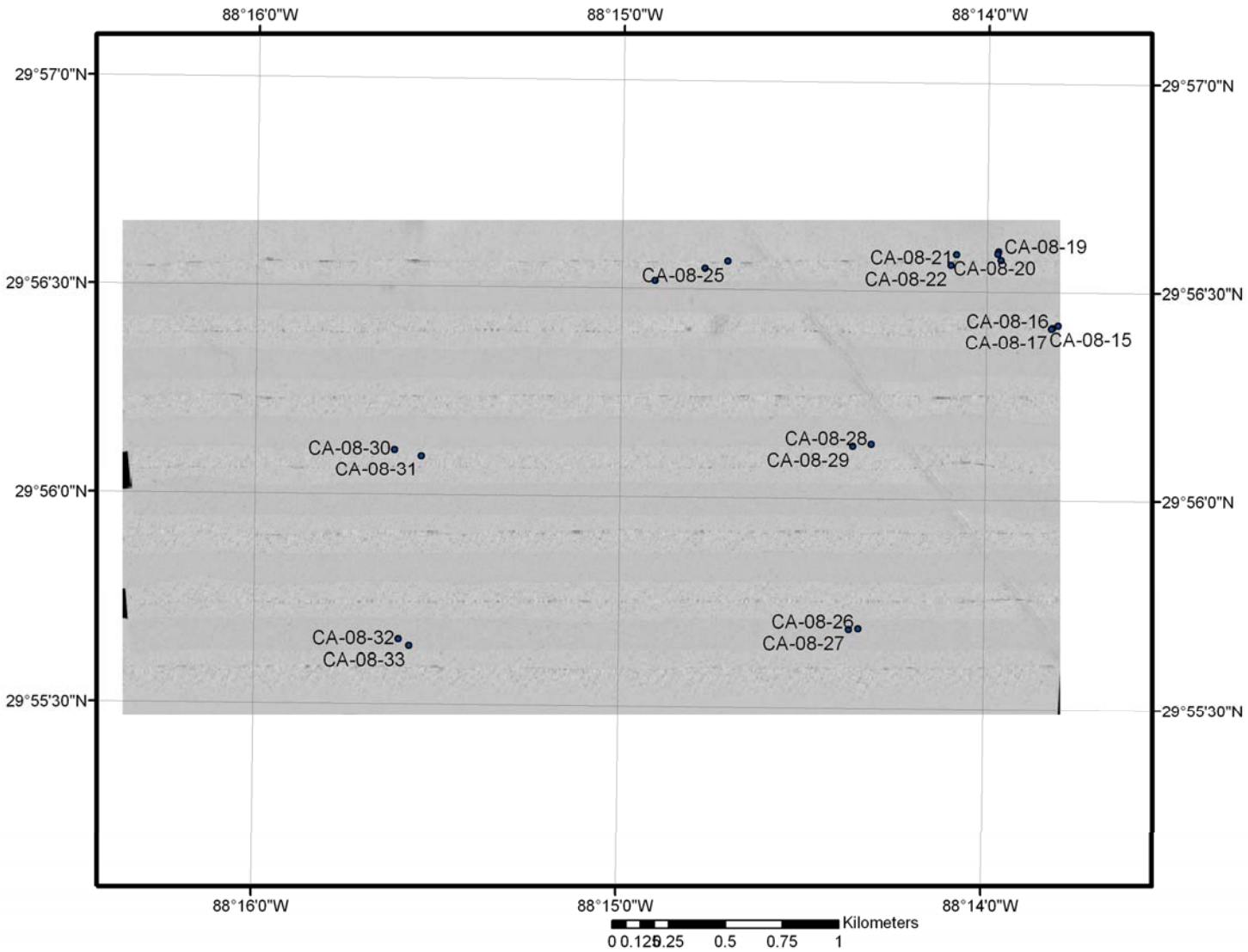

Figure 7. Sidescan sonar mosaic of block C. Core locations and names are displayed. A pipeline in visible in the eastern part of the block. Gray shade refers to low reflectance.

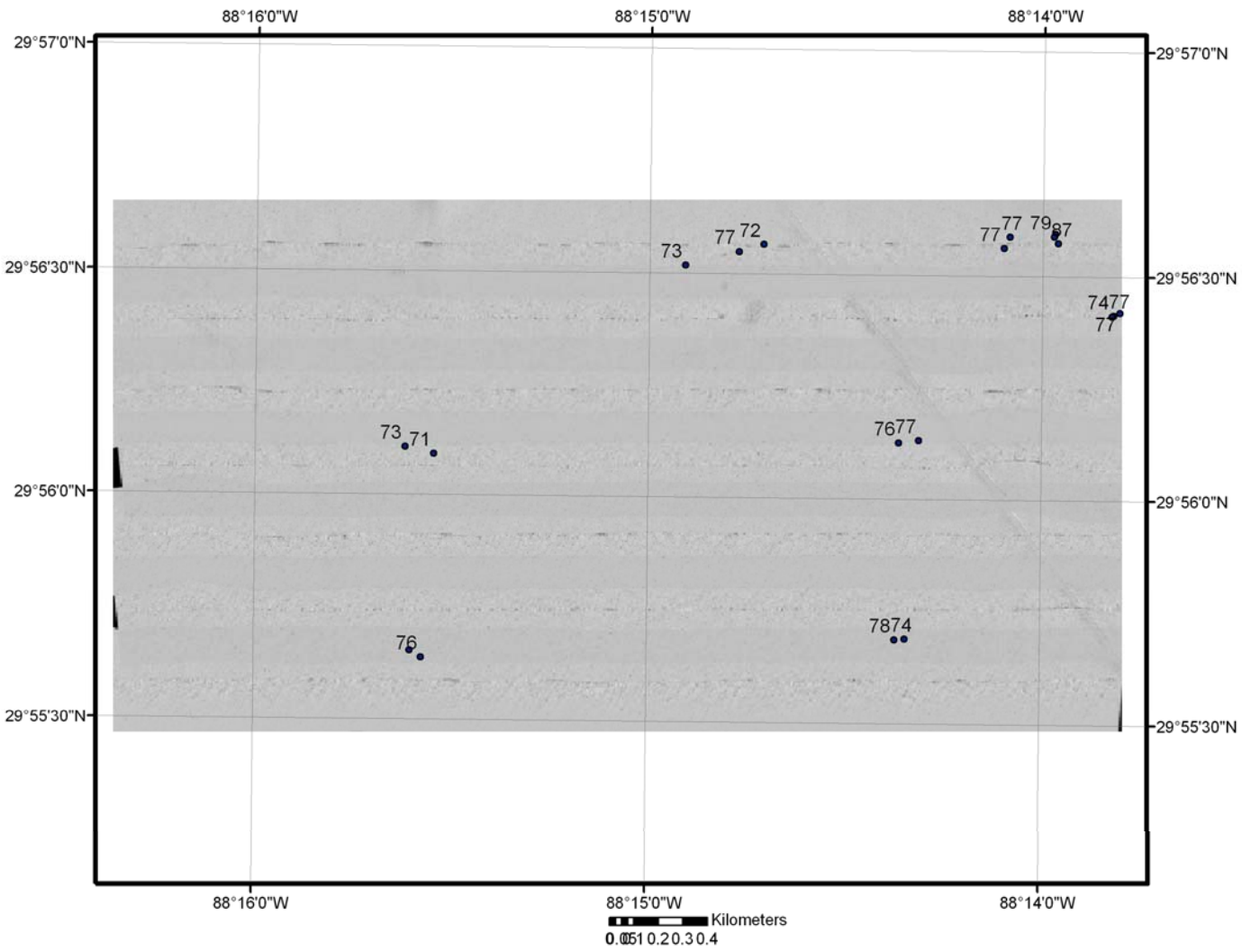

Figure 8. Sidescan sonar image of Block C. Sample locations are shown by circles and values refer to percent of the sample with a grain size >63µ. Pipeline seen in eastern portion of this block.

Table 2. Physical properties of sediments from block C.

Core-ID	% sand	%mud	% CO3	Facies
CA-08-15	76.9	23.1	13.1	sand
CA-08-16	76.5	23.5	13.6	sand
CA-08-17	74.1	25.9	14.4	sand
CA-08-18	80.9	19.1	12.9	sand
CA-08-19	87.0	13.0	12.4	sand
CA-08-20	79.1	20.9	14.8	sand
CA-08-21	76.6	23.5	12.7	sand
CA-08-22	77.1	22.9	14.1	sand
CA-08-23	72.7	27.3	13.1	sand
CA-08-24	77.2	22.8	14.1	sand
CA-08-25	71.5	28.5	14.6	sand
CA-08-26	73.9	26.1	14.4	sand
CA-08-27	78.2	21.8	11.3	sand
CA-08-28	77.4	22.6	12.4	sand
CA-08-29	76.4	23.6	12.0	sand
CA-08-30	73.2	26.8	14.2	sand
CA-08-31	71.4	28.6	14.2	sand
CA-08-32	65.4	34.6	15.0	sand
CA-08-33	76.3	23.7	13.7	sand

location (Figure 9). The long linear feature seen in the eastern portion of the block is a pipeline. No chirp profiles were collected in this region.

Block D

Block D has a pattern of homogenous bottom reflectance that appears similar to Block C (Figure 10). However, the seabed is predominately sandy mud, with sand content <30% (Figure 11) and carbonate content <11% (Figure 12). Further descriptions concentrate on a transect across the center of the block incorporating cores D2A, D4A, and D6B (Figure 10). Block D X-radiographs indicate areas of highly bioturbated muddy sediment with minimal shell fragments in the western core locations (Figure 13). The D6 X-radiograph shows relatively little low-density (muddy) material which appears as the darker areas in the X-radiograph (Figure 13). High-density material (bright areas from increased sand and shell content) becomes more prevalent in x-radiographs to the east.

Gamma spectroscopy indicates the presence of ^{137}Cs and $^{210}Pb_{ex}$ in all cores analyzed. The penetration depths of the cores range from 20cm on the western side of the site to 16 cm in the eastern side of the site. In most cores, ^{137}Cs penetrates only the top 6 cm. In all samples analyzed, ^{7}Be is below detection limits (MDA=~0.3 dpm/g).

Sedigraph results along with sand:mud ratios (Figure 11 and Table 3) show a coarsening trend towards the east. Percent sand content (>63μ) increase from 35% (D2A) in the western portion of the block to >70% (D6B) in the eastern part of site D. Mass frequency distributions (Figure 14) for sand, silt, and clay for a transect through the center of this block reflect these same trends with sand content increasing and clay content decreasing towards the east.

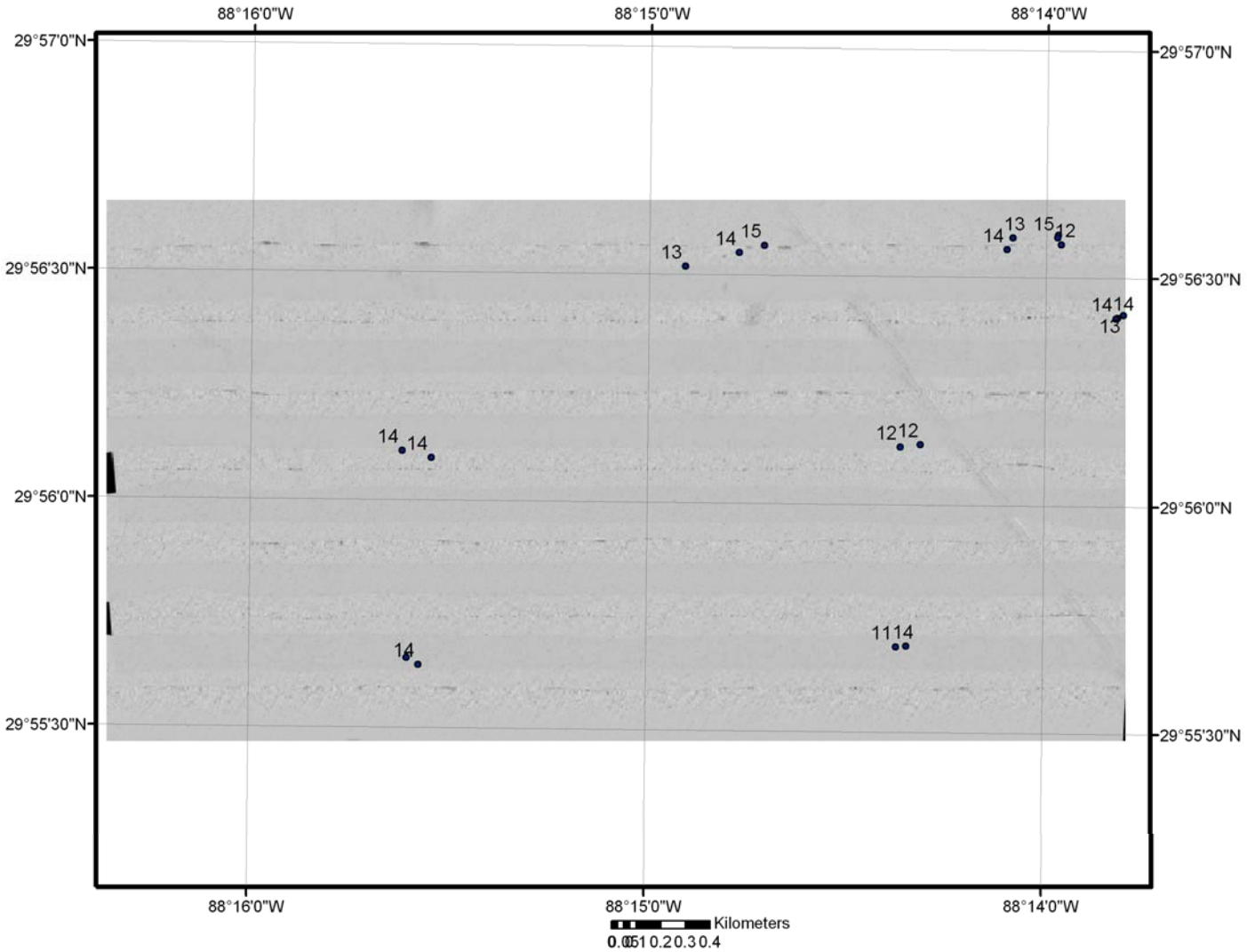

Figure 9. Sidescan sonar image of Block C. Values shown are % carbonate content of surficial sediments. Pipeline located in eastern portion of block.

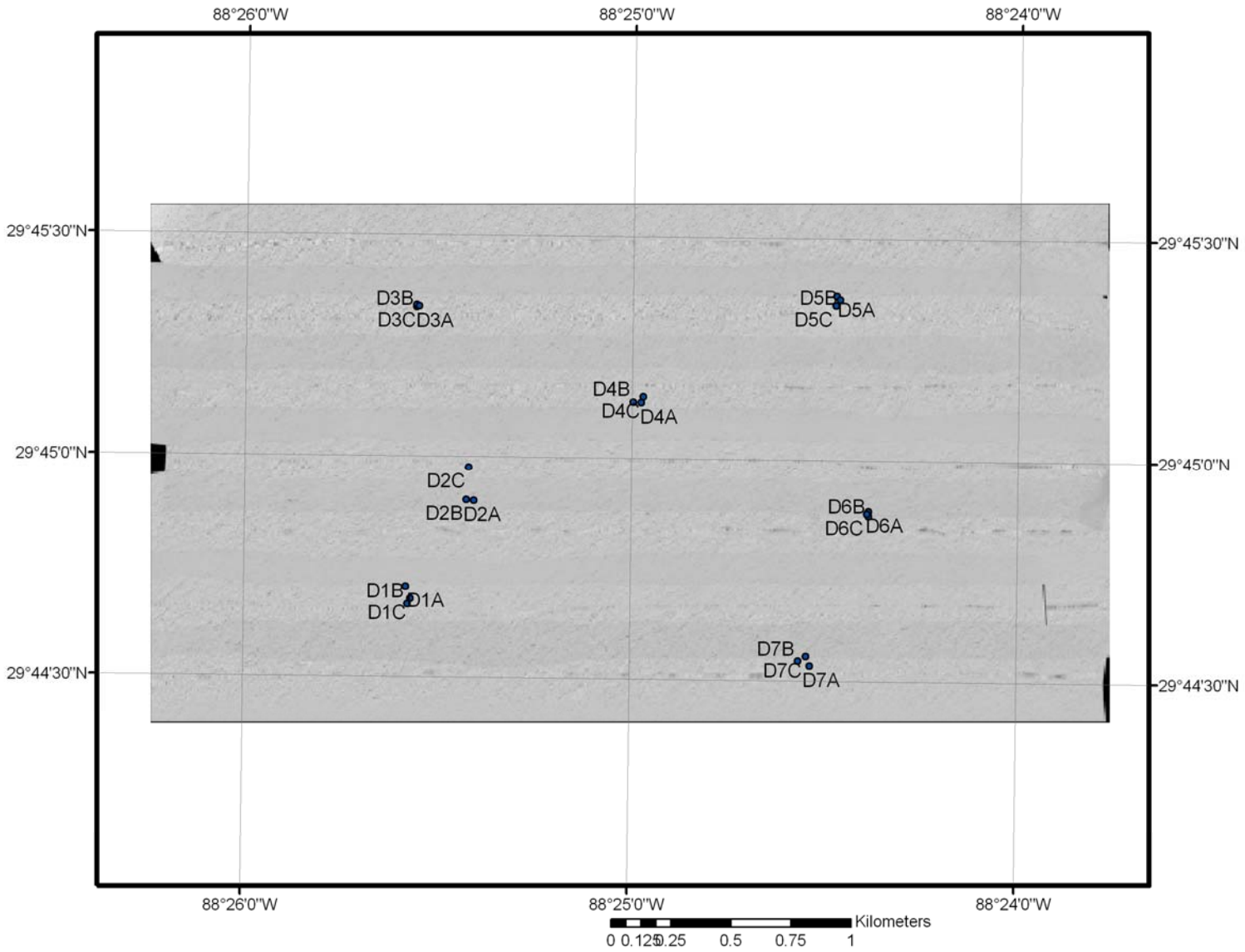

Figure 10. Sidescan sonar mosaic of block D. Core locations and names are displayed. Gray shade indicates low reflectivity.

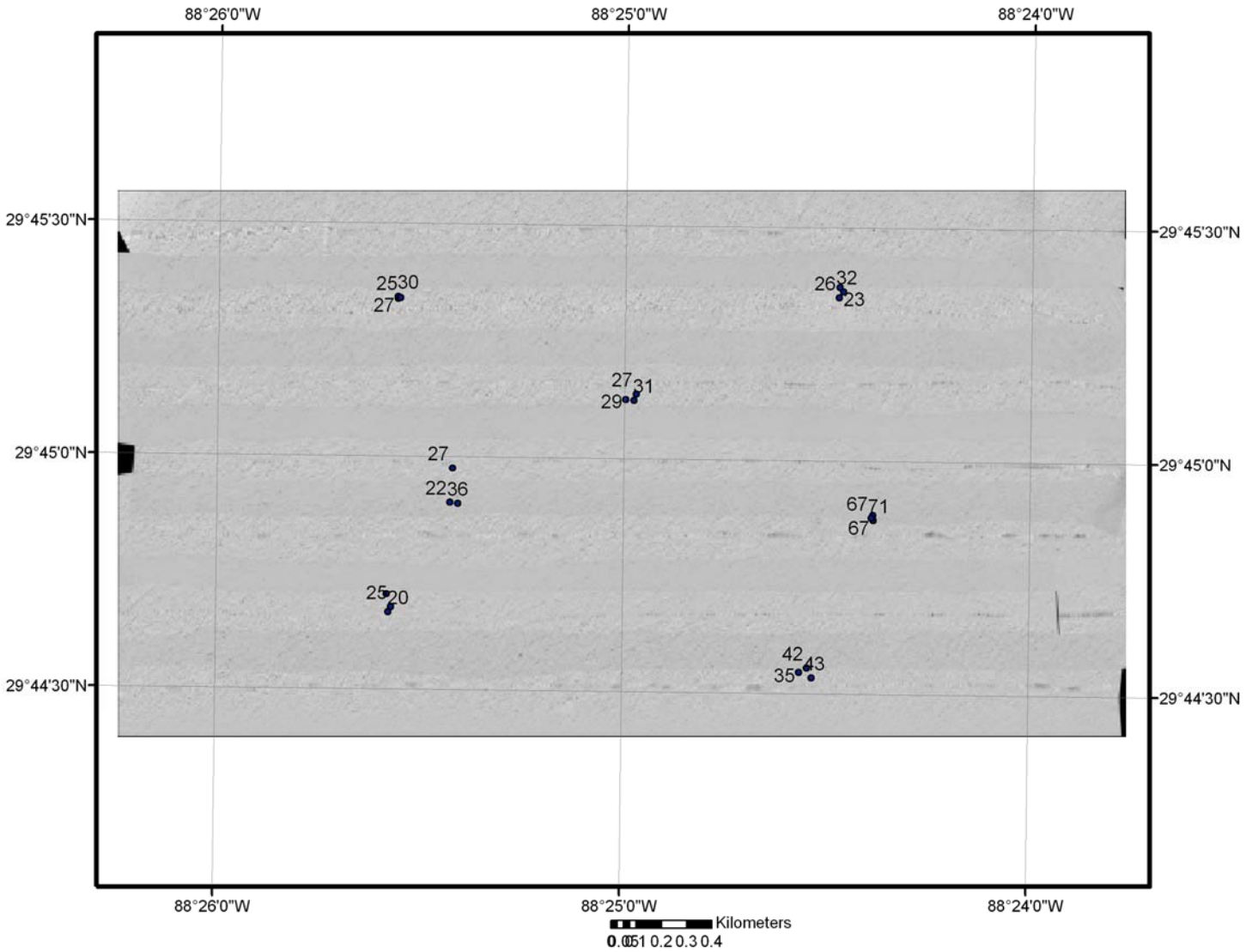

Figure 11. Sidescan sonar image of Block D. Values shown represent the fraction of sample with grain size >63µ.

Figure 12. Sidescan sonar image of Block D. Values shown represent % carbonate content of surficial sediments.

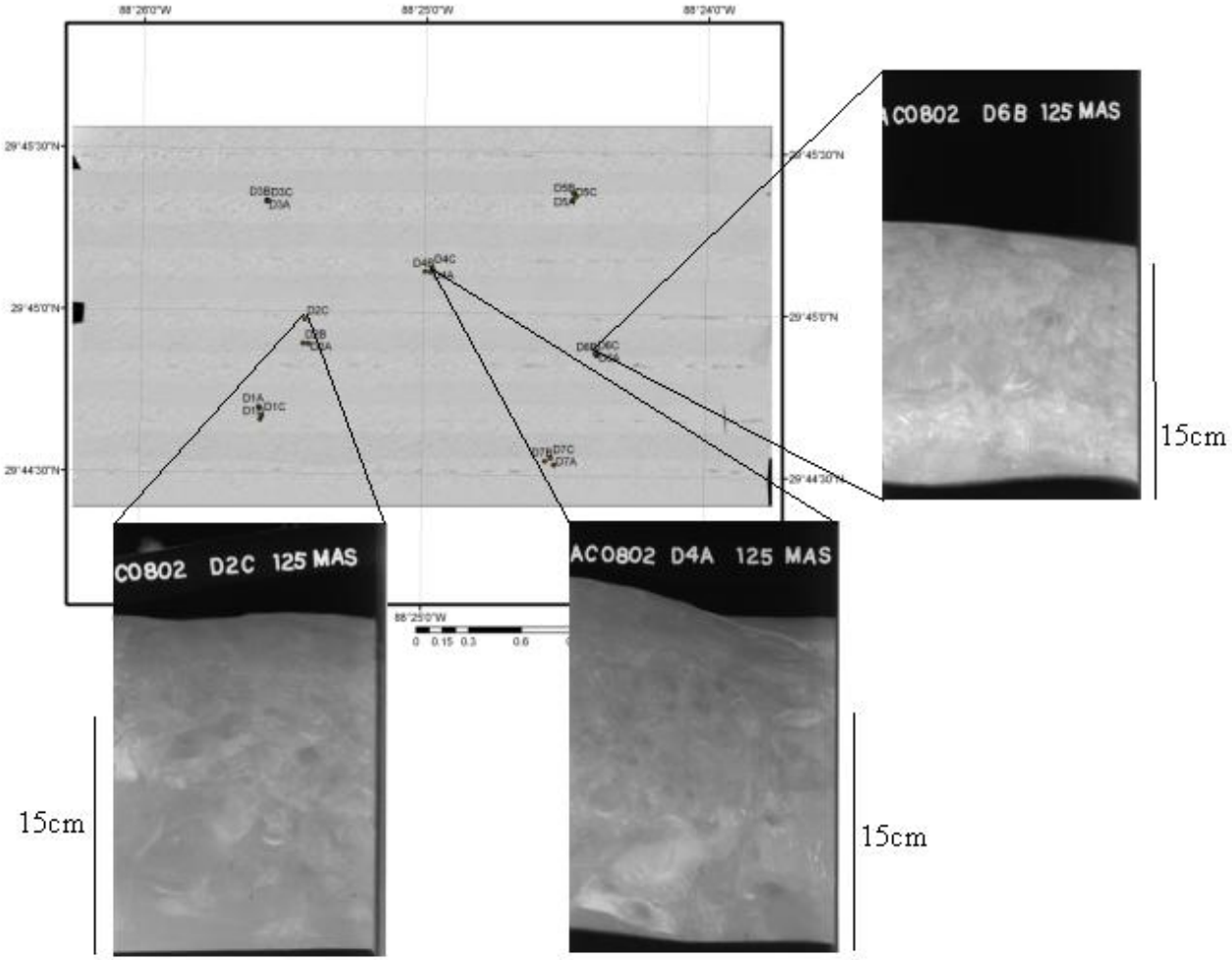

Figure 13. Sonar Image of Block D with X-radiography images and their core locations.

Table 3. Physical properties of sediments from block D.

Core-ID	% sand	%mud	% CO3	Facies
D1A	33.6	66.4	8.5	mud
D1B	19.7	80.3	9.5	mud
D1C	25.3	74.7	9.0	mud
D2A	36.1	63.9	9.7	mud
D2B	21.9	78.1	10.2	mud
D2C	27.3	72.7	10.5	mud
D3A	27.2	72.8	9.4	mud
D3B	29.8	70.2	10.2	mud
D3C	24.6	75.4	10.5	mud
D4A	30.9	69.1	8.6	mud
D4B	29.2	70.8	8.0	mud
D4C	27.3	72.7	8.9	mud
D5A	23.1	76.9	9.5	mud
D5B	32.5	67.6	10.0	mud
D5C	25.6	74.4	9.6	mud
D6A	67.0	33.0	7.0	mud
D6B	70.9	29.1	7.0	mud
D6C	67.1	32.9	8.5	mud
D7A	42.7	57.4	9.3	mud
D7B	34.8	65.2	10.8	mud
D7C	41.5	58.5	9.2	mud

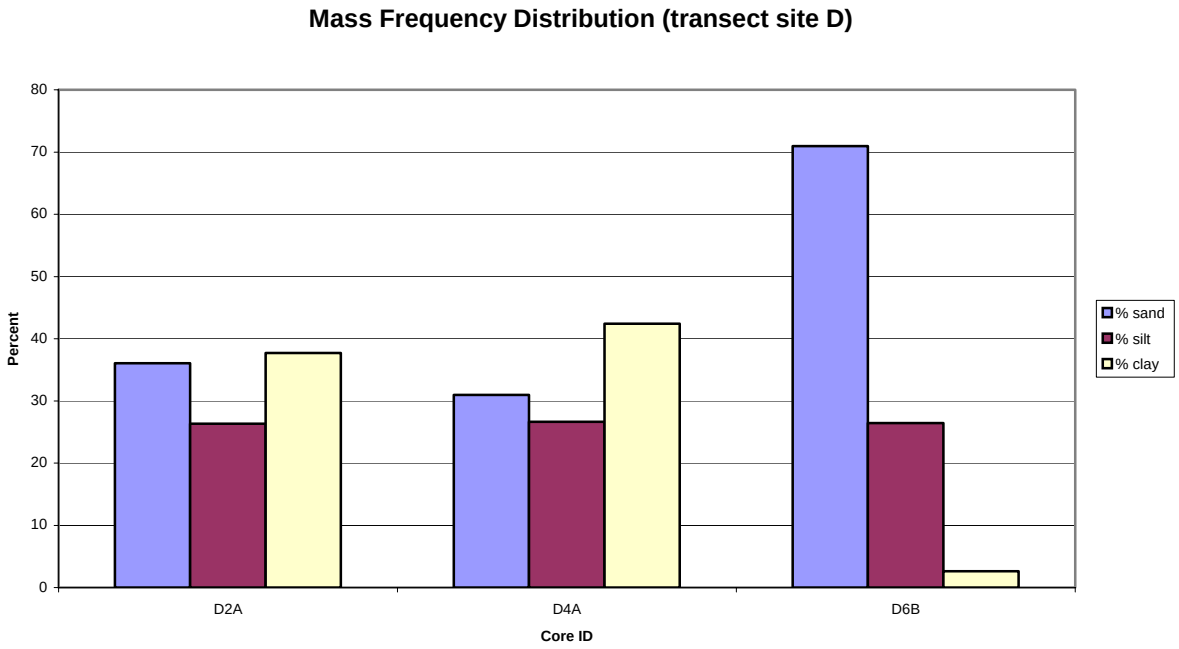

Figure 14. Mass frequency distribution of %sand, %silt, & %clay content in a west to east transect through site D. (see figure 10 for exact core locations)

Chirp subbottom data indicate a thin acoustically transparent veneer with reflectors present (Figure 15). This cover is wedge shaped and appears to terminate against the seabed towards the east. The sediment wedge downlaps onto a hard reflector that is evident at depth to the west and at the surface to the east. The wedge thins from west to east and nearly horizontal reflectors can be seen in the profile. Figure 16 shows an expanded view of this sediment wedge in block D.

Block G

Block G exhibits reflectance patterns similar to Block A, with large, dark, highly reflective features (Figure 17) within a matrix of low and fairly uniform reflectance. NW-SE trending ridges are also apparent but are less prominent than the large patches of highly reflective material. The sand content in all samples is >80%, including coarse shelly debris (Figure 18 and Table 4). Shells from this region comprise both marine and estuarine taxa, including clumps of disarticulated valves of *Crassostrea virginica*, the American oyster. Carbonate content varies from >40% in highly reflective regions to <7% in regions of low reflectance (Figure 19). The highly reflective areas exhibit 1-2 m of vertical relief. Chirp data from this region shows chaotic reflectors at the sea surface with little penetration into the sub-surface where the surface reflectivity is high (Figure 20). Locally, areas of the seabed permit some acoustic penetration and this slightly acoustically transparent material has a hard surface reflector similarly seen in blocks 3 and 4. A series of oyster shells were ^{14}C dated from this area and the values (both radiocarbon ages and calendar ages) are contained in Table 8. Corrected and calibrated dates from oyster shells found at the 40 m isobath range from between 9000-11,000 ybp.

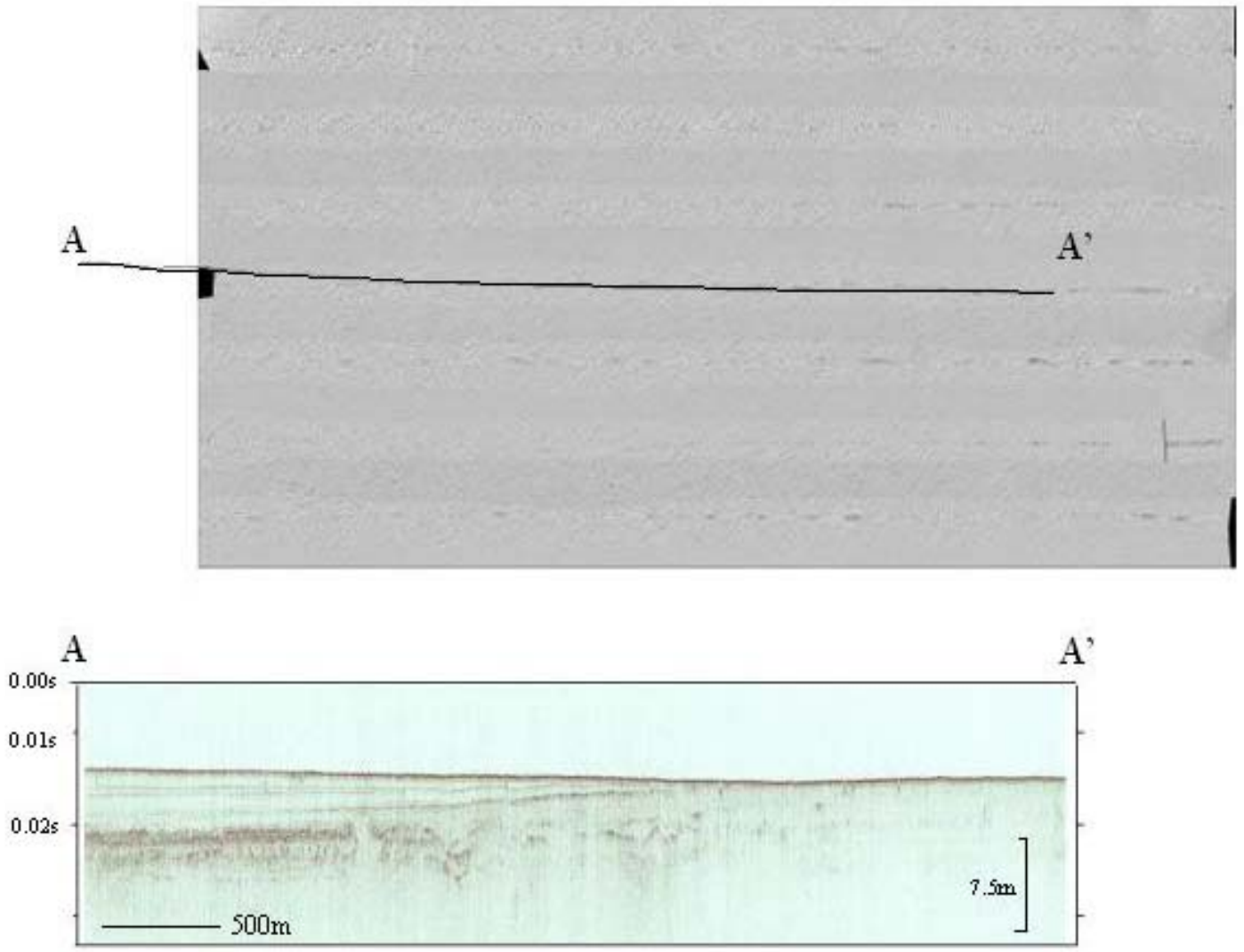

Figure 15. Sidescan sonar image of Block D with the location of the chirp profile. The length of this profile from A-A' is 3.8 km. Times are in two way travel time.

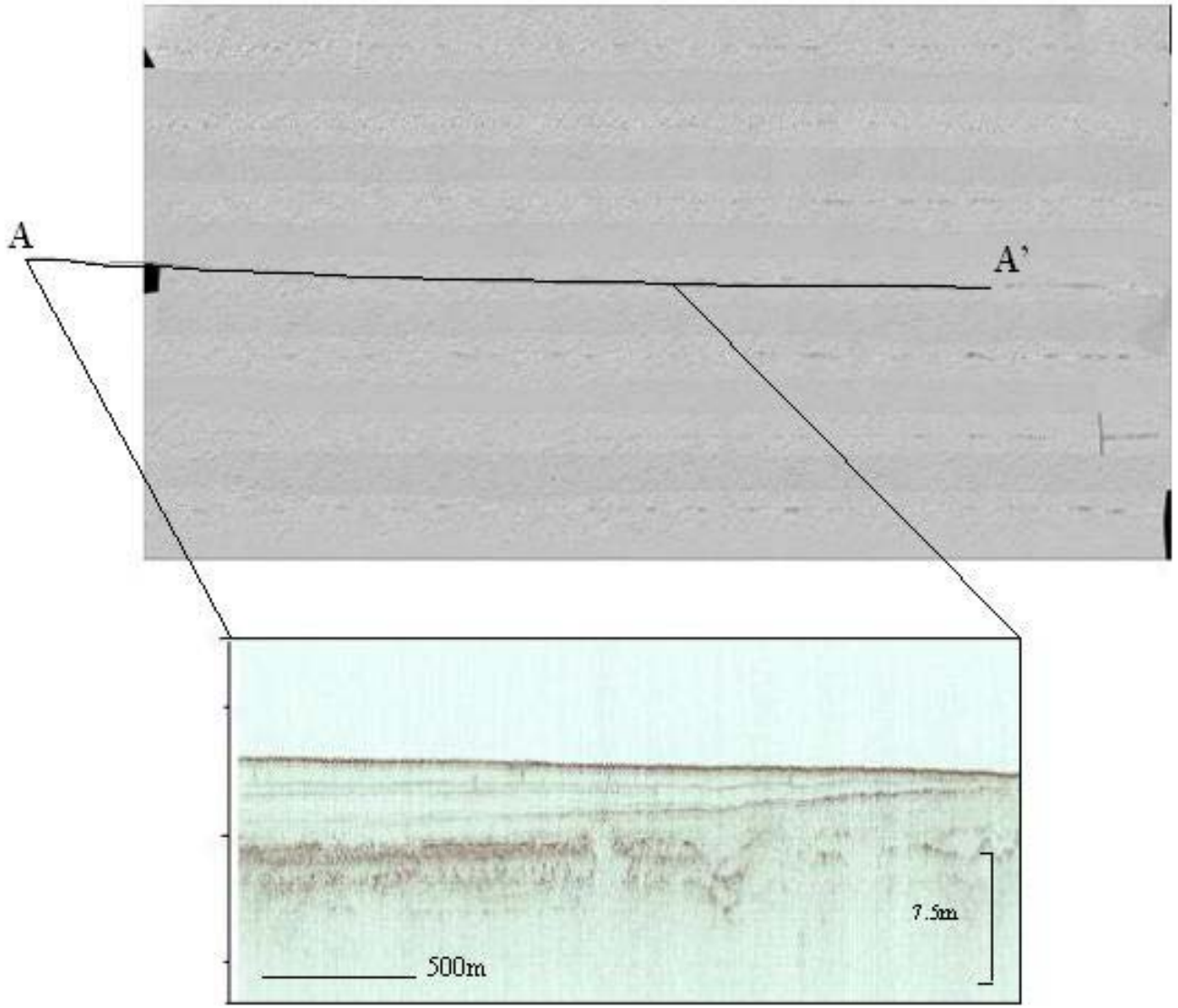

Figure 16. Zoomed in view of the acoustically transparent wedge of sediment at site D.

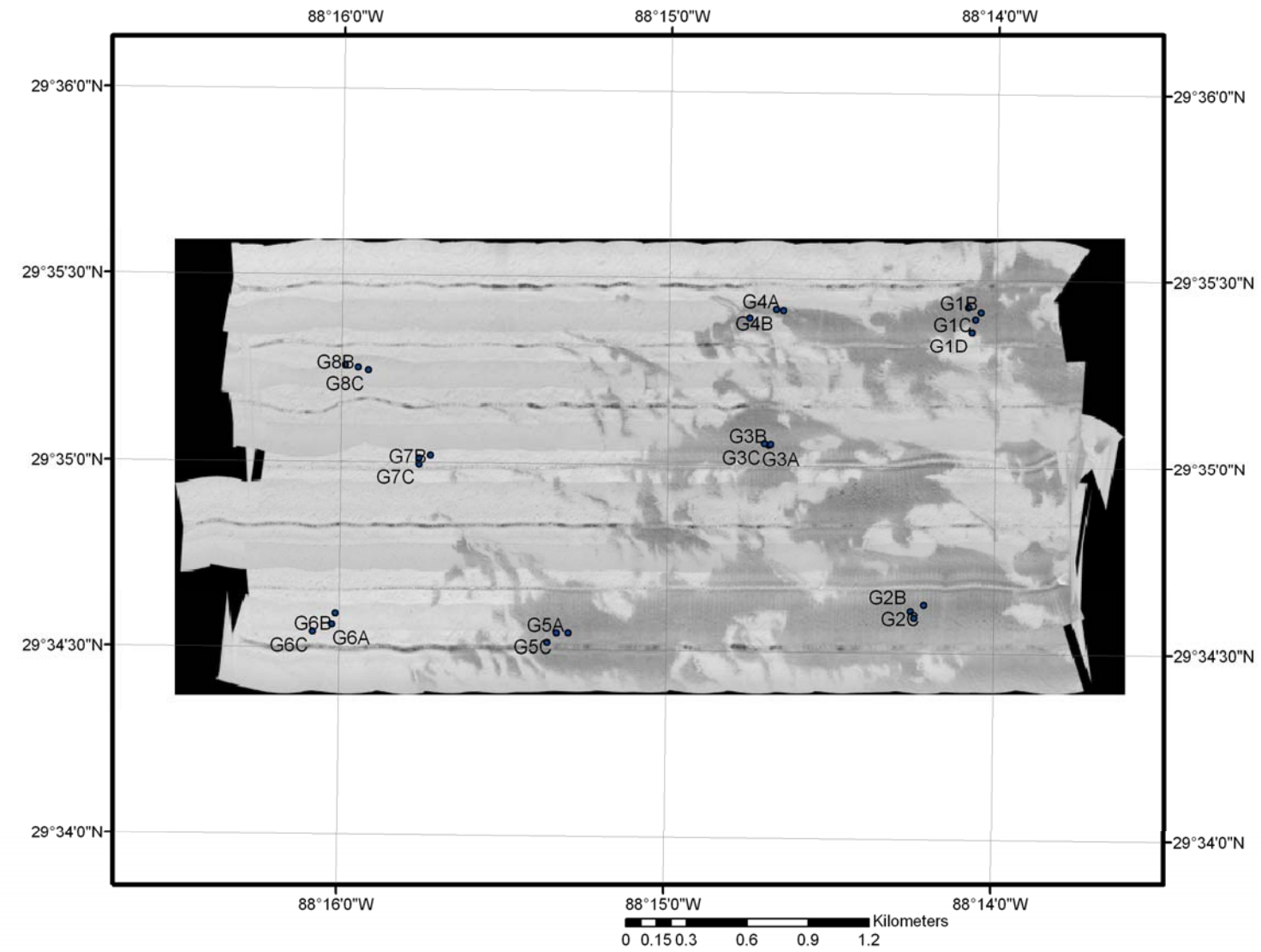

Figure 17. Sidescan sonar mosaic of block G. Core locations and names are displayed. Large patches and linear features of darker shades represent highly reflective features, the remaining lighter gray indicates low reflectivity.

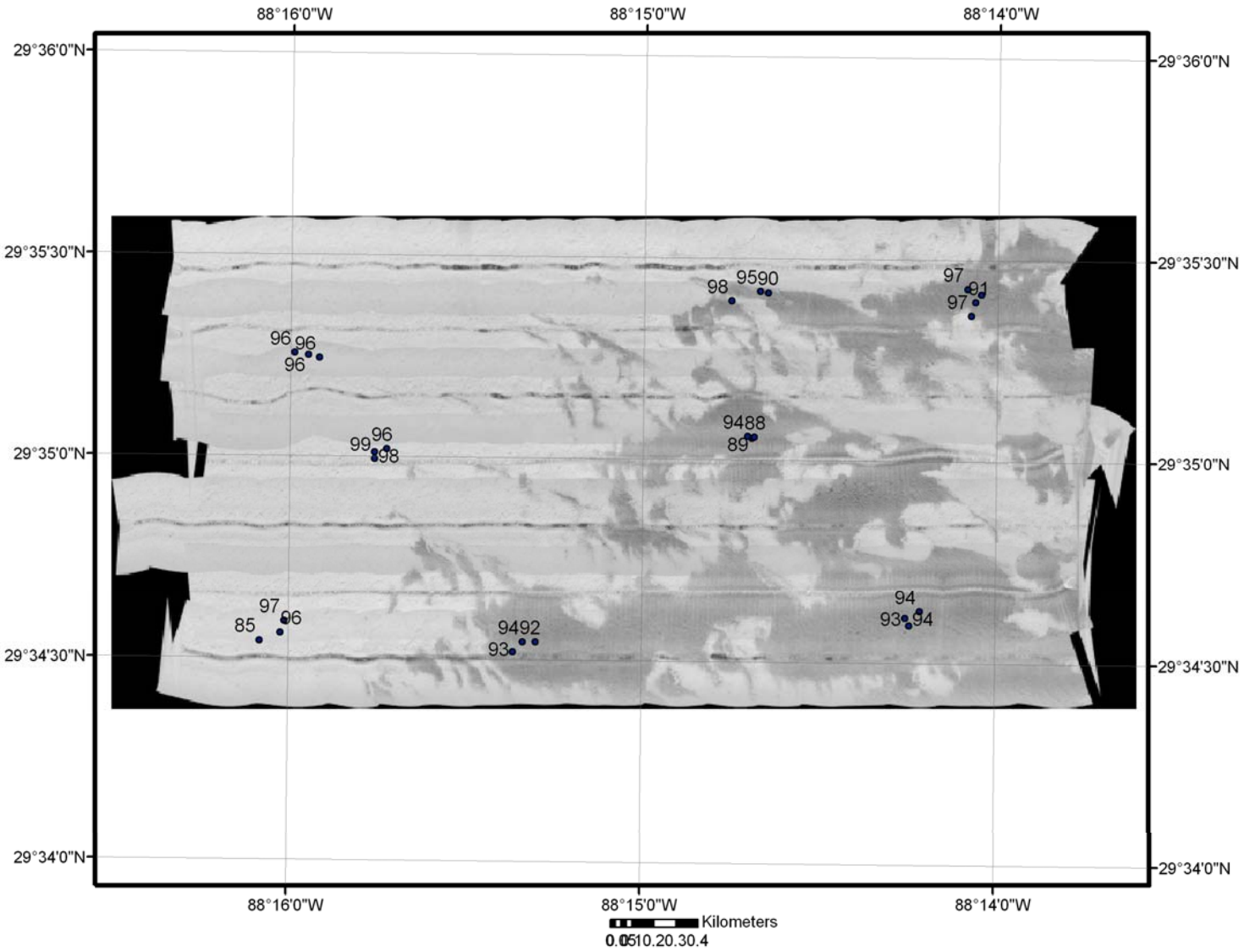

Figure 18. Sidescan sonar image of Block G. Values shown represent to fraction of the sample with a grain size >63µ.

Table 4. Physical properties of sediments from block G.

Core-ID	% sand	%mud	% CO3	Facies
G1A	97.1	3.0	54.4	shell
G1B	89.5	10.5	48.6	shell
G1C	91.2	8.8	50.3	shell
G1D	97.5	2.5	5.9	sand
G2A	93.9	6.1	50.7	shell
G2B	92.9	7.1	45.7	shell
G2C	94.0	6.0	46.6	shell
G3A	89.0	11.0	43.3	shell
G3B	88.0	12.0	43.5	shell
G3C	93.7	6.3	48.1	shell
G4A	89.8	10.2	45.1	shell
G4B	95.3	4.7	49.4	shell
G4.5A	97.6	2.4	5.5	sand
G5A	91.7	8.4	45.4	shell
G5B	93.4	6.6	41.3	shell
G5C	93.6	6.4	47.3	shell
G6A	95.8	4.3	4.1	sand
G6B	96.5	3.5	3.5	sand
G6C	84.7	15.3	4.3	sand
G7A	98.4	1.6	10.3	sand
G7B	96.4	3.6	5.3	sand
G7C	98.6	1.4	6.9	sand
G8A	95.6	4.4	4.7	sand
G8B	95.5	4.5	4.8	sand
G8C	96.1	4.0	5.9	sand

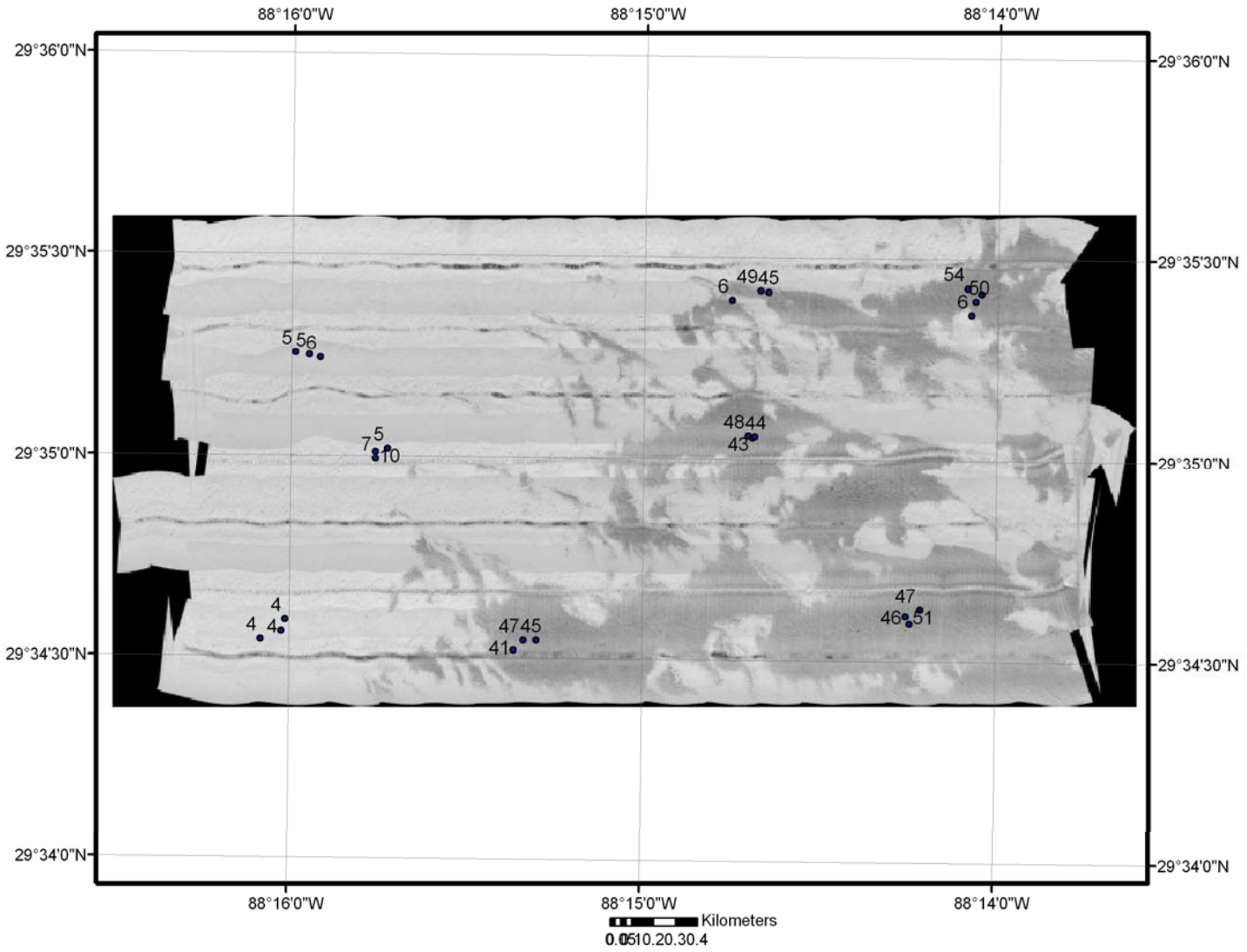

Figure 19. Sidescan sonar image of Block G. Circles represent sample locations and the values are % carbonate content.

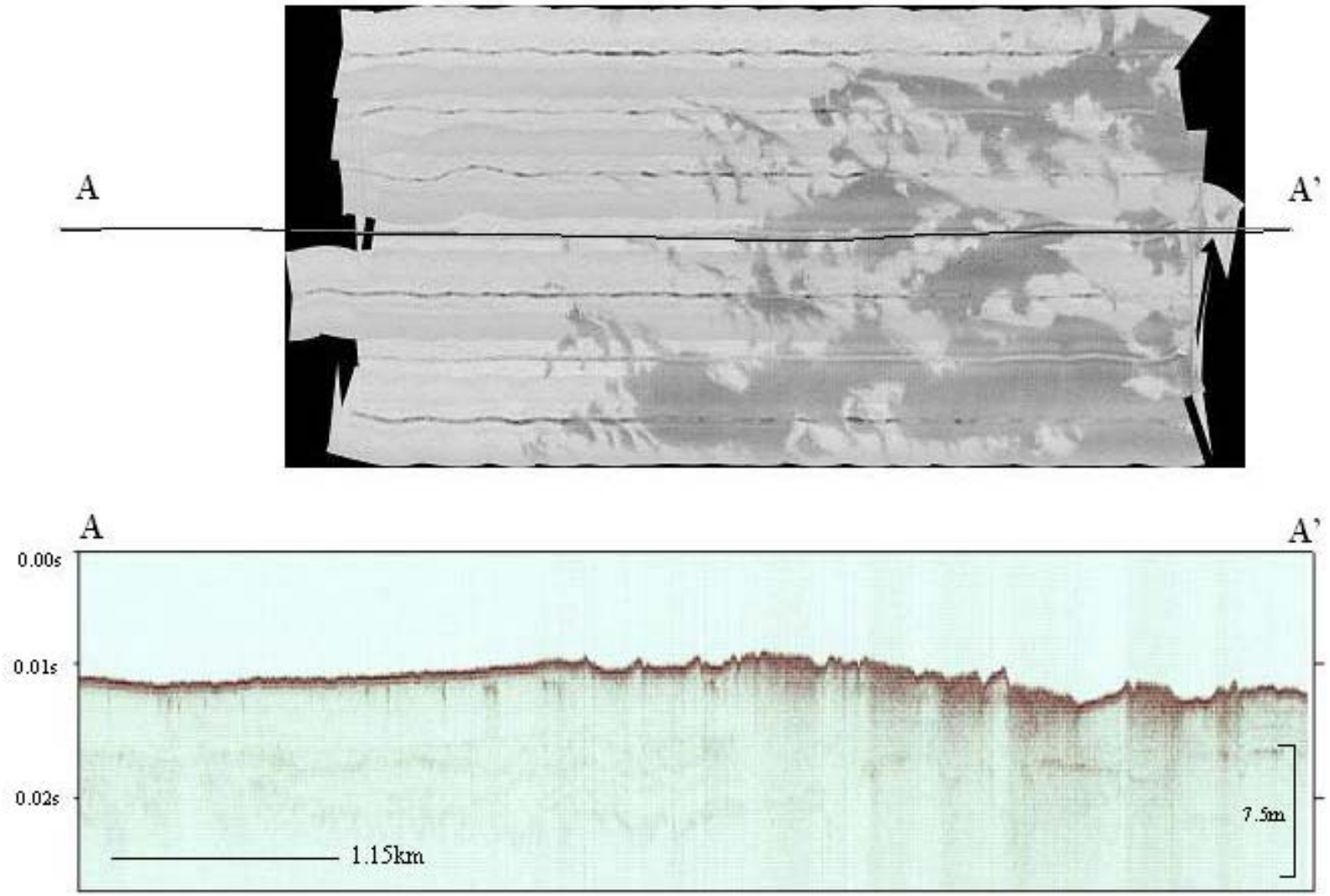

Figure 20. Sidescan sonar image of Block G. The location of the chirp profile is shown as A-A'. The length of this line is 6.2 km. Times are listed in two way travel time.

Block 1

Block 1 exhibits linear and patchy highly reflective regions. The linear features trend NW-SE (Figure 21), similar to blocks A, 2, and Al'02. Some of the highly reflective regions within the sidescan appear to resemble dendritic patterns. Sand content exceeds 90% at most locations (Figure 22 and Table 6). Highly reflective regions are shell hash with a carbonate content greater than 35 %, while the core in the low reflective region (lighter color) consists of muddy sand with a carbonate content less than 10% (Figure 23). These highly reflective regions (darker shades) exhibit 1-2 m of vertical relief from the surrounding seafloor as seen from bathymetric data. Benthic profiling camera pictures illustrate starkly contrasting environments (Figure 24). At areas of higher reflectance, the images display shell hash, while at areas of lower reflectivity the photographs show fairly uniform muddy sand.

Block 2 and Alabama 2000 & 2002

The area consists of primarily large patchy regions of highly reflective material along with areas of almost parallel linear features trending NW-SE (Figure 25). Areas within the sidescan appear to take a pattern of dendritic form near areas of highly reflective material. Sand content exceeds 90% at most locations (Figure 26 and Table 7). In the highly reflective regions (dark areas), the bottom type is shell hash with a carbonate content >40%. The lower reflectance regions (light areas) consist of slightly muddy sand with a carbonate content less than 11% (Figure 27). Bathymetric data indicate that the highly reflective regions show varying amounts of vertical relief from the sea floor. Ridge features stand ~3 m above the surrounding seabed, while larger patches are ~1m above the surrounding seabed. Chirp data from this region show

Table 5. Radiocarbon ages for oyster shells collected at the 40m isobath.

Sample-ID	Water Depth	Sample Type	Measured Age	DC_13	Corrected and Calibrated Age (1sigma)
1	40m	oyster shell	11013 +/- 87	-1.29	10822-10809
2	40m	oyster shell	10936 +/- 76	0.02	10655-10548
3	40m	oyster shell	10911 +/- 85	-1.51	10643-10563
4	40m	oyster shell	10319 +/- 85	-1.23	9383-9077

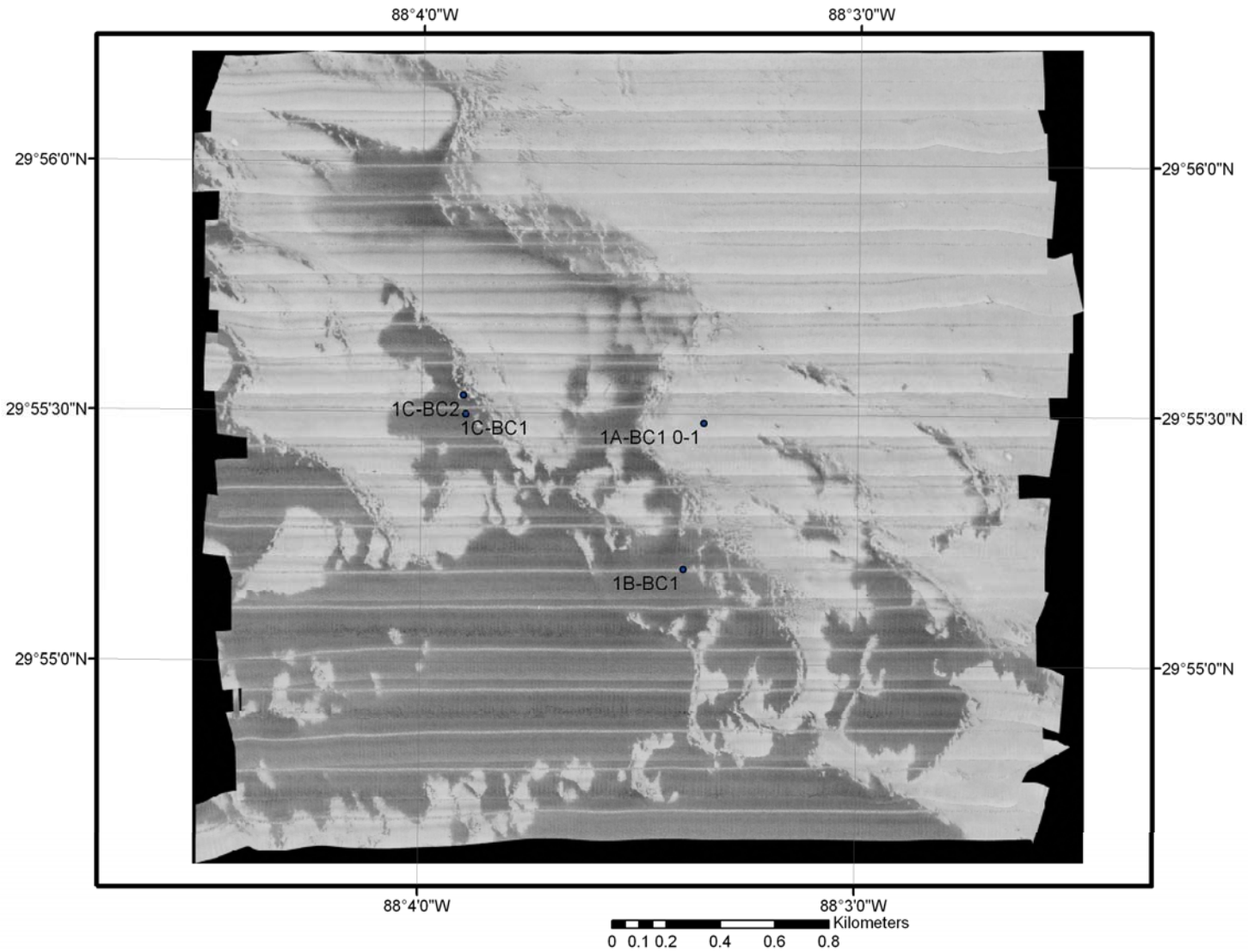

Figure 21. Sidescan sonar mosaic of block 1. Core locations and names are noted. Darker regions are areas of higher reflectivity and lighter areas are regions of low reflectivity.

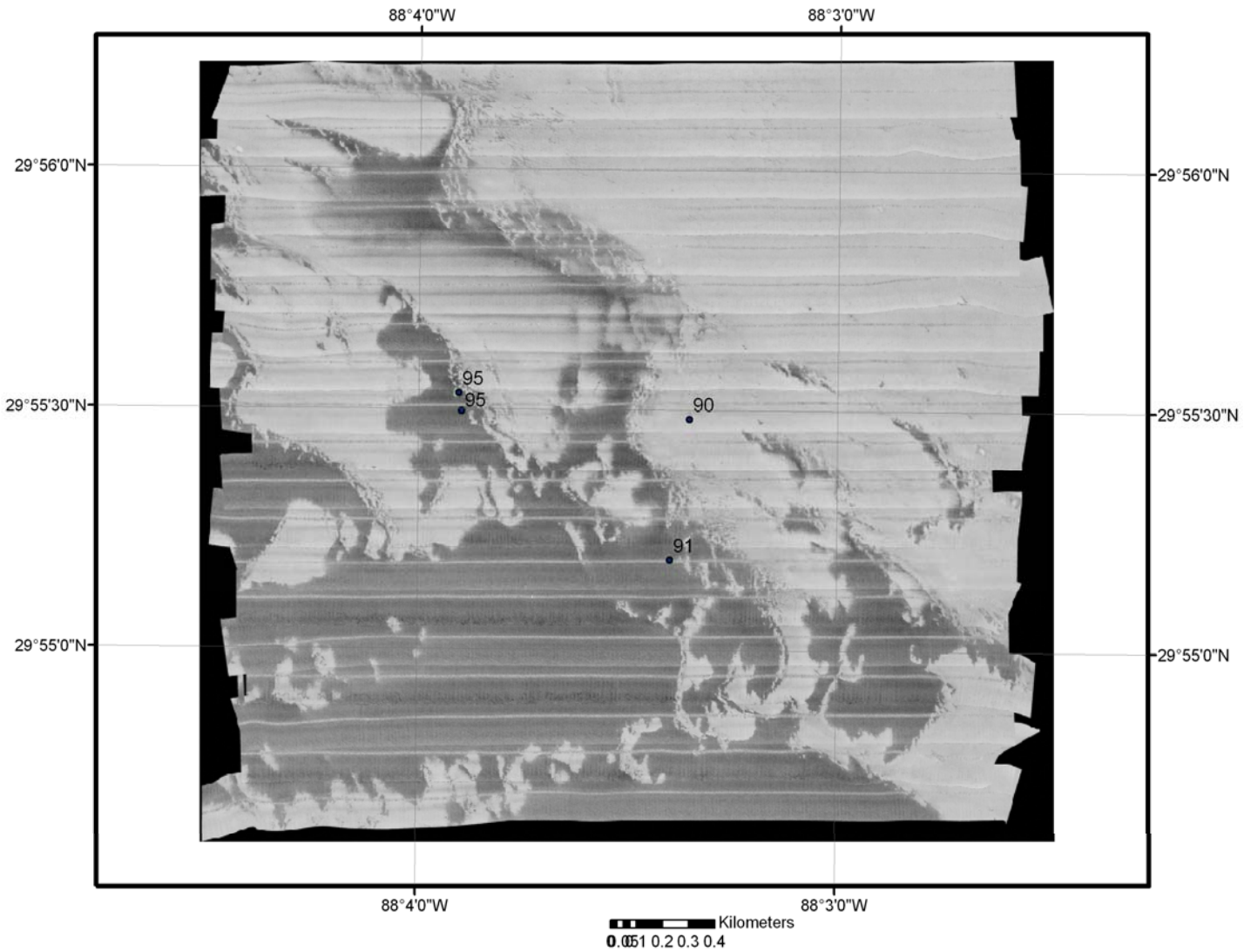

Figure 22. Sidescan sonar image of Block 1. Sample locations are represented by circles and values reflect the fraction of the sample >63µ.

Table 6. Physical properties of sediments from block 1.

Core-ID	%sand	%mud	%CO3	Facies
1A-BC1 0-1	89.6	10.4	5.4	sand
1A-BC1 1-2	91.8	8.2	8.1	sand
1A-BC1 2-3	91.2	8.8	4.8	sand
1A-BC1 3-4	90.6	9.4	4.7	sand
1A-BC1 4-5	89.4	10.6	4.7	sand
1A-BC1 5-6	89.3	10.7	5.4	sand
1A-BC1 6-7	90.2	9.8	8.2	sand
1A-BC1 7-8	89.2	10.8	6.8	sand
1B-BC1	91.5	8.5	36.5	shell
1C-BC1	95.1	4.9	43.5	shell
1C-BC2	95.1	4.9	39.4	shell

.

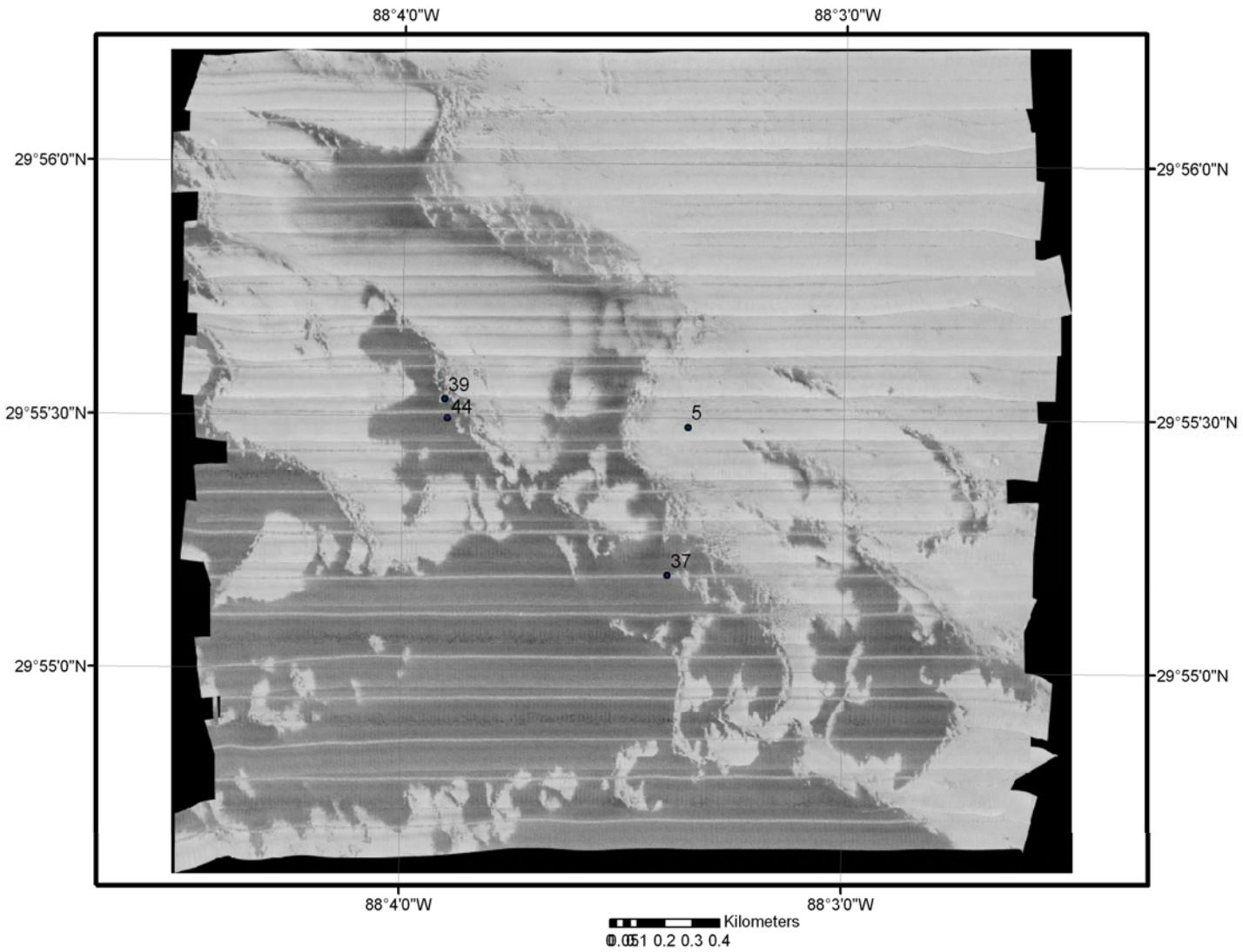

Figure 23. Sidescan sonar image of Block 1. Sample locations are noted and the values refer to the % carbonate found in the surficial samples.

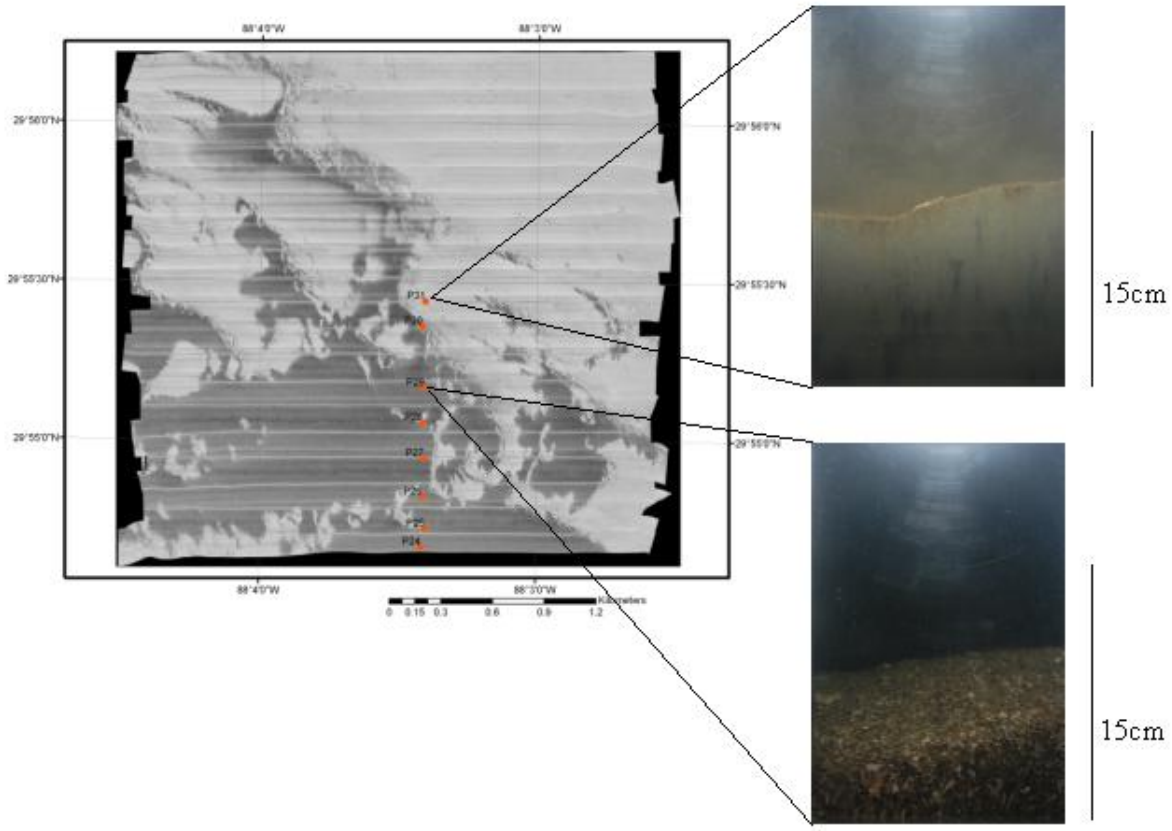

Figure 24. Benthic photographs from Block 1. Upper photograph of muddy sand was taken in the lower reflectivity regions and the shell hash photograph was taken in the high reflectivity region.

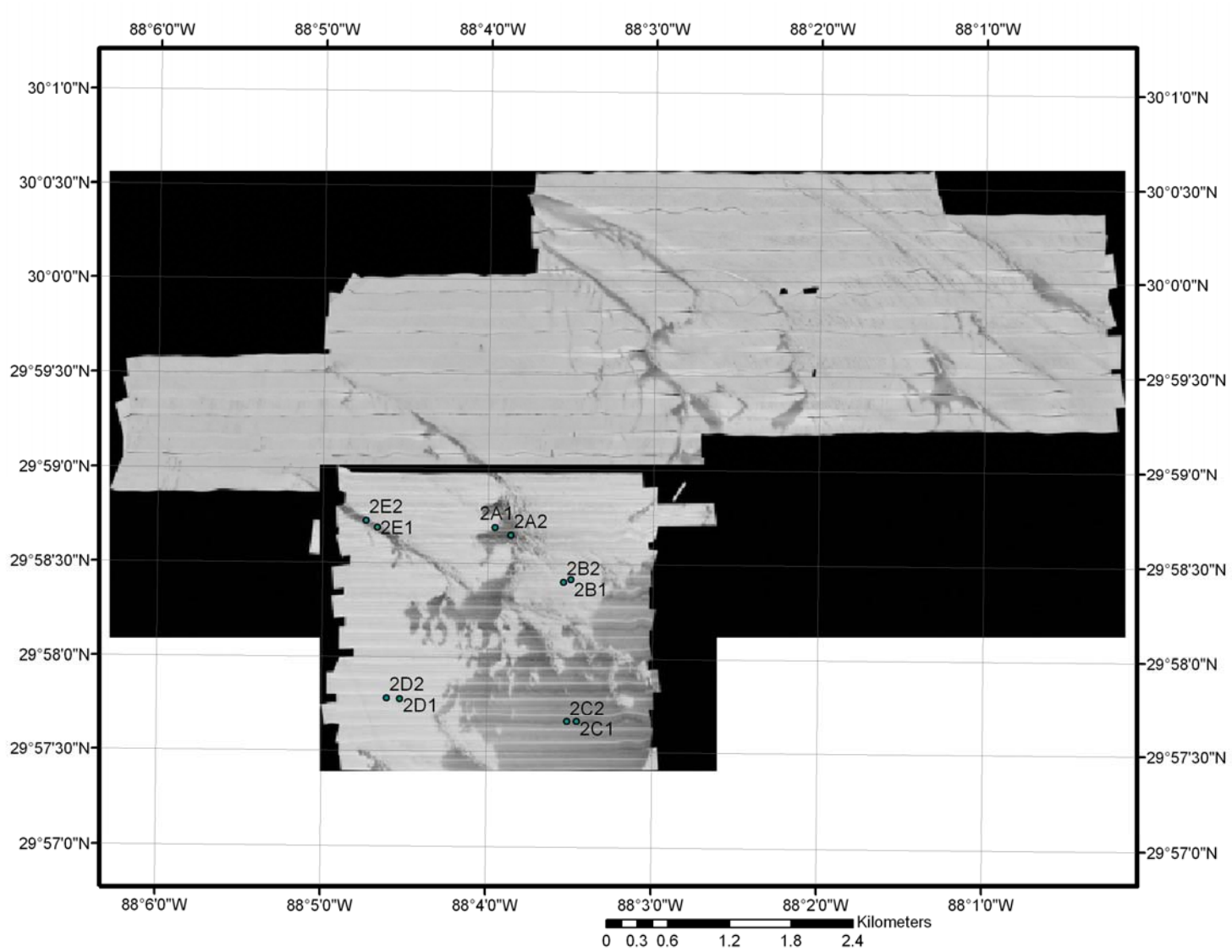

Figure 25. Sidescan sonar mosaic of block 2 and Al'02. Core locations and names are noted. High reflectivity is seen as the darker areas in the mosaic and low reflectivity is seen as lighter shades of gray.

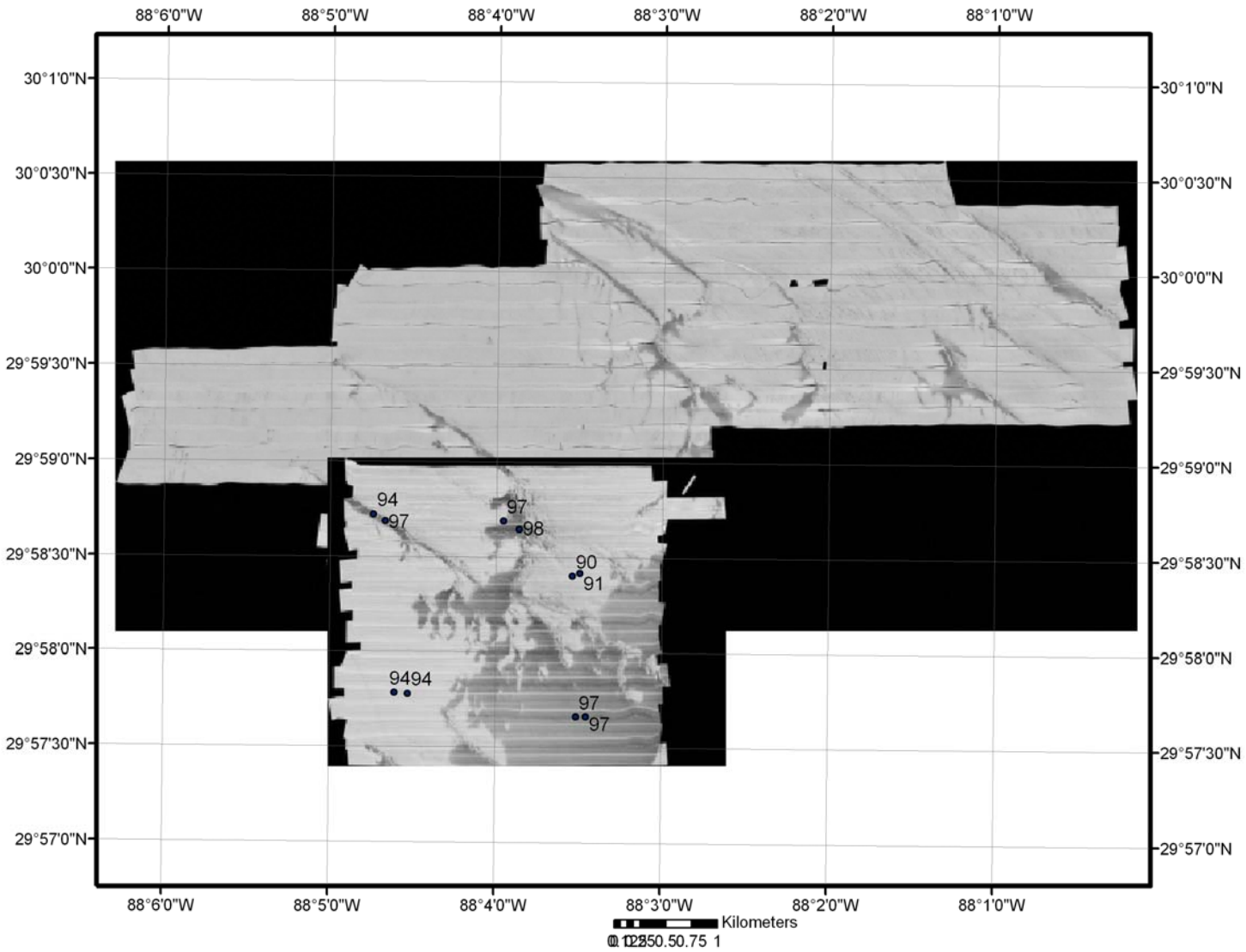

Figure 26. Sidescan sonar image of Block 2 & Al'02. Core locations are circles and values represent the fraction of that sample with grain size >63µ.

Table 7. Physical properties of sediments from block 2.

Core-ID	%sand	%mud	%CO3	Facies
2A-BC1	97.2	2.8	54.5	shell
2A-BC2	97.8	2.2	51.4	shell
2B-BC1	91.0	9.0	4.6	sand
2B-BC2	89.5	10.5	11.6	sand
2C-BC1	96.9	3.1	41.3	shell
2C-BC2	97.0	3.0	45.6	shell
2D-BC1	93.7	6.3	n/a	sand
2D-BC2	93.7	6.3	5.0	sand
2E-BC1	96.6	3.4	40.8	shell
2E-BC2	94.2	5.8	46.6	shell

asymmetrical reflectors with up to 3 m of vertical relief (Figure 28). These ridge-like features either have a steep landward slope with a long trailing edge seaward or they appear to have two separate elements. In the latter case, lens shaped features exists with an adjacent wedge of slightly acoustically transparent sediment downlapping onto a hard reflector near the surface of the seabed (Figure 29). At the highly reflective regions, seabed photos show shell rubble. Photos of lower reflectance areas show muddy sand (Figure 30).

Blocks 3 & 4

Sidescan from blocks 3 and 4 shows a predominantly homogeneous bottom reflectance (Figure 31), except in the northeastern area of the block 3 where a small patch of high reflectivity is evident in the sidescan image. A pipeline is also visible in the sonar at the southeastern corner of block 3. Three replicate cores taken within the highly reflective region show that 95% of the material is greater than 63μ (Figure 32 and Table 8). Sediment from two cores taken directly in this region contained sandy shell hash with >25% carbonate, whereas sediment from a core located adjacent to this highly reflective patch contained <5% carbonate in slightly muddy sand. Other cores taken within the remainder of blocks 3 and 4 contained >92% sand and <8% carbonate, except for a single core in block 4 containing 19% carbonate (Figure 33). Two cores were also taken near the pipeline in the southeastern corner and have sand contents greater than 55% and carbonate values less than 10%. Benthic profile images of this region show muddy sand (Figure 34).

The size of site 4 was reduced from its original specifications due to its presence in relation to a major shipping channel for Mobile Bay. This region was chosen for

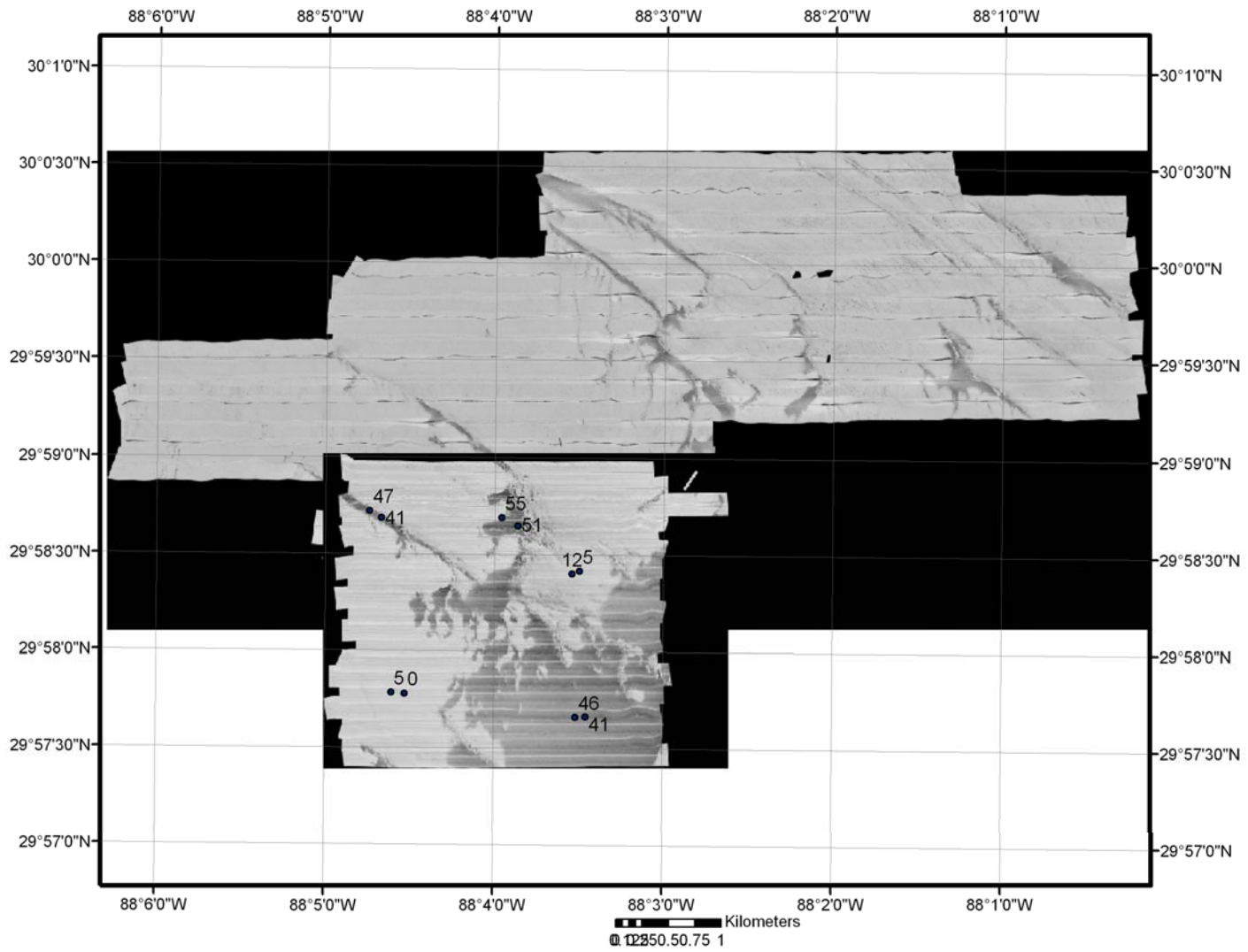

Figure 27. Sidescan sonar image of Block 2 & Al'02. Core locations are noted and values represent the % carbonate content of surficial sediments found at each site.

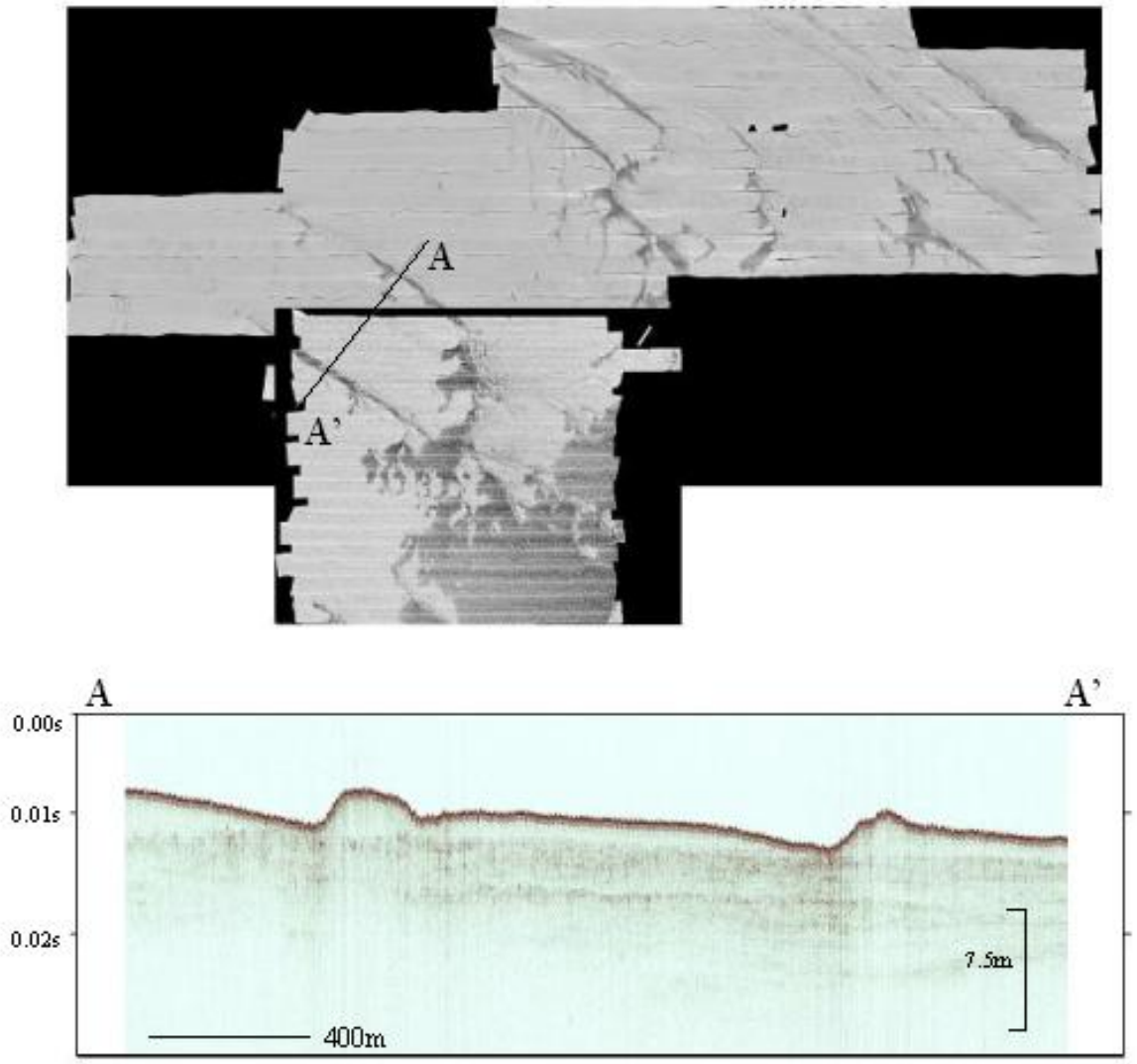

Figure 28. Sidescan Sonar image of Block 2 & Al'02 with the location of chirp profile. The length of the profile from A-A' is 2.1 km. Times are listed in two way travel time.

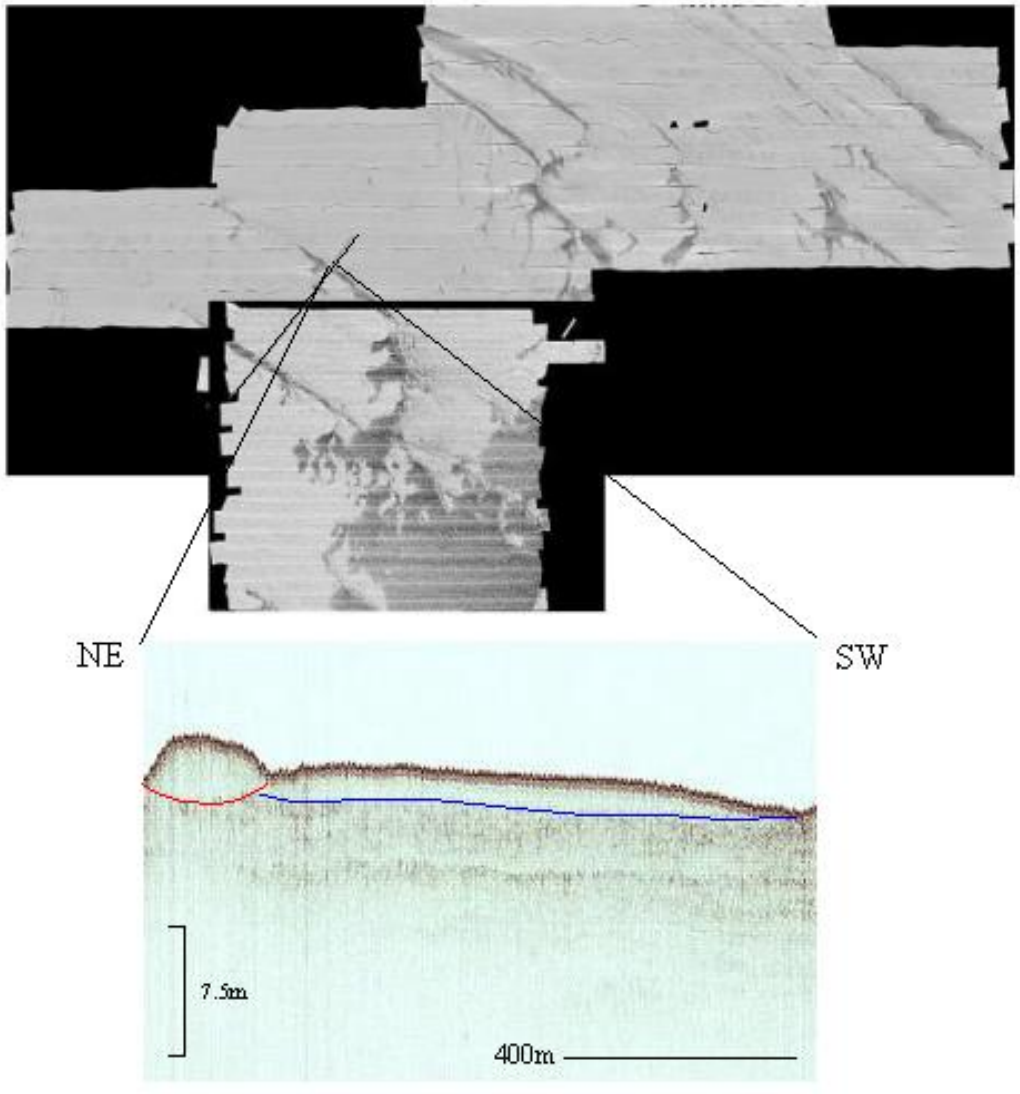

Figure 29. Chirp profile from Blocks 2 & Al'02. Notice the wedge of slightly acoustically transparent sediment that sits atop the harder reflector and the geometry of the shell ridge.

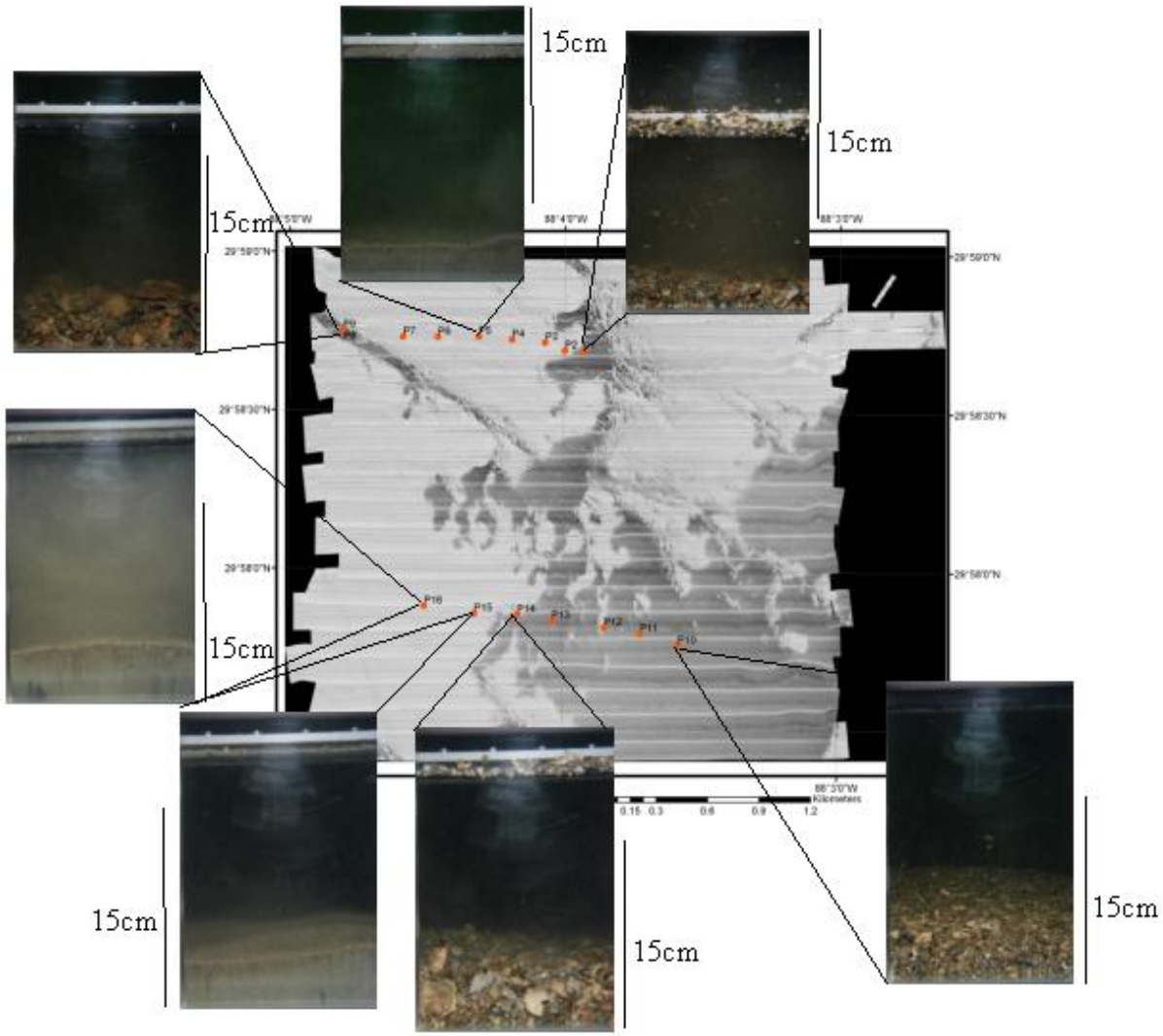

Figure 30. Benthic photographs from transects taken at Block 2.

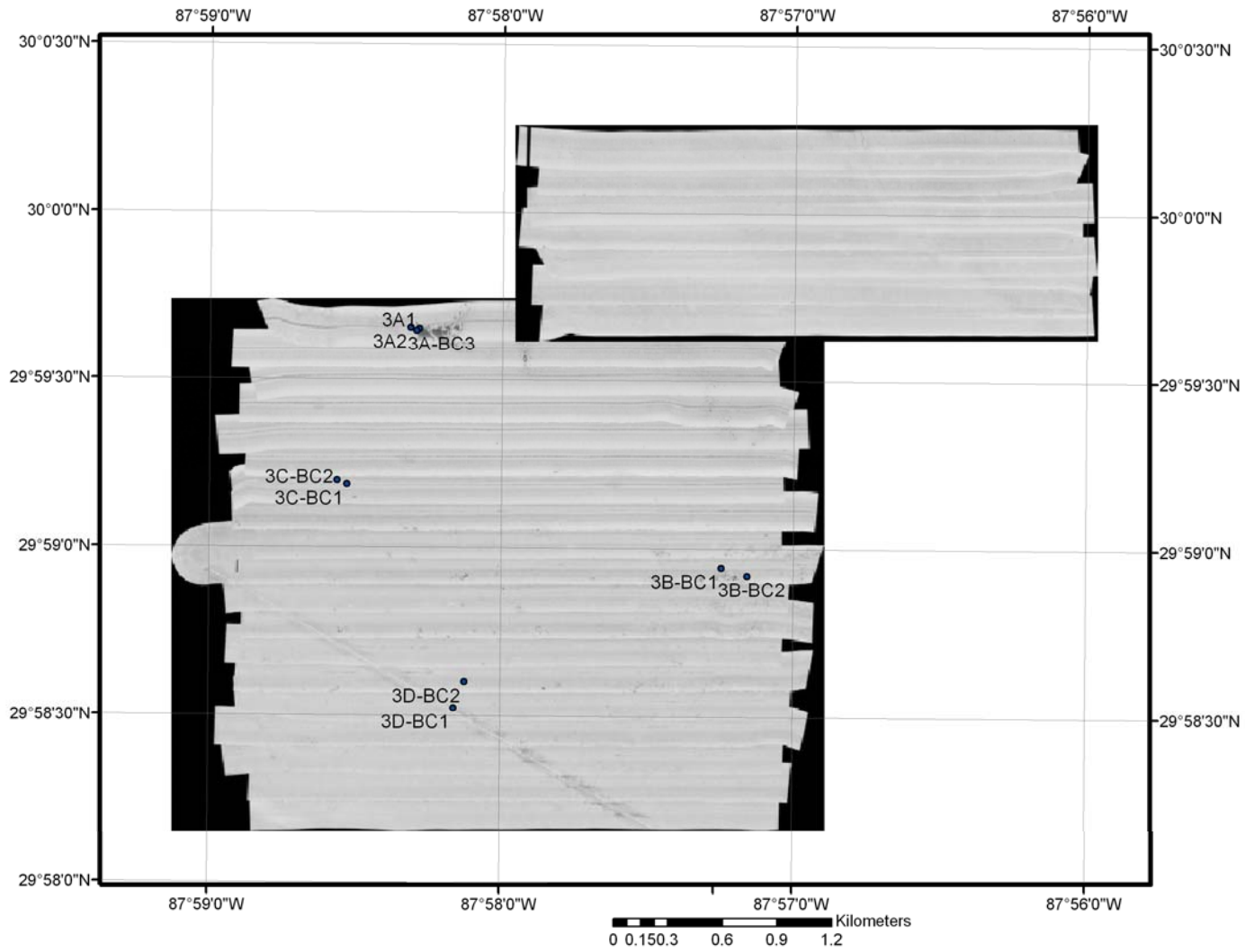

Figure 31. Sidescan sonar mosaic of blocks 3 & 4. Block 3 is the larger southern block and block 4 is the smaller northern block. Core locations and names are noted. Darker areas indicate higher reflectivity and the lighter gray areas are regions of low reflectance. A pipeline is visible in the SW of block 3.

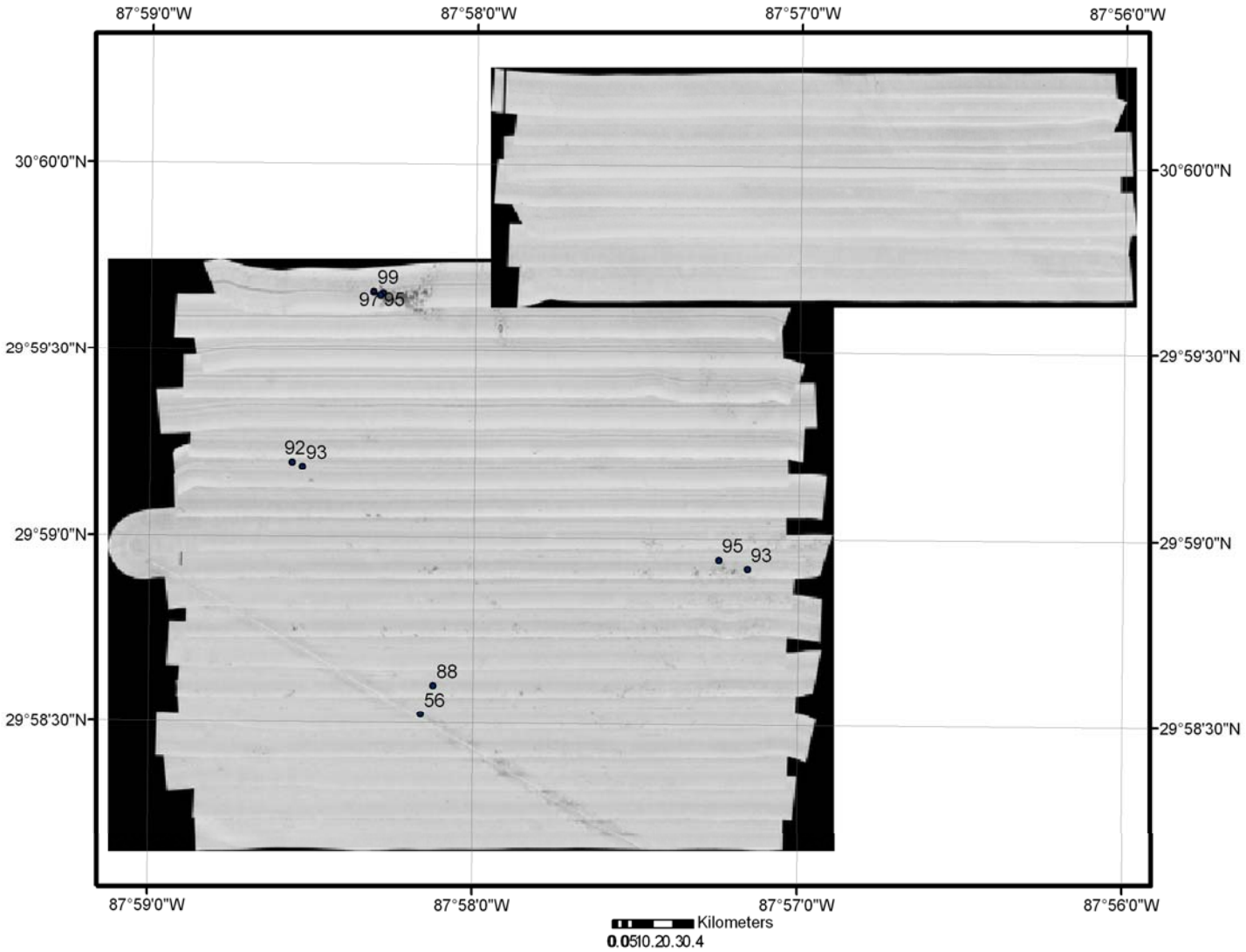

Figure 32. Sidescan sonar image of Blocks 3 & 4. Values are the percent of the sample with a grain size >63µ. Block 3 is the larger block to the south and block 4 is the smaller block to the north.

Table 8. Physical properties of sediments from blocks 3 & 4.

Core-ID	%sand	%mud	%CO3	Facies
3A-BC1	96.9	3.1	35.4	shell
3A-BC2	98.9	1.1	4.6	sand
3A-BC3	95.4	4.6	25.2	shell
3B-BC1	94.8	5.2	8.1	sand
3B-BC2	93.2	6.8	5.4	sand
3C-BC1	93.3	6.7	5.4	sand
3C-BC2	92.4	7.6	5.4	sand
3D-BC1	55.8	44.2	10.1	dredge
4A-BC1	96.9	3.1	19.3	sand

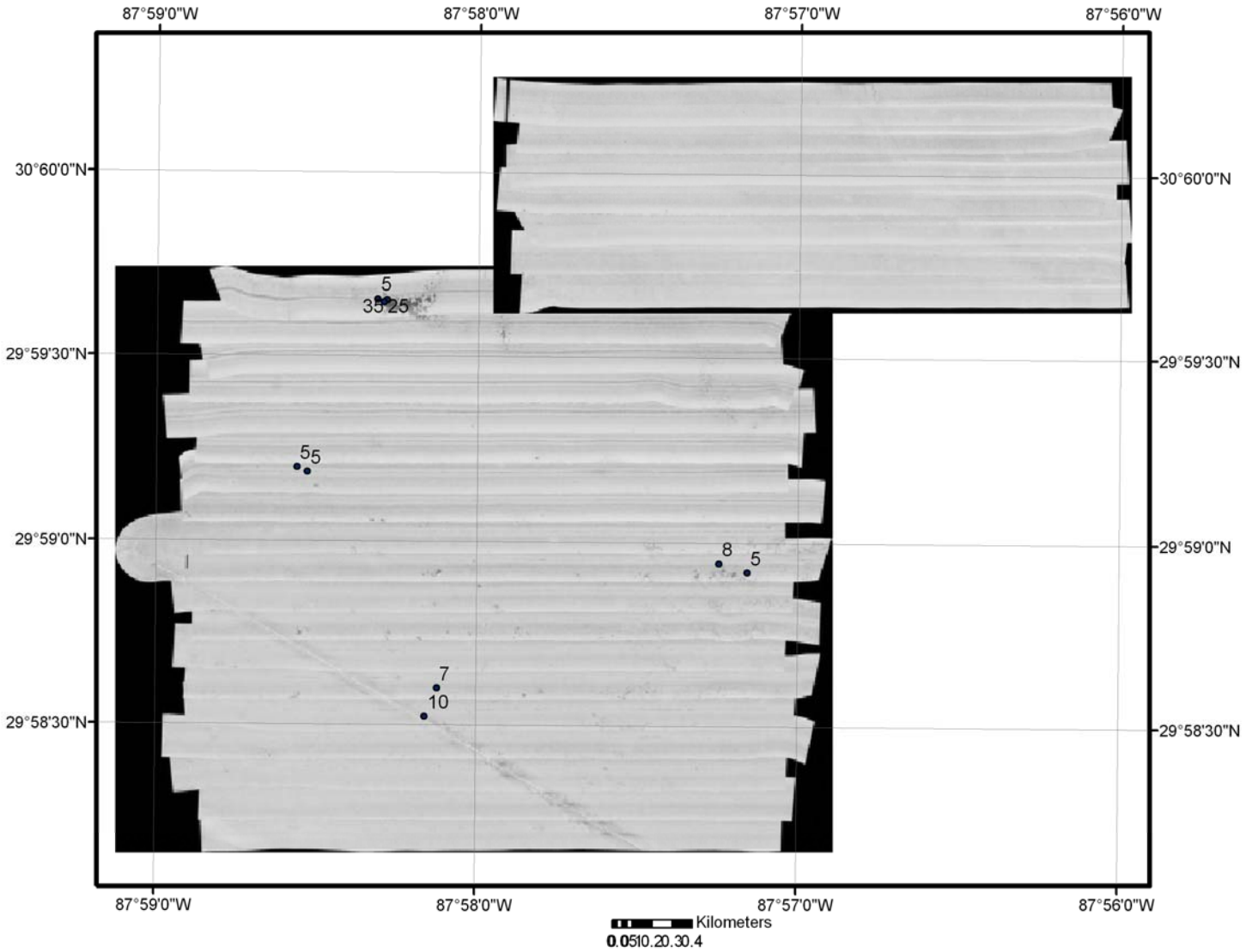

Figure 33. Sidescan sonar image of Blocks 3 & 4. Values are % carbonate content of surficial sediments. Block 3 is the larger block to the south and block 4 is the smaller block to the north.

seafloor characterization because of the Southeast Banks feature present on the seafloor. Southeast Banks lies on the Alabama inner shelf at water depths ranging from 17-28 m. This region consists of many ridges composed of shell and sand and a large patch of shell-sand-mud within a larger sand facies. Parker et al. (1992) believe this feature arises from shoreface-connected ridges that were detached during sea level rise. Chirp subbottom data from this area (sites 3 and 4) show a sharp surface echo and few, if any, subsurface reflectors (Figure 35). Vertical relief is seen in the northern part of the line.

Juvenile Red Snapper EFH

The relationship between sediment properties (sand:mud ratio, organic carbon, and carbonate content) and juvenile red snapper catch data, were compared in selected samples. These samples were selected based on close proximity of the trawls in reference to the core sediment samples. An average of the data points was taken for each location for each data type and were plotted (x vs. y) to examine a correlation. The results are contained in Figures 36 and 37. A positive correlation (r^2=0.5, n=10) was observed for the juvenile snapper density versus sand:mud (Figure 36). A negative correlation (r^2=0.65, n=11) was observed for juvenile snapper density versus organic content of sediments (Figure 37).

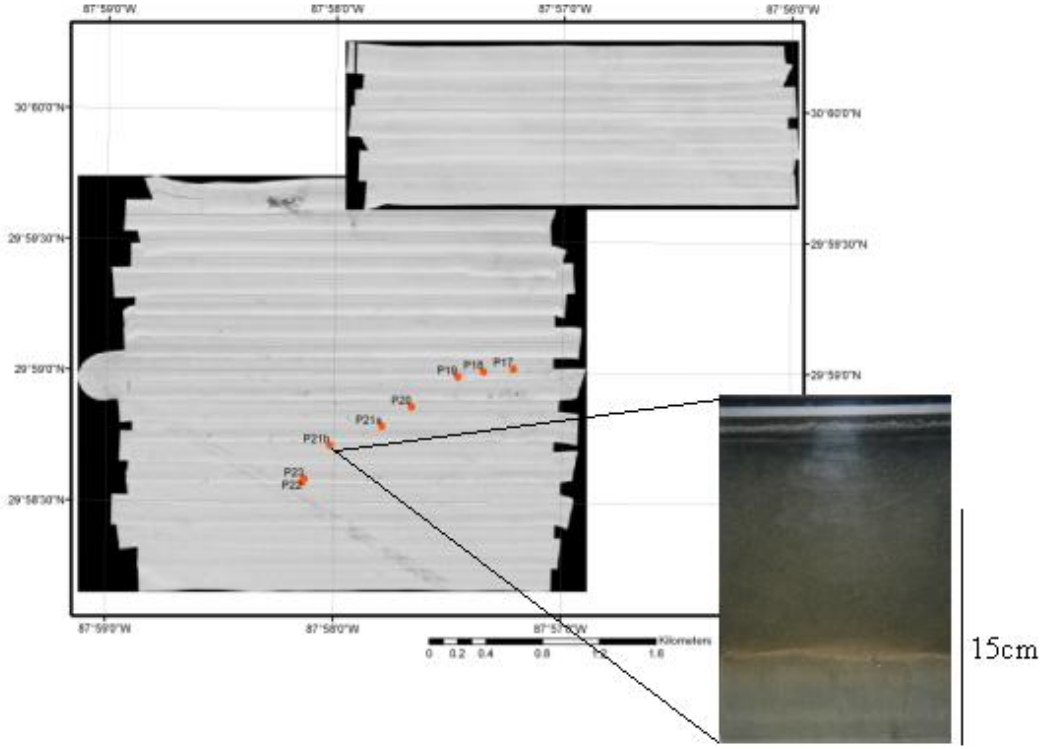

Figure 34. Benthic Photograph taken at Blocks 3 & 4.

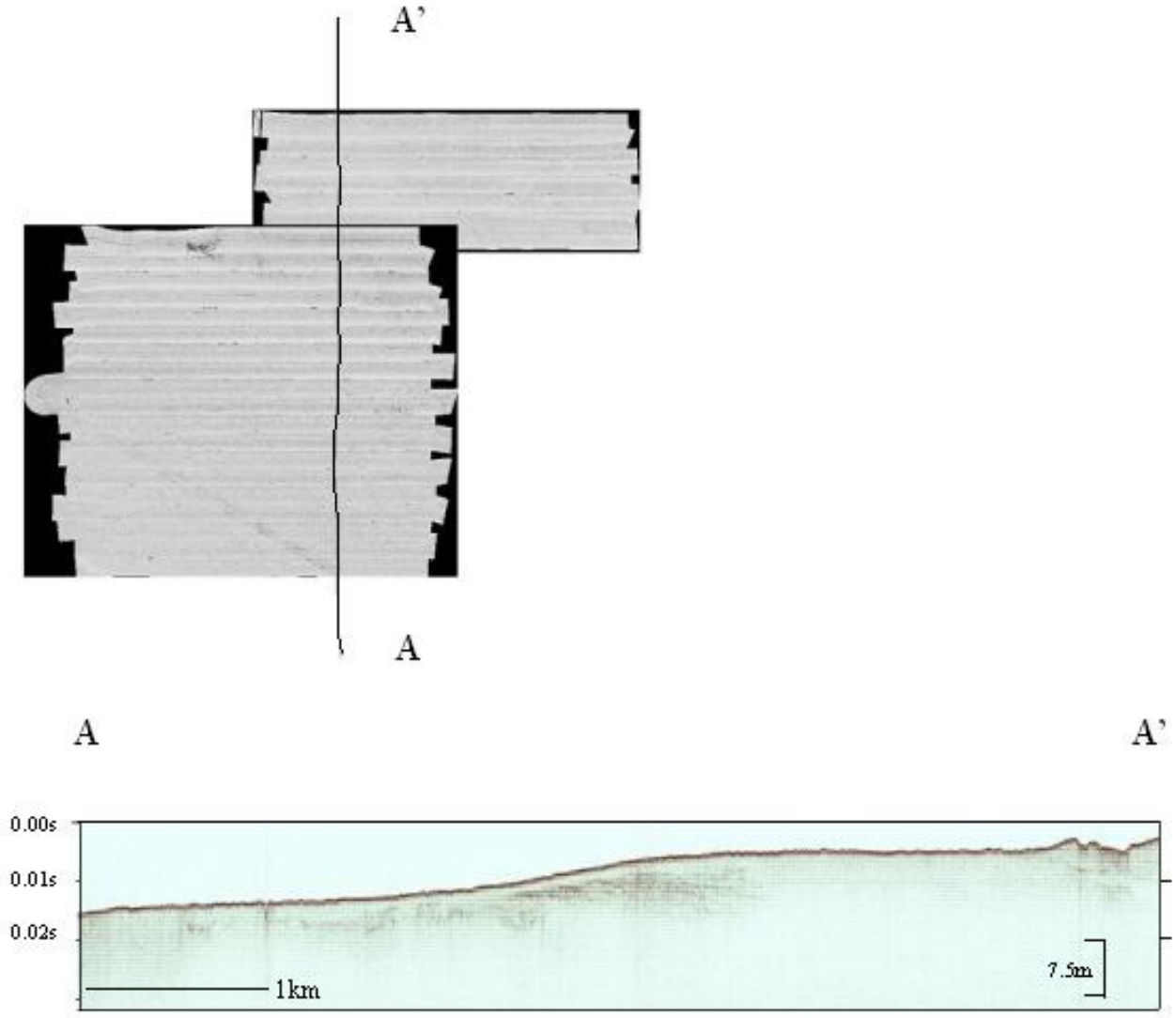

Figure 35. Sidescan sonar image of Blocks 3 & 4 with the location of the chirp profile. The length of the profile from A-A' is 7.9 km. Times are listed in two way travel time.

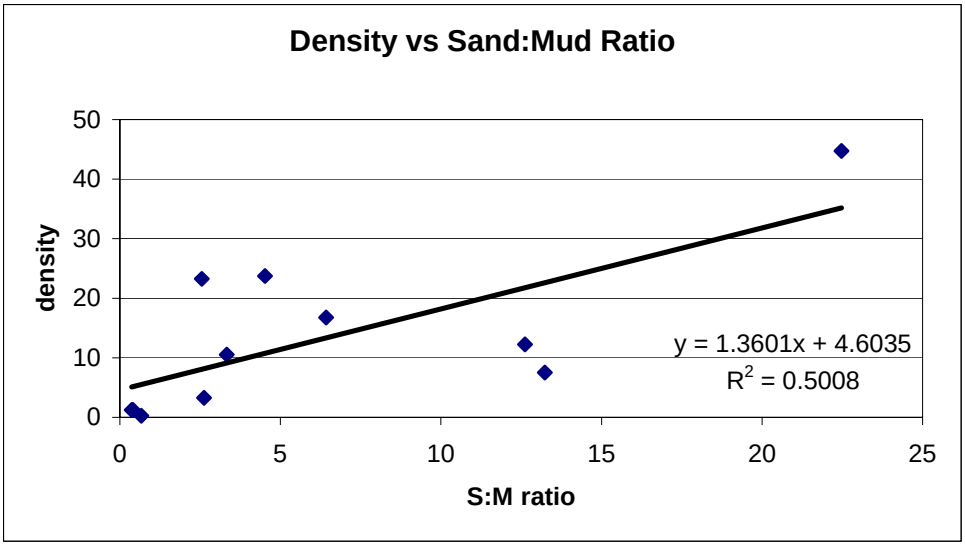

Figure 36. Juvenile Snapper Density versus Sand:Mud Ratio

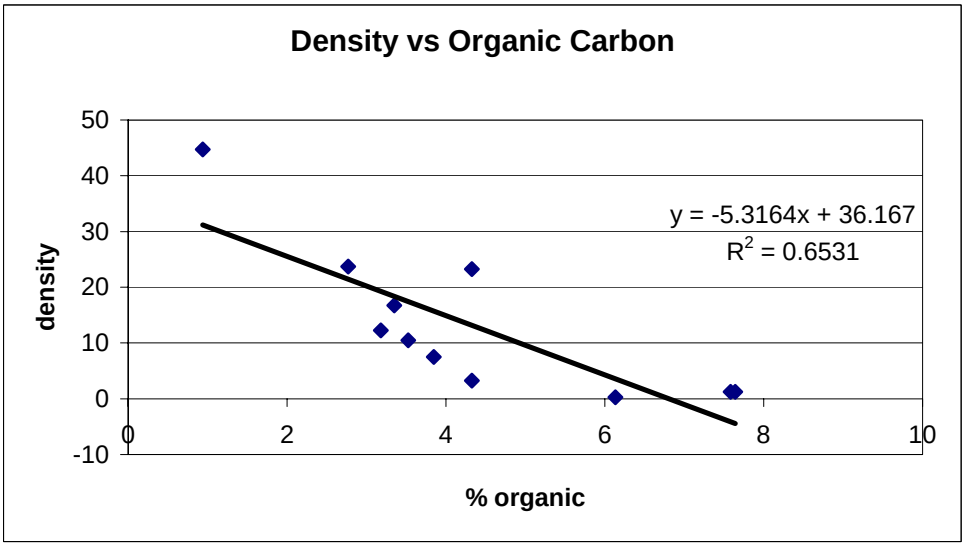

Figure 37. Juvenile Snapper Density versus Organic Carbon Content

DISCUSSION

Geologic Interpretations

Based on the results from surficial sediment properties and sonar classification, there appear to be three depositional environments present on the Mississippi-Alabama continental shelf. These environments include (1) MAFLA Sands; (2) shoreface shell ridges and lagoonal shell reefs/patches; and (3) prodelta muds. These different environments reflect varying combinations of marine and/or estuarine origins.

Surficial Sands

It appears that the sandy sediments found within all of the study areas can be classified as part of the eastern sand sheet or MAFLA complex. McBride et al (1999), state that the source of the MAFLA sand sheet is from the eroding shoreface that has been reworked by storms from sediment winnowing during Holocene transgression. They also note that this sand sheet thins towards the west. The thickness of this sediment package does not exceed 10m and the sediments within this package usually have a sand content >90% (Ludwick, 1964; Doyle and Sparks, 1980; McBride, 1999). Sandy sediment collected in the eastern sites (Blocks 1, 2, 3, 4, Al'02, and C) exhibit typical sediment parameters as previously documented for the eastern sand sheet (MAFLA). Block C contains sand content greater than 70% and can be classified as a low-relief muddy sand sheet. All sites (Blocks A, 5, C, and G) within the western region of the overall study area still exhibit similar MAFLA sediment properties but are slightly muddier. Prodelta clay deposits from the St. Bernard and Balize delta lobes of the Mississippi River are likely sources for these muds, along with sediments delivered from Mobile Bay. Figure 38 demonstrates a map of interpreted facies seen in the study area.

Shell Beds and Ridges

Shallow sites A, 5 (approximately 20 m water depth, Figure 4), Al'02, 2 (approx 25-30 m water depth, Figure 25), and 1 (approximately 32 m water depth, Figure 21) are characterized by sandy substrate with easily distinguishable highly reflective linear ridges. The ridges are composed of slightly sandy shell, and have 1-2 m relief above the surrounding slightly muddy sand seabed. Shell fragments include encrusted and bored oyster-shell debris and marine taxa. The ridges can extend for kilometers in lengths and usually have widths of about 100 m. These almost parallel features are oriented NW-SE and are exposed on the seafloor surface. Distances between the ridges vary from 450 m to 1.2 km. The composition of the ridges contrast with the muddy sand seabed immediately adjacent and show an abrupt change between sediment types.

The size and scale of the ridges do not appear to be wave-generated bedforms nor does the sediment composition of the ridges favor this development. The reflection geometry of the ridges recorded in the subbottom profile display characteristic morphology of shoreline deposits (either barrier or shoreface ridge). Parker et al. (1992) and Schroeder et al. (1988), both conclude that the most likely mechanism for the formation of the ridges at Southeast Banks (slightly north of our study area) is shoreface-connected ridges that were detached and then drowned by sea level rise. Along the New Jersey continental shelf, Stubblefied et al. (1984) recognize both transgressive and post-transgressive features. In this case, two mechanisms were proposed for formation: (1) post-transgressive reworked shoreface-connected ridges, and (2) transgressive drowned barriers. Surficial sediments associated with the Stubblefied et al. (1984) study are all sands. Orientation of these ridges (this study; Parker et al., 1992 and Stubblefied et al.,

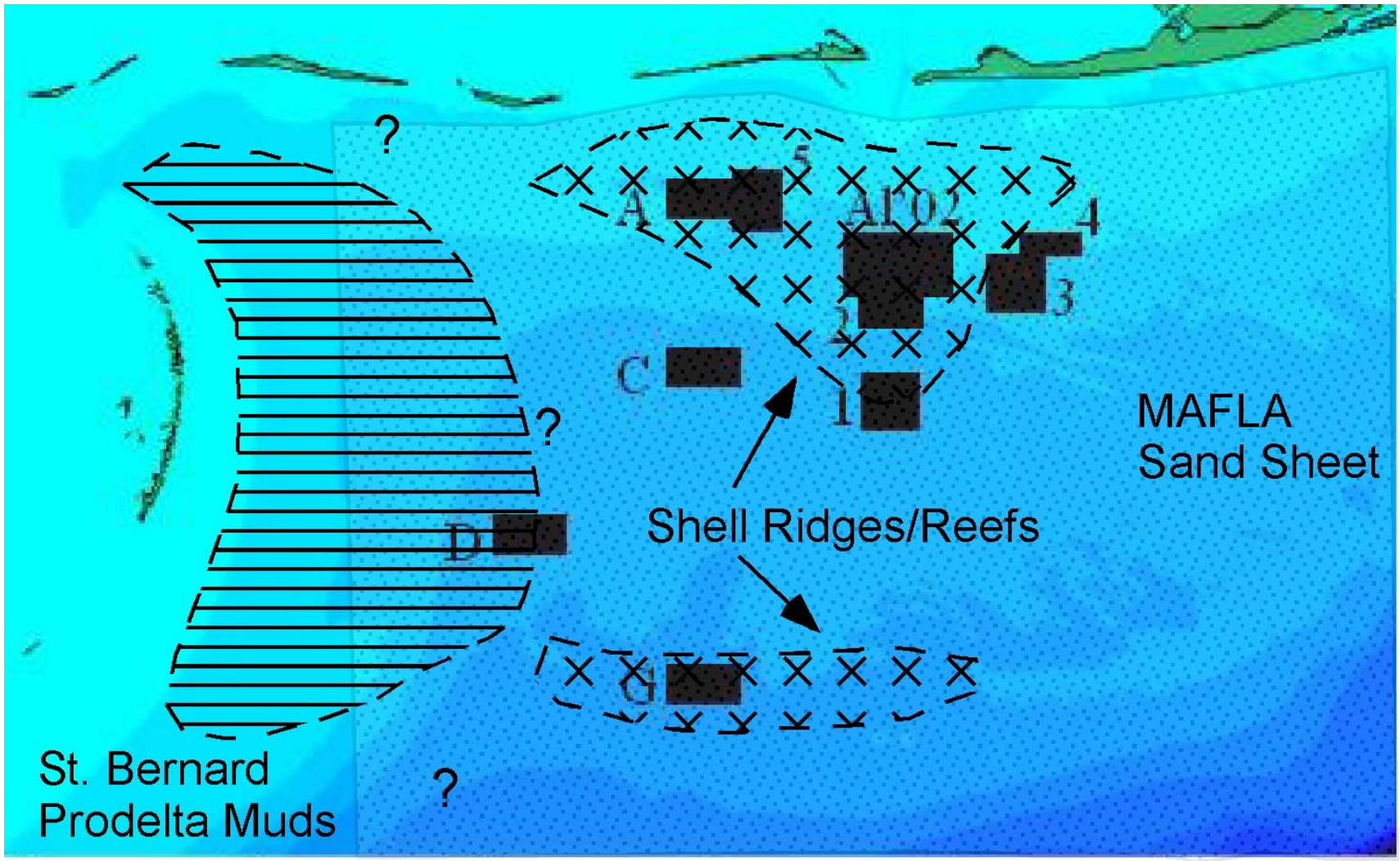

Figure 38. Map of interpreted facies of the Northern GOM continental shelf. MAFLA sand sheet cover most of the region with shell reefs and ridges and St Bernard prodelta deposits at their proposed locations.

1984) may be shore oblique; but surface sediment composition of these ridges between the Mississippi-Alabama shelf and the New Jersey shelf differ greatly. However, we have no subsurface sediment data in this study. Whether the ridges are drowned shoreface-connected ridges or degraded barriers, both are indicators of historical shorelines and can therefore be used to track approximate sea level position in the Holocene.

Based on composition and geometry, the shoreline ridges were probably created near the shoreface, and then subsequently drowned from rapid sea level rise. As sea level continued to rise, winnowing of remaining sediments left sands to be deposited between and up against the *in-situ* shell ridges; therefore, creating the surficial features that are observed on the seafloor presently (as seen in Figures 4 and 25).

The patchy highly reflective features also observed in site 2 and 1 on the inner shelf, and in site G (approx 40 m water depth) on the mid-shelf include both broad patches and narrow shell ridges, separated by sand. Some reflectance patterns within the sidescan, at these areas, appear to be dendritic in nature with channel-like features branching from large areas of highly reflective shell material. This pattern is similar to what may be seen in present estuarine/lagoonal environments and their associated tidal channels.

In a large shelly patch, within block 1 (Figure 21), masses of blue and orange clay were found among the shell hash collected. The soil-like appearance of these masses suggests that they are paleosols. The presence of paleosols within the large shell beds indicates that the reef-like features may be composed of older Pleistocene muds. These are old deposits that were weathered subaerially. Presently, estuaries are the dominant

low-energy, muddy facies along the gulf coast (e.g. Bentley et al., 2002). Carbonate percentages vary from >45% at the ridges/reefs to less than 10% at the adjacent bed. The shell debris is primarily composed of fragmentary and entire valves (site G) of *Crassostrea virginica*, an estuarine species, with fully marine gastropods, bivalves, and serpulid polycheates, as seen in benthic photographs (Figures 24 and 30). When examined upon collection, clusters or clumps of oyster valves were observed, indicating no transport from other areas and thus *in-situ* preservation (Figure 39). The profiles indicated chaotic surface reflection and either acoustic washout below or prolonged high amplitude subsurface echoes at the reef areas (Figure 20). Surrounding these reef areas are pockets of somewhat acoustically transparent material that form lenses and terminate against the hardbottom regions (Figure 20). Sediment samples indicate that the slightly acoustically transparent material consists primarily of sand (Figures 17, 19 and Table 4). Since these sands onlap onto the reef-like structures, they are believed to have been deposited around these shell beds after the initial formation and submergence of the shell beds from sea level rise.

Radiocarbon ages of oyster shells found in the southern most region, site G (40 m isobath), indicate shell formation between 9,000-10,000 ybp (corrected ages). Disarticulated oyster valves are widespread along the GOM continental shelf, however previous studies (Schroeder et al., 1995) have documented that oyster shells recovered near the 40 m isobath on the GOM shelf have uncorrected ages of 11000-10000 ypb and can be attributed to paleo-estuarine conditions. These uncorrected ages correspond to the uncorrected ages found in this study. In addition, the extent and morphology of the large patches suggests that they may be, in part, relict features, not post-transgressive marine

Figure 39. Picture of oyster shells collected at the surface of the seabed at the 40 m isobath (Site G).

features. Schroeder et al. (1995) also note that cross-shelf transport of these shells was not likely due to the relatively good conditions of the shells found in their study. *In-situ* preservation of the oyster shells is also believed to be the case in this study. Due to the age, orientation and size, subsurface geometry, and composition, these features are believed to be remnants of lagoonal/estuarine sediments (possibly *in-situ* estuarine oyster reefs) developed and subsequently submerged during Holocene transgression.

Using the general Holocene sea level curve (Figure 40) from Perillo (1995) based on uncalibrated radiocarbon datasets, an age-depth relationship can be examined. Sea level rose rapidly from 15000-12000 ybp and some fluctuation in the general trend of the curve appears at approximately 10500-9000 ybp. From these curves, sea level appears to have slowed down and possibly receded a few meters at approximately 40 m below present level. Radiocarbon dates obtained from oyster shells collected at the 40 m isobath return ages within this range (Figure 40). Oyster shells are assumed to be *in-situ* in this region for the following reasons: (1) separate independent studies of radiocarbon dating of oyster shells and sea level studies yielded comparable results, and (2) the extensive, irregular nature of the shell beds from which the oyster valves were recovered are not typical of post-transgressive marine features. Sea level then rose rapidly until approximately 8000 ypb and 20-25 m below present sea level. At this time, sea level rise appears to have slowed and possibly receded slightly. The depth associated with this interval at ~8000 ybp corresponds to the linear ridge features seen in the northern sites (Figures 4, 21, and 25). After this date, sea level rose more rapidly until 7000-6000 ybp, when sea level approached its present elevation, although details of Holocene fluctuations are under study (Blum et al., 2002).

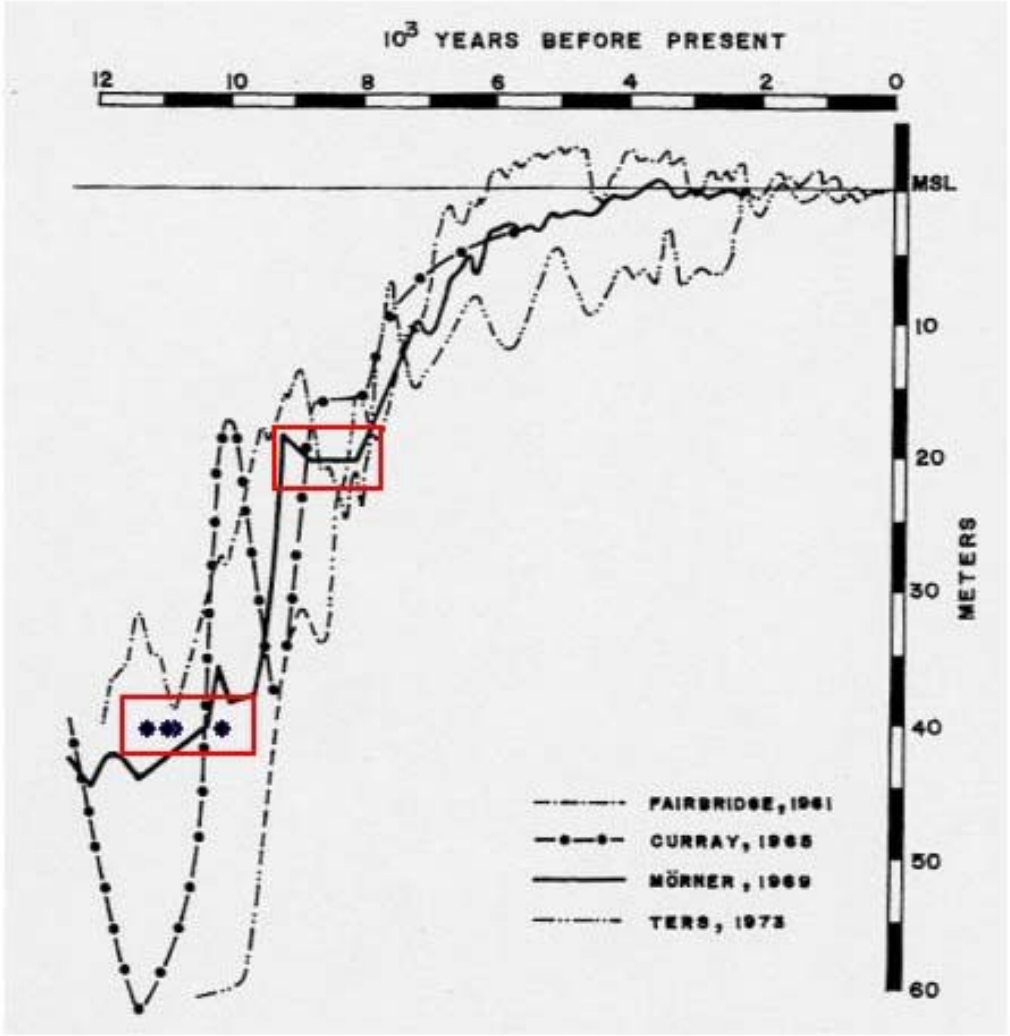

Figure 40. Sea Level curve from Perillo (1995) using uncalibrated datasets. Depths of shell features are outlined with their approximated ages and radiocarbon dated shells (uncorrected radiocarbon ages of the samples) from the 40m isobath are shown as filled circles.

McBride and Byrnes (1995) indicated that the Eastern Alabama-Florida shelf is dominated by 2 shelf-parallel (shore-oblique) sand shoals. The North Perdido shoal occurs in approximately 20-25 m water depth while the South Perdido shoal is in water depths ranging from 25-40 m. Water depths of the shoals deepen towards the west; both of these shoals appear to terminate to the east of our study area (McBride et al., 1999). According to McBride et al. (1999), North Perdido shoal is no longer visible in surficial bathymetry south and west of Perdido Bay, Florida, while South Perdido shoal is recognizable westward in bathymetry until south of the Morgan Peninsula, Alabama. McBride (1997) states that the surficial sediments present on this shelf are "fine-to-coarse quartz sand with widely scattered shell fragments". These shoals are reworked transgressive barrier/beach deposits and are oriented and positioned overlying transgressive topography or escarpments (McBride, 1997). The depths of these shoals are similar to the depths of the ridge (Blocks A, 5, Al'02 and 2 at 20-26 m water depth) and reef features (Blocks 1 and G at 33 to 40 m water depth) observed to the west. If the trend of North Perdido shoal were to be extended to the west, it would exist slightly deeper than the shallow blocks associated with this study. If the trend of South Perdido shoal were to extend to the west it would also run slightly deeper than the most offshore blocks of our study area (Figure 41). This tenuous association suggests that, if our ridges and shell beds developed at or near the same time as North and South Perdido shoal, then the ridges and shell beds may have been landward of the shoreface. Given that the North and South Perdido shoals may have developed during periods of sea level stillstands and indicate possible Holocene shoreline locations and/or terraces, it is highly likely that the features observed to the west, in our study area, may have related origins.

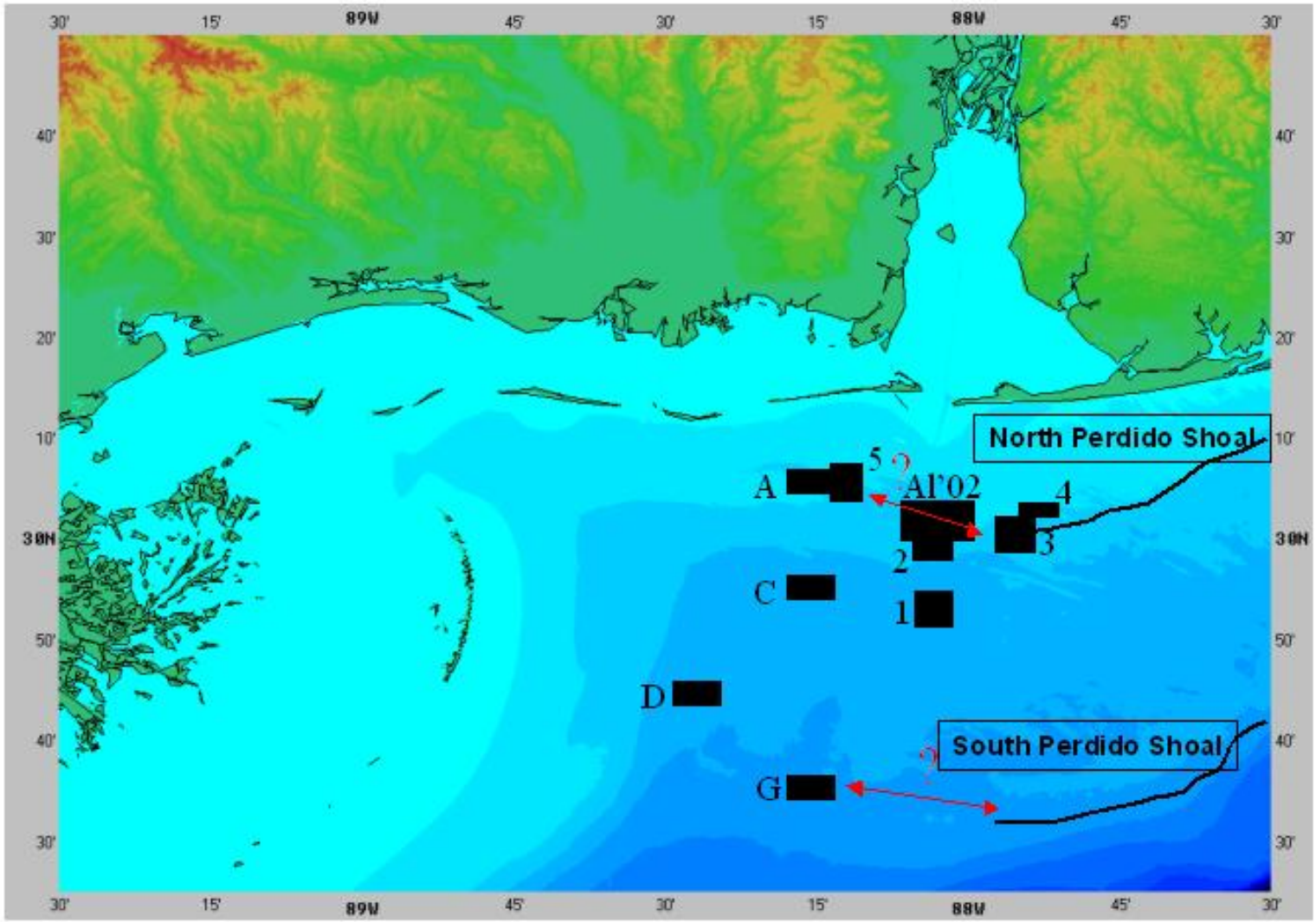

Figure 41. Study Area map with locations of North Perdido Shoal and South Perdido Shoal. Locations and depths of these shoals are adapted from McBride and Byrnes (1995), McBride (1997), & McBride et al. (1999).

Variable depth of each shoal and the differences in depths between the shoals to the east and the features to the west suggests that if they were formed as a coastal features, differential subsidence and uplift has occurred since initial formation. This neotectonic activity may be related to deltaic loading and faster subsidence at areas closer to the MS River deltas. The closer the features are to the MS deltas the faster they would have subsided. This allows for better preservation of these features and explains the depth variations seen (deeper to the west, shallower to the east).

Relict Deltaic Deposits

Block D, although similar in reflectance to the sandy Block C, is composed of homogeneous sandy mud with over 70% silt and clay particles (Figure 10). This contrasts greatly with the shell and sand features documented on previous pages. The carbonate content of this site is <10%, much lower than ridges and shell beds found in blocks A, 5, 1, 2, Al'02, and G. There is also an eastward coarsening trend associated with the surficial sediments in block D (Figure 11).

Chirp profiles indicate a wedge-shaped package of acoustically transparent sediment (probably mud) that downlaps onto the eastern portion of the site (Figures 15 and 16). This thin veneer corresponds to the eastern most extent of the St. Bernard prodelta (Figure 42). Cores D2 and D4 are both located within the boundaries of the wedge of muddy sediment, while D6 exists further east of the mud veneer (Figures 10, 14, and 15).

The X-ray of this site show intensely bioturbated sediment lacking in any apparent physical stratification (Figure 13). It is likely that fine sediments supplied by Holocene Mississippi River deltas were mixed with pre-existing sands by biological

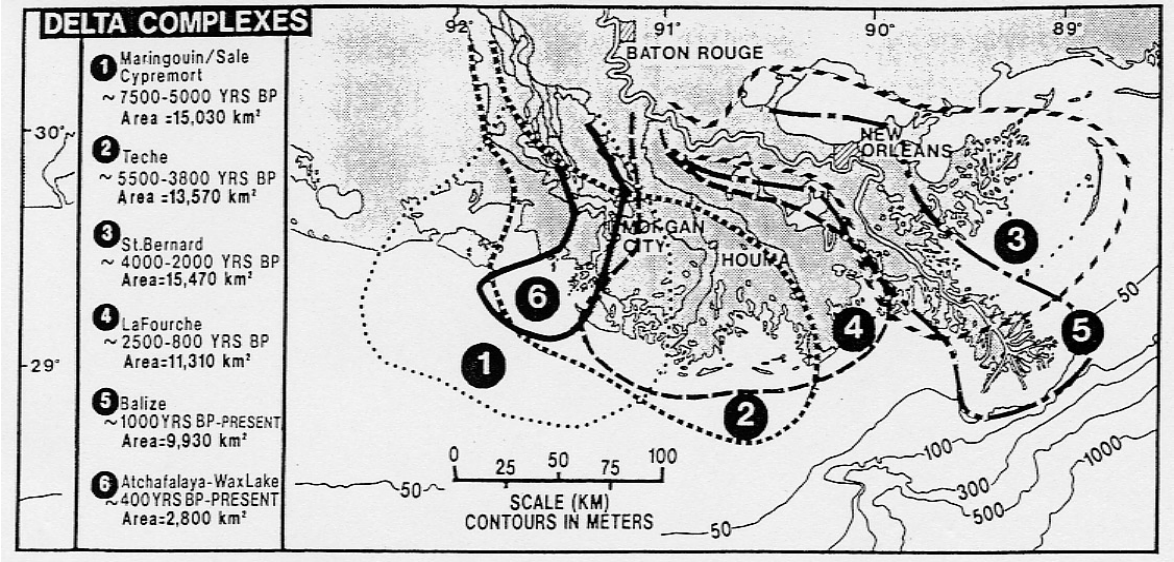

Figure 42. The Delta Lobes of the Mississippi River (From Roberts, 1997). Concentrate on the location and age of the St. Bernard lobe (~4000-2000 ypb).

processes, thus accounting for the range of particle sizes, and apparent lack of stratification.

The absence of ^{7}Be in surficial sediment provides evidence that there has been negligible sediment derived from fluvial sources during the few months prior to sampling. Within the transect, ^{137}Cs disappears at approximately 6cm. Thus, some portion of sediment to ~6cm can be inferred to have been deposited since 1954. Although excess ^{210}Pb is present in all cores, it diminishes greatly in activity with depth. The presence of excess ^{210}Pb in the cores suggests that new sediments are being supplied to this region and mixed downward by bioturbating organisms as shown in the x-radiographs. Also, surficial sediment properties indicate prodelta deposition by the modern Balize delta lobe during times of extremely high river discharge (i.e. major floods). This will be addressed later in this section. However, both the deposition and the mixing are slow, making accumulation rates difficult to calculate using these methods. Overall, the radioisotopes suggest delivery of fresh sediment to this area, but results preclude more detailed analysis.

This site is most likely near the eastern edge of deltaic mud deposits of the St Bernard delta lobe (Figure 42) active 4000-2000 ybp (Roberts, 1997) along with smaller amounts of surficial prodelta sediments from the Modern Mississippi River. Progradation of this delta lobe covered the Mississippi inner continental shelf with approximately 4m of sediment (Kindinger, 1988). The chirp profile for block D shows a similar sediment thickness in the western part of the line (Figures 15 and 16).

This is the most western site of the study and can also be influenced by the sediment plume of the Modern Mississippi delta when major floods occur (Figure 43).

Walker et al (1994), document this process in a satellite image displaying suspended sediments in the Mississippi River plume. Clay-mineral suites from Southeast Banks (eastern part of the study area) report high-illite contents and may reflect an influence of the Mississippi River in this region (Parker et al 1992). Sediments from the Mobile River could also be delivered to the inner shelf regions but most likely not to this study area (Site D).

A Model of Facies Evolution

From the variety of data collected in this region, we propose a conceptual geologic model for the Holocene geologic evolution of this region (Figure 44). At the last glaciation (Late Wisconsinan), the Mobile River prograded across the Northern GOM shelf (Figure 45) and formed the Lagniappe Delta (Kindinger, 1989; Sydow and Roberts, 1994). Holocene transgression began approximately 18,000 ypb; at which time, sea level rise was rapid. At 10,000-9,000 ybp, the rate of sea level rise slowed and allowed for coastal sediment accumulations and reworking along the coast (near S. Perdido shoal, Blocks G and 1). This led to development of coastal and lagoonal environments, that produced features like the estuarine shell reefs in Figures 17 and 20, and relict shoreface deposits at what is presently 40 m water depth. This is confirmed by radiocarbon ages of relatively pristine oyster shells located at the 40 m isobath (Figure 40 and Table 8). Sea level began to rise rapidly again submerging the features before they could be completely reworked and destroyed by wave action and erosion. The ridges and reefs became topographic high spots along the continental shelf. This rapid rise continued until approximately 8000 ybp when either the rate decreased or increased sediment supply allowed for coastal progradation to keep up. Shoreline features such as shoreface ridges

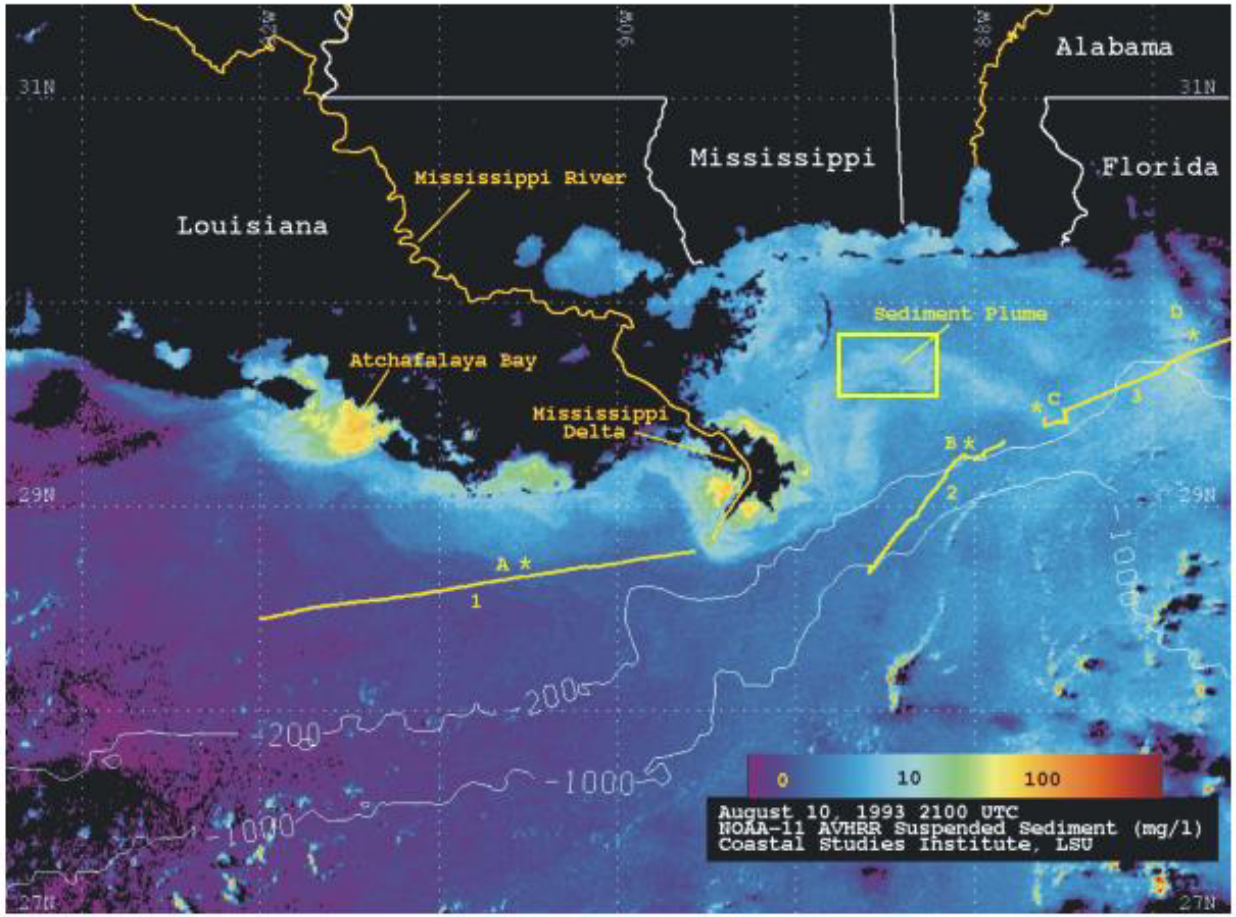

Figure 43. Satellite Image of the sediment plume from the Mississippi River after the summer flood of 1993 (From Walker et al, 1994).

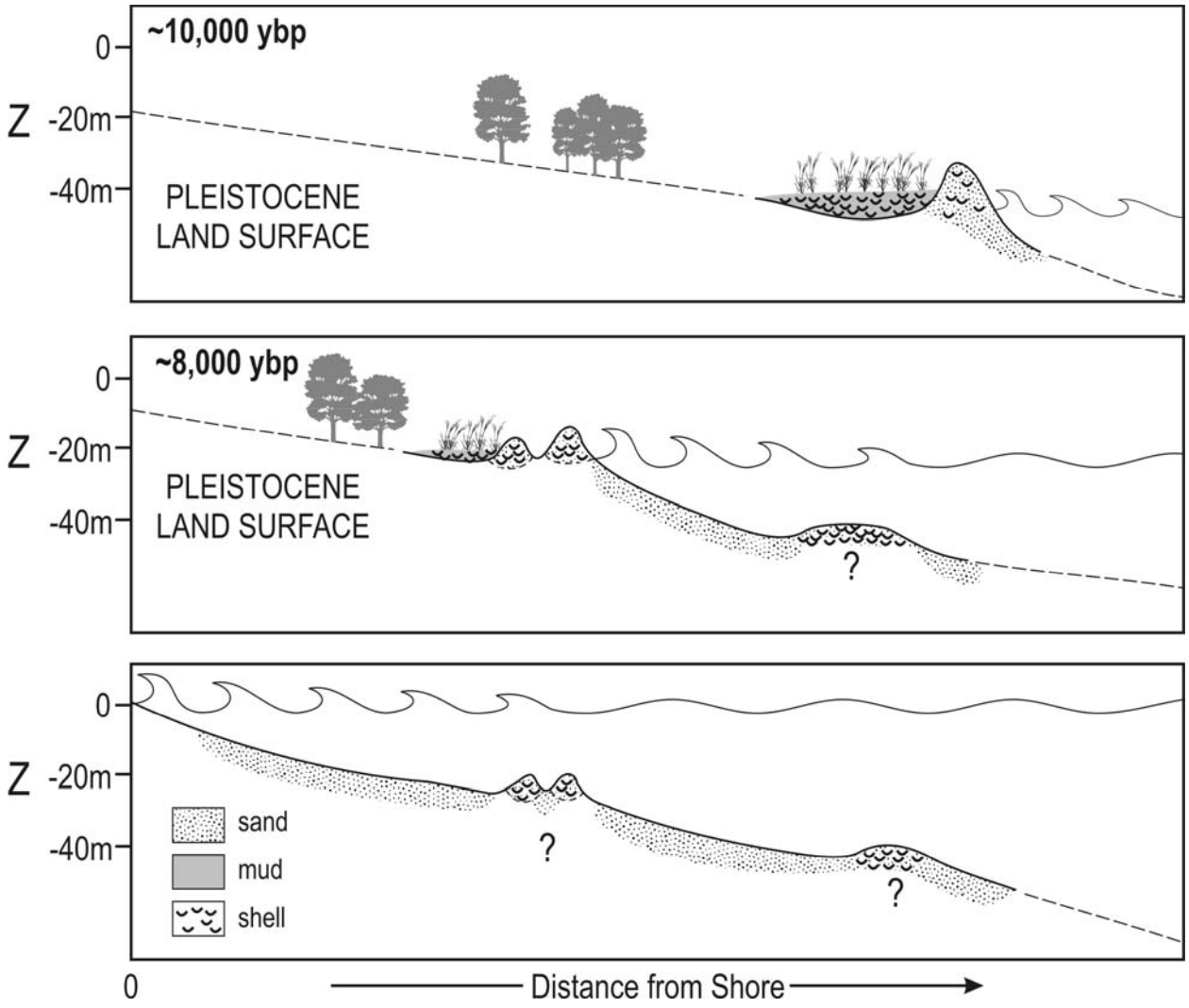

Figure 44. Conceptual geologic model for Holocene evolution of Northern Gulf of Mexico continental shelf.

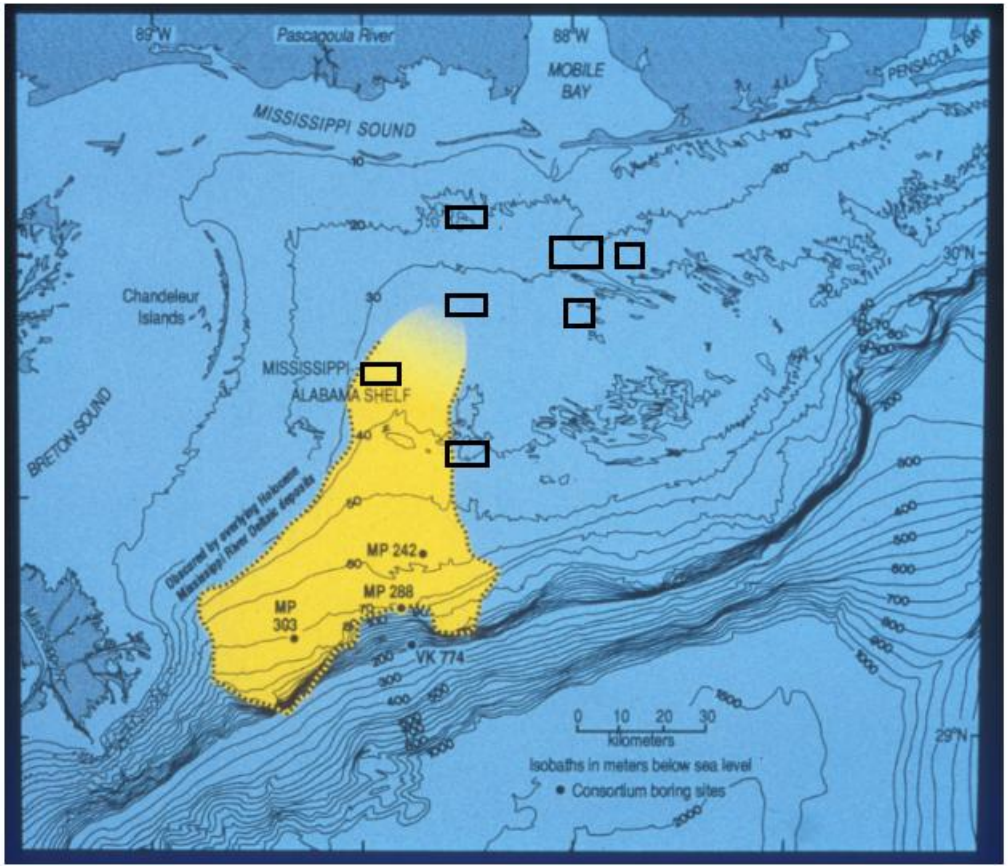

Figure 45. Location of the Late Pleistocene Lagniappe Delta. (adapted from H.H. Roberts) Location of study sites are outlined.

and to a lesser extent estuarine shell beds were deposited at this time (Figures 38 and 40). Rapid transgression then resumed, submerging these features before they could be completely reworked, and leaving them exposed on the shelf as topographic highs. Sea level then continued to rise to its present state. Throughout this entire sequence, shelf hydrodynamic processes winnowed out the fine sediments leaving a relatively clean homogenous sand sheet (MAFLA) around these paleotopographic highs. More recent deposition of ancestral Mississippi River sediments (St Bernard delta lobe) and modern sediments from the Mississippi River plume added fine-grained material to pre-existing sand deposits (Figures 38, 42, and 44).

In order to get a full and complete validation of the model proposed, vibracores are needed to calibrate chirp records and document subsurface sediment properties. By examining the underlying sediments associated with these features, our suggested model could be better evaluated. Having chirp subbottom profile data from the shelf break to the beach would be beneficial to explore the subsurface of the entire shelf and relate back to sea level history. However, existing facies show that this region is unique in that marine, estuarine, and shoreface deposits are seen preserved and exposed on the continental shelf. What was consistently thought of as a continuously homogenous sand sheet can now be seen as an area of mud deposition and exposed paleogeographic shell ridges and reefs. The Mississippi-Alabama inner-to middle continental shelf may be similar in process and form to that described by McBride (1997) for the Eastern Alabama-Florida Panhandle shelf. However, the paleogeographic features (ridges and reefs) observed to the west (MS-AL shelf) appear to have a depositional history that

favors rapid submergence and preservation of coastal environments rather than post-transgressive reworking of transgressive shoreline deposits.

Implications to Juvenile Red Snapper Essential Fish Habitat

In an effort to contribute to the study of EFH for juvenile red snapper, we compared physical sediment properties to juvenile fish density using regression techniques (Figures 36 and 37). Fish trawl data were obtained from Will Patterson by personal communication. The presence of these hard-bottom sediments appears to be related to spatial distributions of juvenile red snapper, as shown below.

Juvenile red snapper density versus Sand:Mud ratio is shown in Figure 36. A positive relationship (r^2=0.5, n=10) exists between density of juveniles and grain size, indicating that more juveniles are found in areas of coarser sediment. Juveniles apparently display an affinity for the low-relief shell structures observed on the sea floor in this area.

Juvenile red snapper density versus % organic matter is observed in Figure 37. A negative relationship was observed between juvenile snapper density and % organic matter in the sediments (r^2=0.65, n=11). This negative correlation may be influenced by grain size, as well, if most of the organic matter present is associated with the finest sediments.

These preliminary analyses suggest that a spatial relationship exists between juvenile snapper densities and physical sediment properties. A spatial extent of these large-scale topographic features and their influence on juvenile red snapper cannot be determined here because of the tracklines for individual trawls and the sampling scheme of the trawls. Further study and high-resolution mapping of the sea floor in conjunction

with better coordinated trawl location need to be accomplished in order to determine the spatial extent of these features and their influence on juvenile red snapper distributions. However, an initial overall estimate of the study sites suggests that 15% of the seabed is composed of shell ridge and reef sediments. A better picture of these features on a larger scale could be obtained with multi-beam bathymetry. Then areas can be further targeted for sonar mapping and sampling to characterize the bottom sediments and relate them to essential fish habitat.

CONCLUSIONS

The surficial sediments associated with the Mississippi-Alabama continental shelf have been long considered either a transitional zone between the prodelta muds of the Mississippi River and the MAFLA sand sheet or a continuation of this eastern sand sheet, as suggested by Ludwick (1964). However, geoacoustic methods and sampling have documented a more complex assemblage of shelf and estuarine/coastal facies. Along the Mississippi-Alabama inner-to-mid continental shelf, three primary facies exist (1) MAFLA sand sheet; (2) Inner and Middle shelf shell ridges and reefs; and (3) Modern prodelta mud facies. These different environments represent geological processes active since the early-mid Holocene to recent time. This study has delineated seven main conclusions.

(1) A more detailed history of the Holocene has been preserved on the Mississippi-Alabama continental shelf than has been previously thought.

(2) Relict shell ridges and reefs produced in coastal/estuarine locations appear to have been preserved and are presently exposed on the shelf.

(3) Radiocarbon ages of shells and age/depth relationships associated with sea level fluctuations support hypotheses of relict features exposed on the shelf. Whether they are drowned reefs or slightly reworked shoreface deposits, the features represent a record of coastal evolution during the Mid-Holocene.

(4) Better preservation of these features along with age-depth relationships suggest more rapid submergence westwrd, closer to the MS delta than to the east.

(5) Sonar mapping and bottom characterization of the surficial sediments is proving to be an effective means of delineating juvenile red snapper habitat.

(6) Based on preliminary analyses, Juvenile red snapper seem to prefer coarser shell ridges that exhibit some vertical relief.

(7) For mapping and trawl coordination, we suggest trawling along the orientation of the ridges and reef features. This would allow for better comparisons to be made between specific sediment types and juvenile red snapper density with regards to habitat preference.

Deciphering this record is being made possible by the powerful combination of acoustic seabed mapping and direct sampling methods. Together they are instrumental in investigating depositional history and relating geology to biology. Utilizing an interdisciplinary approach to understanding habitat for threatened and endangered species is proving vital in determining essential fish habitat.

REFERENCES

Anderson, L.C., and McBride, R,A., 1996. Taphonomic and Paleoenvrionmental Evidence of Holocene Shell-Bed Genesis and History on the Northeastern Gulf of Mexico Shelf. Palaios, v.11, p. 532-549.

Appleby, P.G., Oldfield, F., 1978. The calculation of ^{210}Pb dates assuming a constant rate of supply of unsupported ^{210}Pb to the sediment. Cantena 5, 1-8.

Bentley, S.J., Keen, T.R., Blain, C.A., Vaughan, W.C., 2002. The Origin and Preservation of a Major Hurricane Event Bed in the Northern Gulf of Mexico; Hurricane Camille, 1969. Marine Geology, v. 186(3-4), p. 423-446.

Blondel, P.J., and Murton, B.J., 1997. Handbook of Seafloor Sonar Imagery. PRAXIS-Wiley & Sons. 314 p.

Blum, M.D., Carter, A.E., Zayac, T., Goble, R.J., 2002. Middle Holocene Sea-Level and Evolution of the Gulf of Mexico Coast (USA). Journal of Coastal Research. Special Issue 36, p. 65-80.

Bryant, W.R., Lugo, J., Cordova, C., and Salvador, A., 1991. Gulf of Mexico Physiography and Bathymetry. In: Salvador (editor) The Gulf of Mexico Basin. Geological Society of America, p. 13-30.

Brooks, G.R., Kindinger, J.L., Penland, S., Williams, S.J., McBride, R.A., 1995. Journal of Coastal Research, v.11(4), p. 1026-1036.

Buffler R.Y., 1991. Early Evolution of the Gulf of Mexico Basin. In: Goldthwaite, D. (editor) Introduction to Central Gulf Coast Geology. N.O.G.S. publication, p.1-15.

Carver, R.E., 1971. Procedures in Sedimentary Petrology. Wiley-Interscience, New York.

Coakley, J.P. and Syvitski, J.P.M., 1991. Sedigraph technique: *in*, Syvitski, J.P.M., ed., Principles, Methods, and Application of Particle Size Analysis: Cambridge, Cambridge University Press, 368 p.

Coleman, J.M and Gagliano, S.M., 1964. Cyclic sedimentation in the Mississippi River Deltaic Plain. Gulf Coast Association Geological Societies Transactions, v.14, p.67-80.

Donoghue, J.F., 1993. Late Wisconsinan and Holocene depositional history, Northeastern Gulf of Mexico. Marine Geology. v. 112, p. 185-205.

Doyle, L.J., and Sparks, T.N., 1980. Sediments of the Mississippi, Alabama, and Florida (MAFLA) Continental Shelf. Journal of Sedimentary Petrology, v.50(3), p. 905-916.

Ewing, T.E., 1991. Structural Framework, Gulf of Mexico. In: Salvador (editor) The Gulf of Mexico Basin. Geological Society of America, p. 31-52.

Frazier, D.E., 1967. Recent Deltaic deposits of the Mississippi River: Their Development and Chronology. Gulf Coast Association Geological Societies Transactions, v.17, p. 287-315.

Freitas, R., Silva, S., Quintino, V., Rodrigues, A.M., Rhynas, K., Collins W.T., 2003. Acoustic Seabed Classification of Marine Habitats: studies in the western coastal-shelf of Portugal. ICES Journal of Marine Science, v. 60, 599-608.

Kennicutt II, M.C., and Schroeder, W.W., Brooks, J.M., 1995. Temporal and Spatial Variations in Sediment Characteristics on the Mississippi-Alabama Continental Shelf. Continental Shelf Research, v.15(1), p. 1-18.

Kenny, A.J., Cato, I. Desprez, M., Fader, G. Schuttenhelm, R.T.E., Side J., 2003. An Overview of Seabed Mapping Techniques in the Context of Marine Habitat Classification. ICES Journal of Marine Science, v. 60, p. 411-418.

Kindinger, J.L., 1988. Seismic Stratigraphy of the Mississippi-Alabama Shelf and Upper Continental Slope. Marine Geology, v.83, p. 79-94.

Kindinger, J.L., 1989. Depositional History of the Lagniappe Delta, Northern Gulf of Mexico. Geo-Marine Letters, v.9, p. 59-66.

Kindinger, J.L, Penland, S., Williams, S.J., Suter, J.R., 1989. Inner Shelf Deposits of the Louisiana-Mississippi-Alabama Region, Gulf of Mexico. Transactions- Gulf Coast Association of Geological Societies, v. 39, p. 413-420.

Larsen, L.C., 2002. Notes on Real-Time Interpretation of Seafloor Survey Data. In: Wright, D.J. (editor) Undersea with GIS, ESRI Press, p. 23-31.

Ludwick, J.C., 1964. Sediments in Northeastern Gulf of Mexico. In: Miller, R.L. (editor) Papers in Marine Geology. Macmillan Co., New York, NY, p. 204-238.

Mazzullo, J., and Bates, C., 1985. Sources of Pleistocene and Holocene Sand for the Northeast Gulf of Mexico Shelf and the Mississippi Fan. Gulf Coast Association of Geological Societies Transactions, v.35, p. 457-466.

McBride, R.A., 1997. Seafloor Morphology, Geologic Framework, and Sedimentary

Processes of a Sand-Rich Shelf Offshore Alabama and Northwest Florida: Northeastern Gulf of Mexico. Ph.D. Dissertation. Louisiana State University, Baton Rouge, 509 p.

McBride, R.A., Anderson,L.C., Tudoran, A., Roberts, H.H., 1999. Holocene Stratigraphic Architecture of a Sand-Rich Shelf and the Origin of Linear Shoals: Northeastern Gulf of Mexico. SEPM special publication 64, Isolated shallow marine sand bodies: sequence stratigraphic analysis and sedimentologic interpretation, p. 95-126.

McBride, R.A., & Byrnes, M.R., 1995. Surficial Sediments and Morphology of the Southwestern Alabama/Western Florida Panhandle Coast and Shelf. Transactions-Gulf Coast Association of Geological Societies, v. 45, p. 393-404.

McBride, R.A., Byrnes, M.R., Penland, S., Pope, D.L., Kindinger, J., 1991. Geomorphic History, Geologic Framework, and Hard Mineral Resources of the Petit Bois Pass Area, Mississippi-Alabama. GCSSEPM Foundation Twelfth Annual Research Conference, p. 116-127.

Noller, J.S., 2000. Lead-210 Geochronology. In: Quaternary Geology: Methods and Applications. AGU Reference Shelf 4, p. 115-120.

Parker, S.J., Schultz, A.W., Schroeder, W.W. (1992). Sediment Characteristics and Seafloor Topography of a Palimpsest Shelf, Mississippi-Alabama Continental Shelf. In: Fletcher III, C.H & Wehimiller, J.F. (editors) Quaternary Coasts of the United States: Marine and Lacustrine Systems (SEPM Special Publication 48), p. 243-251.

Patterson,W.F., Wilson, C.A., Bentley, S.J., Cowan, J.H., Henwood, T., Allen, Y.C., Dufrene, T.A., In press. Delineating juvenile red snapper habitat on the northern Gulf of Mexico continental shelf. Pages XXX in P. Barnes and J. Thomas, Editors. American Fisheries Society Symposium XXX: Benthic Habitats and the Effects of Fishing.

Perillo, G.M.E. 1995. Geomorphology and Sedimentology of Estuaries: An Introduction. In: Perillo, G.M.E. (editor) Geomorphology and Sedimentology of Estuaries. Developments in Sedimentology 53, Elsiever, p. 1-15.

Roberts, H.H., 1997. Dynamic changes of the Holocene Mississippi River Delta Plain: The Delta Cycle. Journal of Coastal Research, v. 13(3), p. 605-627.

Roberts, H.H., Wilson, Charles A., Supan, J., Winans, W., 1999. New Technology for Characterizing Louisiana's Shallow Coastal Water Bottoms and Predicting Future Changes. Transactions- Gulf Coastal Association of Geological Societies. v. 49, p. 452-460.

Roberts, H.H., Wilson, Charles A., Supan, J., 2000. Acoustic Surveying of Ultra-Shallow Water Bottoms (<2.0 m) for both Engineering, and Environmental Applications. In: Proceedings- Offshore Technology Conference. v. 32(1), p. 571-580.

Sager, W.W., Schroeder, W.W., Davis, K.S., Resak, R., 1999. A Tale of Two Deltas: seismic mapping of the ear surface sediments on the Misssissippi-Alabama outer shelf and implications for recent sea level fluctuations. Marine Geology. v. 160, p. 119-136.

Sager, W.W., Schoeder, W.W., Laswell, J.S., Davis, K.S., Resak, R, Gittings, S.R., 1992. Mississippi-Alabama Outer Continental Shelf Topographic Features formed during the Late Pleistocene-Holocene Transgression. Geo-Marine Letters, v. 12, p.41-48.

Schroeder, W.W., Gittings, S.R., Dardeau, M.R., Fleisher, P., Sager, W.W., Shultz, Resak, R., 1989. Topographic Features of the L'MAFLA Continental Shelf, Northern Gulf of Mexico. Oceans '89 Proceedings, IEEE Publication No. 89CH2780-5, New York, p. 54-58.

Schroeder, W.W., Schultz, Dindo, J.J., 1988. Inner-Shelf Hardbottom Areas, Northeastern Gulf of Mexico. Transactions- Gulf Coast Association of Geological Societies, v. 38, p. 535-541.

Schroeder, W.W., Schultz, A.W., Pilkey, O.H., 1995. Late Quaternary Oyster Shells and Sea-Level History, Inner Shelf, Northeast Gulf of Mexico. Journal of Coastal Research, v.11(3), p.664-674.

Sommerfield, C.K., Nittrouer, C.A., Alexander, C.R., 1999. ^{7}Be as a tracer of flood sedimentation on the northern California continental margin. Continental Shelf Research, v. 19, 335-361.

Stubblefied, W.L., McGrail, D.W., Kersey, D.G., 1984. Recognition of Transgressive and Post-Transgressive Sand Ridges on the New Jersey Continental Shelf. In: Tillman, R.W. & Siemers, C.T. (editors) Siliciclastic Shelf Sediments. SEPM Special Publication No. 34, p. 1-24.

Stuvier, M., and Reimer, P.J., 1993. Extended ^{14}C database and revised CALIB 3.0 ^{14}C age calibration program. Radiocarbon. v. 35(1), p. 215-230.

Suter, J.R., and Berryhill, H.L., 1985. Late Quaternary Shelf-Margin Deltas, Northwest Gulf of Mexico. The American Association of Petroleum Geologists Bulletin. v. 69(1), p. 77-91.

Sydow, J., and Roberts, H.H., 1994. Stratigraphic Framework of a Late Pleistocene Shelf-edge Delta, Northeast Gulf of Mexico. American Association of Petroleum Geologists Bulletin. v. 78, p. 1276-1312.

Valentine, P.C., Cochrane, G.R., Scanlon, K.M., 2003. Mapping the Seabed and Habitats in the National Marine Sanctuaries- Examples from the East, Gulf and West Coasts. Marine Technology Society Journal, v. 37(1), p. 10-17.

Walker, N.D., Fargion, G.S., Rouse, L.J., Biggs, D.G., 1994. The Great Flood of Summer 1993: Mississippi River Discharge Studied. EOS, Transactions, American Geophysical Union, v.75(36), p. 409, 414-15.

Winker, C., 1982. Cenozoic Shelf Margins, Northern Gulf of Mexico. Gulf Coast Association of Geological Societies Transactions v. 43: 427-448.

APPENDIX A

CHIRP SUBBOTTOM PROFILES

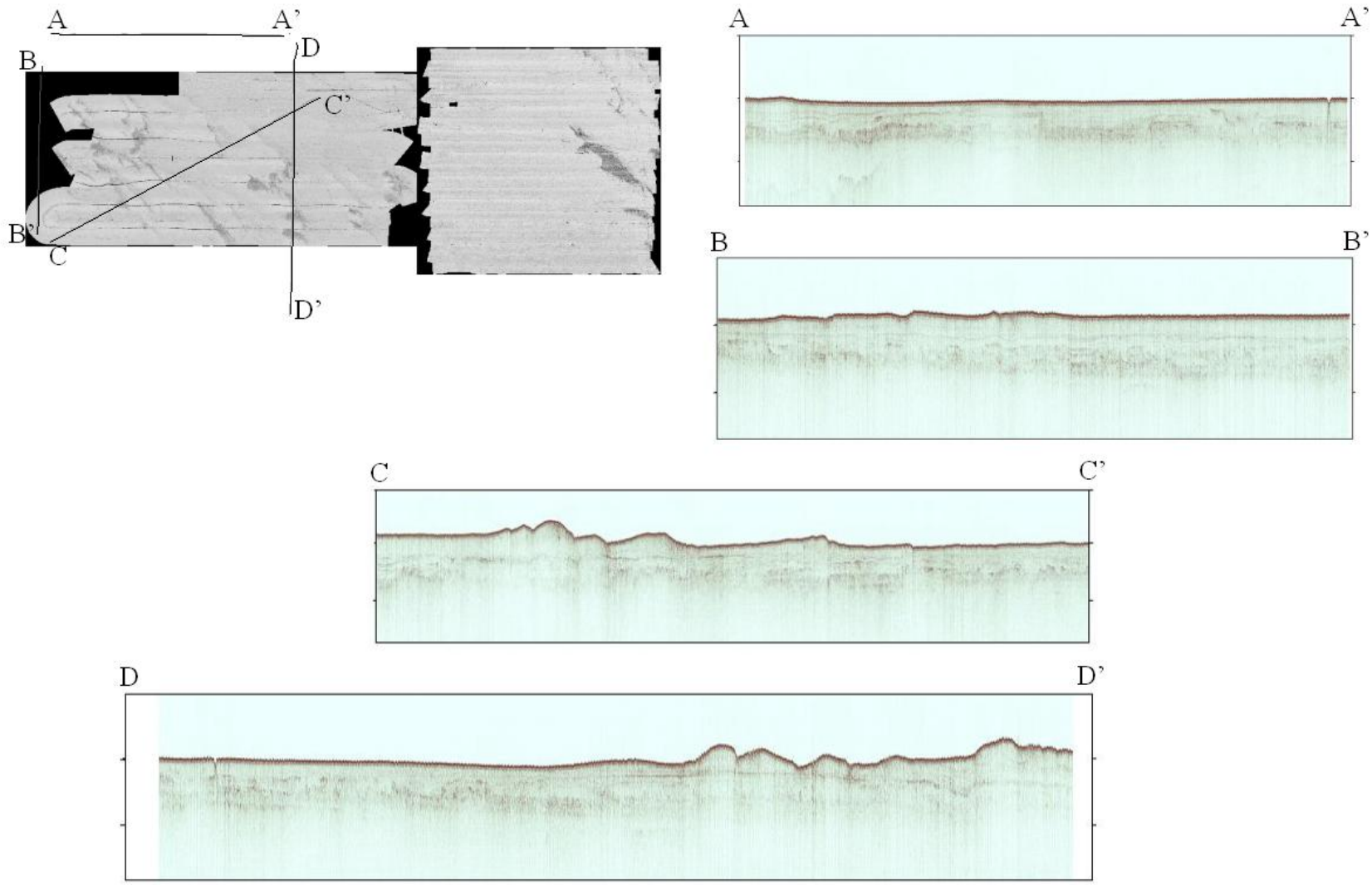

Figure 46. Chirp subbottom profiles within blocks A & 5.

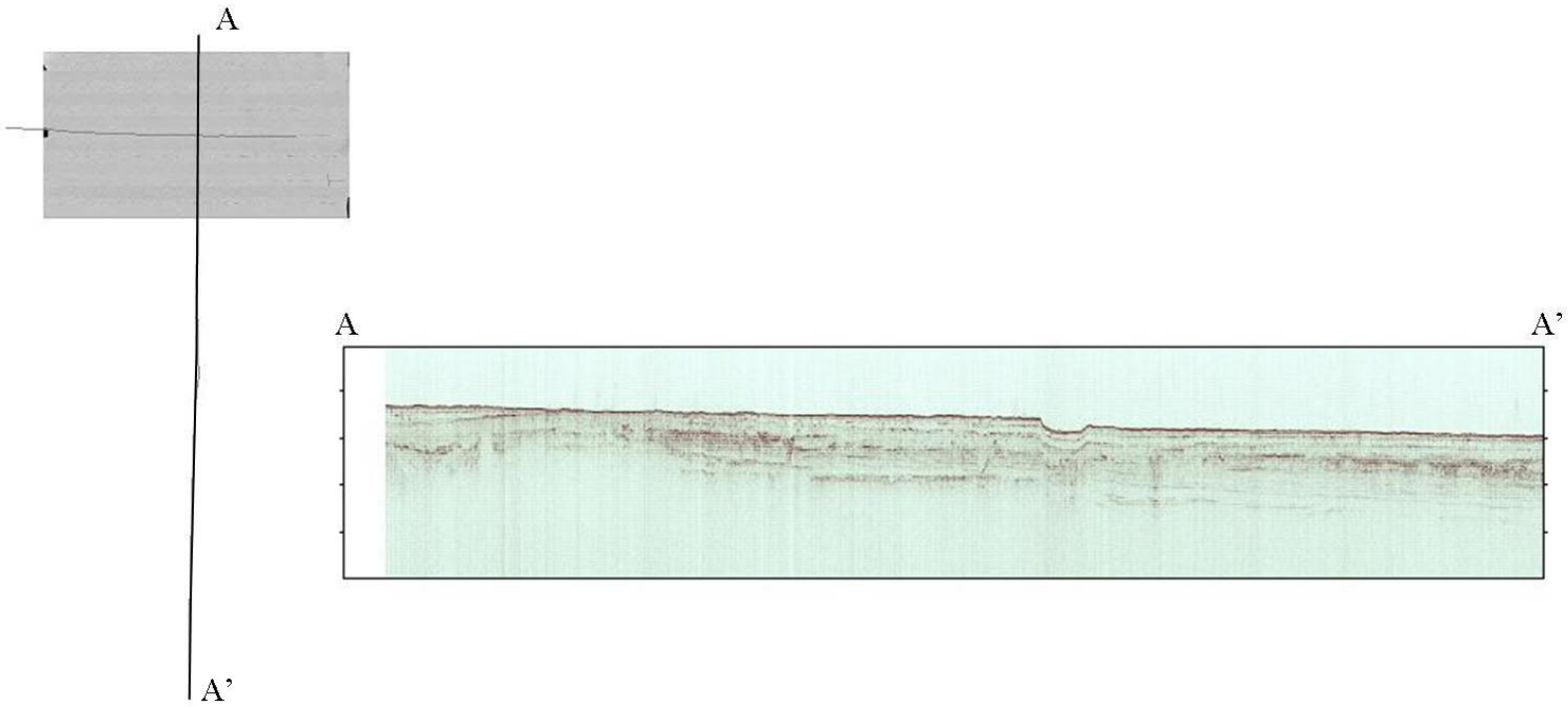

Figure 47. Chirp subbottom profile from block D.

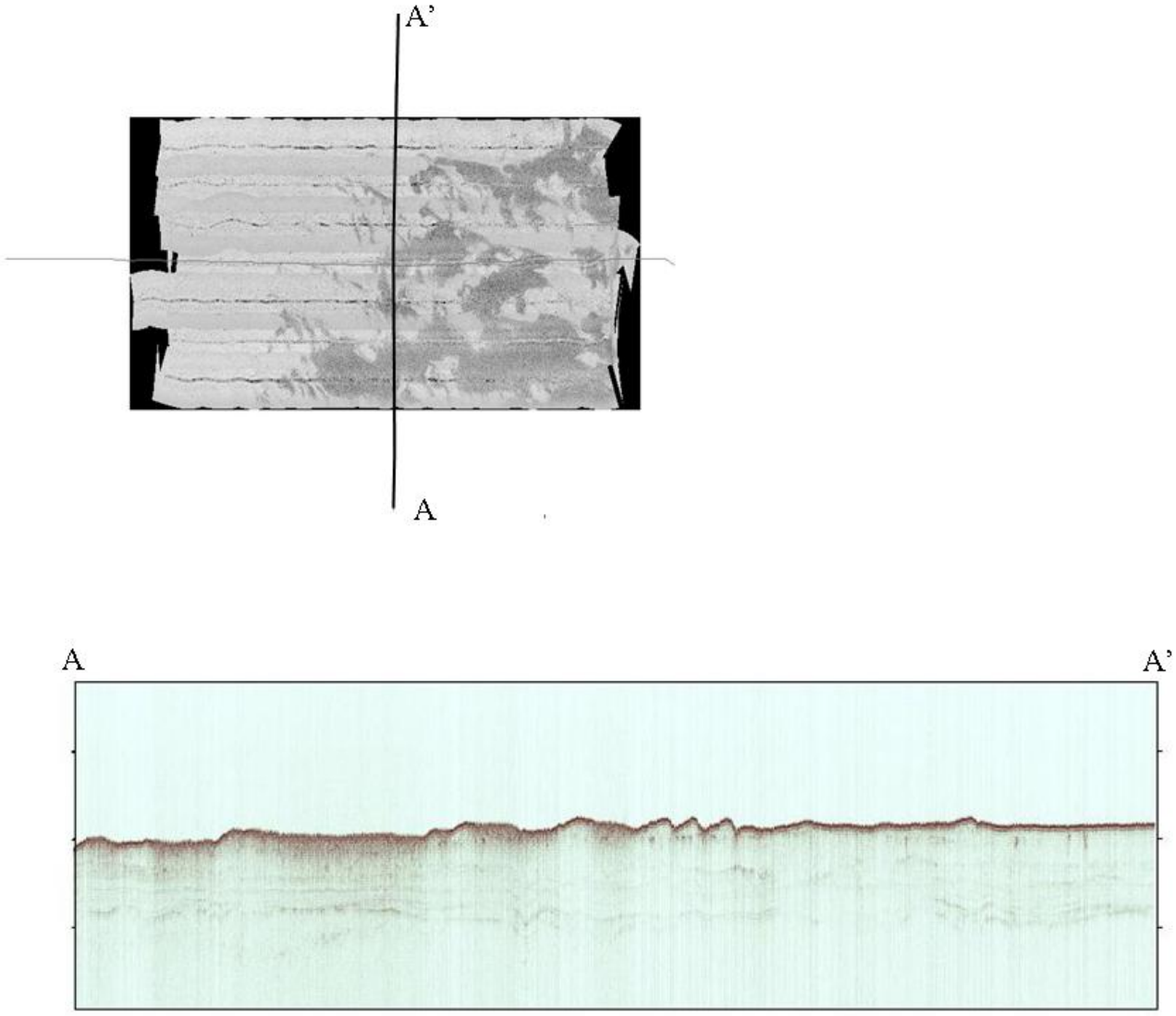

Figure 48. Chirp subbottom profile from block G.

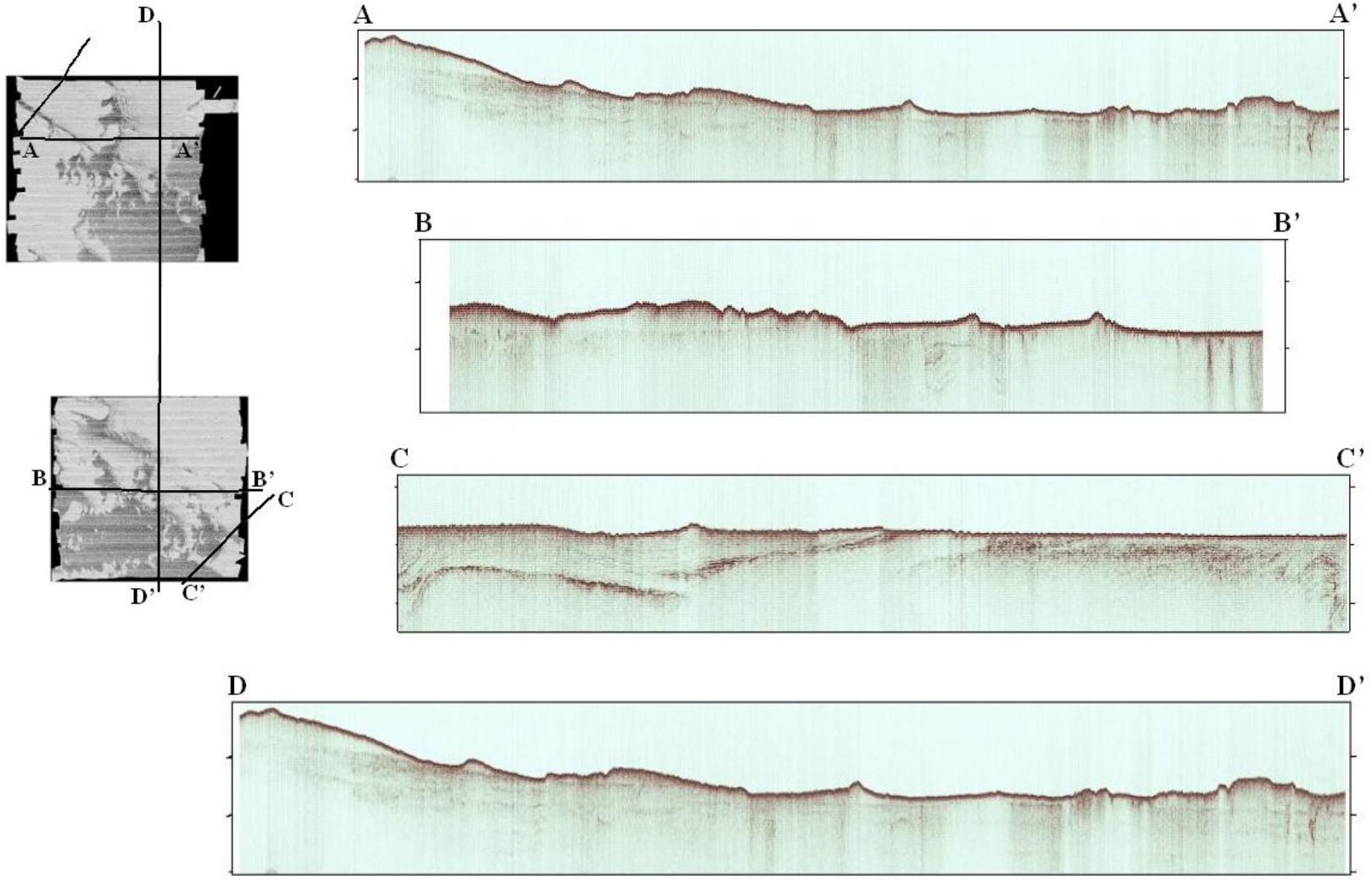

Figure 49. Chirp subbottom profiles from blocks 1 & 2.

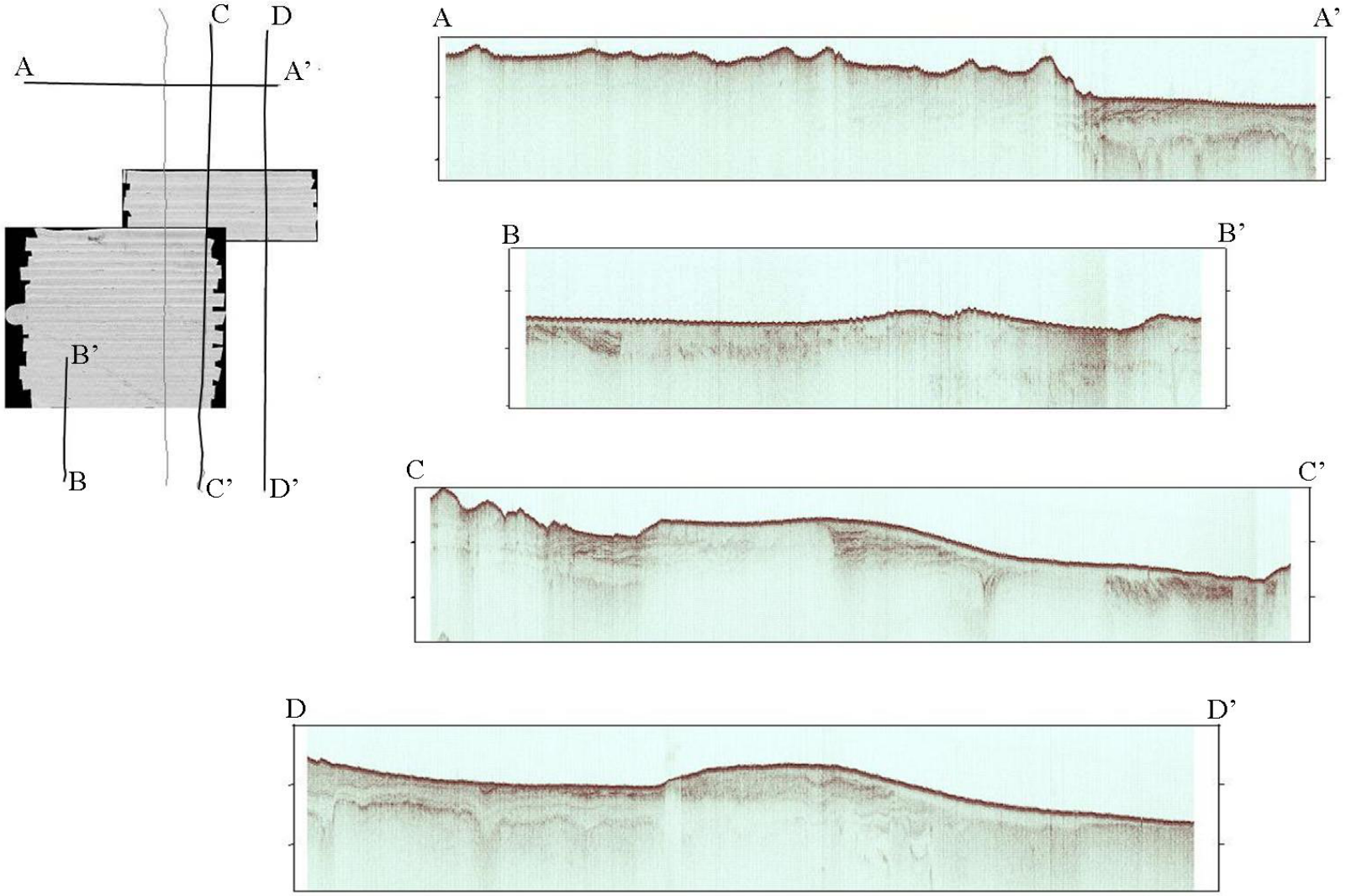

Figure 50. Chirp subbottom profiles from blocks 3 & 4.

APPENDIX B

SEDIMENT DATA FROM AC0802 SITE D

Table 9. Grain Size and Gamma Spectrometry results from core location D1. (29º44.7' N -088º25.6' W)

Core	Depth (cm)	Cs-137 Activity (dpm/g)	Pb-210 Activity(dpm/g)	% sand	% silt	% clay
D1A	0-5			33.61	29.34	37.05
D1A	5-10			32.79	17.83	49.38
D1B	0-2	0.3±0.047	10.8±0.38	19.75	30.66	49.59
D1B	2-4	0.26±0.053	11.4±0.38	23.91	30.04	46.05
D1B	4-8	0.29±0.051	9.8±0.36	28.51	33.25	38.24
D1B	8-12			24.16	34.40	41.44
D1B	12-16			23.09	29.56	47.35
D1B	16-20	ND*	2.1±0.2			
D1C	0-2			25.33	30.85	43.83

*ND= Not Detectable

Table 10. Grain Size and Gamma Spectrometry results from core location D2. (29º44.9'N -088º25.4'W)

Core	Depth (cm)	Cs-137 Activity (dpm/g)	Pb-210 Activity(dpm/g)	% sand	% silt	% clay
D2A	0-2	0.25±0.047	8.95±0.34	36.02	26.31	37.67
D2A	2-4	0.17±0.052	8.28±0.34	44.70	28.83	26.47
D2A	4-6			53.19	29.42	17.38
D2A	6-8	ND	5.4±0.22	43.91	26.61	29.47
D2A	8-10			36.52	28.42	35.06
D2A	10-12			46.05	28.47	25.48
D2A	12-14	ND	3.14±0.21	45.17	28.59	26.23
D2A	14-16			29.04	27.79	43.17
D2A	16-18			14.57	25.23	60.19
D2A	18-20	ND	0.6±0.09			
D2B	0-2			21.91	29.14	48.95
D2C	0-2			27.25	25.73	47.02

Table 11. Grain Size and Gamma Spectrometry results from core location D3. (29º45.3'N -088º25.5"W)

Core	Depth (cm)	Cs-137 Activity (dpm/g)	Pb-210 Activity(dpm/g)	% sand	% silt	% clay
D3A	0-2	0.18±0.06	10.07±0.36	27.19	30.91	41.90
D3A	2-4	0.1±0.05	10.85±0.36	25.26	30.43	44.31
D3A	4-6			35.89	27.96	36.15
D3A	6-8	0.3±0.05	9.64±0.33	29.52	29.01	41.47
D3A	8-10			33.95	28.41	37.64
D3A	10-12			32.21	29.22	38.57
D3A	12-14	0.21±0.04	6.64±0.30	36.02	29.11	34.87
D3A	14-16			23.00	30.88	46.12
D3A	16-18			21.93	29.05	49.02
D3A	18-20	0.1±0.04	3.76±0.29	21.54	29.08	49.39
D3A	20-22			14.23	26.44	59.33
D3A	22-24			14.90	24.07	61.03
D3B	0-2			29.89	26.50	43.61
D3C	0-2			24.72	26.46	48.82

Table 12. Grain Size and Gamma Spectrometry results from core location D4. (29º45.1'N -088º24.9'W)

Core	Depth (cm)	Cs-137 Activity (dpm/g)	Pb-210 Activity(dpm/g)	% sand	% silt	% clay
D4A	0-2	0.145±0.05	10.9±0.36	30.94	26.64	42.42
D4A	2-4	0.16±0.05	8.79±0.34	35.32	28.36	36.32
D4A	4-6			40.92	28.44	30.64
D4A	6-8	0.072±0.03	7.98±0.32	36.97	26.42	36.61
D4A	8-10			34.61	28.78	36.60
D4A	10-12					
D4A	12-14	ND	3.9±0.21	40.15	29.49	30.37
D4A	14-16			31.99	24.14	43.88
D4A	16-18			18.07	20.57	61.35
D4B	0-2			29.10	24.73	46.17
D4C	0-2			27.23	26.33	46.44

Table 13. Grain Size and Gamma Spectrometry results from core location D5. (29º45.3'N -088º24.4'W)

Core	Depth (cm)	Cs-137 Activity (dpm/g)	Pb-210 Activity(dpm/g)	% sand	% silt	% clay
D5A	0-2			22.97	31.35	45.68
D5B	0-2	0.3±0.04	10.9±0.36	32.43	28.79	38.79
D5B	2-4	0.2±0.05	9.8±0.35	32.54	28.46	39.00
D5B	4-6			49.24	26.33	24.44
D5B	6-8	ND	4.3±0.24	47.44	26.71	25.86
D5B	8-10			28.96	29.34	41.70
D5B	10-12			35.59	29.81	34.60
D5B	12-14	ND	6.3±0.3	38.86	28.73	32.42
D5B	14-16			38.93	28.99	32.08
D5C	0-2			25.52	28.55	45.93

Table 14. Grain Size and Gamma Spectrometry results from core location D6. (29º44.8'N -088º24.4'W)

Core	Depth (cm)	Cs-137 Activity (dpm/g)	Pb-210 Activity(dpm/g)	% sand	% silt	% clay
D6A	0-2			66.88	29.64	3.48
D6B	0-2	0.14±0.046	5.58±0.27	70.94	26.43	2.63
D6B	2-4	0.06±0.035	4.68±0.25	69.81	24.94	5.25
D6B	4-6			65.67	24.30	10.03
D6B	6-8	ND	8.18±0.33	61.76	25.06	13.18
D6B	8-10			61.60	25.30	13.11
D6B	10-12			62.64	27.93	9.43
D6B	12-14	ND	1.8±0.14	65.33	28.25	6.42
D6B	14-16			60.85	29.70	9.45
D6C	0-2			67.08	28.44	4.49

Table 15. Grain Size and Gamma Spectrometry results from core location D7. (29º44.5'N -088º24.5'W)

Core	Depth (cm)	Cs-137 Activity (dpm/g)	Pb-210 Activity(dpm/g)	% sand	% silt	% clay
D7A	0-2			42.79	32.74	24.47
D7B	0-2			34.65	30.51	34.84
D7C	0-2	0.24±0.05	10.1±0.35	41.58	27.02	31.39
D7C	2-4	0.22±0.05	804±0.33	36.58	30.24	33.18
D7C	4-6			40.86	28.80	30.34
D7C	6-8			39.68	27.59	32.73
D7C	8-10			37.70	28.04	34.26
D7C	10-12			42.39	31.00	26.61
D7C	12-14			45.01	32.33	22.66
D7C	14-16			44.15	30.53	25.32
D7C	16-18			49.51	30.51	19.99

VITA

Triniti Dufrene was born in October of 1978, in New Orleans, Louisiana. She graduated from St. Mary's Dominican High School in 1996 and then moved to South Carolina to attend Coastal Carolina University. There she obtained a Bachelor of Science degree in marine science with an emphasis in coastal geology in 2001. She worked as a GIS research specialist at the Center for Marine and Wetlands Studies mapping historical shorelines, until she decided to attend graduate school at LSU, in the Coastal Studies Institute in the Department of Oceanography and Coastal Sciences in August 2002. Triniti is presently a candidate for the Master of Science in the Department of Oceanography and Coastal Sciences.